Paper:
Gil, A. & Ortigosa, R. (2016). A new framework for large strain electromechanics based on convex multi-variable strain energies: Variational formulation and material characterisation. *Computer Methods in Applied Mechanics and Engineering, 302*, 293-328.
http://dx.doi.org/10.1016/j.cma.2015.11.036

A new framework for large strain electromechanics based on convex multi-variable strain energies: Variational formulation and material characterisation

Antonio J. Gil, Rogelio Ortigosa

PII: S0045-7825(15)00416-8
DOI: http://dx.doi.org/10.1016/j.cma.2015.11.036
Reference: CMA 10790

To appear in: *Comput. Methods Appl. Mech. Engrg.*

A new framework for large strain electromechanics based on convex multi-variable strain energies: variational formulation and material characterisation.

Antonio J. Gil[1], Rogelio Ortigosa

Zienkiewicz Centre for Computational Engineering, College of Engineering Swansea University, Bay Campus, SA1 8EN, United Kingdom

Abstract

Following the recent work of Bonet et al.[1], this paper postulates a new convex multi-variable variational framework for the analysis of Electro Active Polymers (EAP) in the context of reversible nonlinear electro-elasticity. This extends the concept of polyconvexity [2] to strain energies which depend on non-strain based variables introducing other physical measures such as the electric displacement. Six key novelties are incorporated in this work. First, a new definition of the electro-mechanical internal energy is introduced expressed as a convex multi-variable function of a new extended set of electromechanical arguments. Crucially, this new definition of the internal energy enables the most accepted constitutive inequality, namely ellipticity, to be extended to the entire range of deformations and electric fields and, in addition, to incorporate the electro-mechanical energy of the vacuum, and hence that for ideal dielectric elastomers, as a degenerate case. Second, a new extended set of variables, work conjugate to those characterising the new definition of multi-variable convexity, is introduced in this paper. Third, both new sets of variables enable the definition of novel extended Hu-Washizu type of mixed variational principles which are presented in this paper for the first time in the context of nonlinear electro-elasticity. Fourth, some simple strategies to create appropriate convex multi-variable energy functionals (in terms of convex multi-variable invariants) by incorporating minor modifications to a priori non-convex multi-variable functionals are also presented. Fifth, a tensor cross product operation [3] used in [1] to facilitate the algebra associ-

[1]Corresponding author: a.j.gil@swansea.ac.uk

Preprint submitted to Computer Methods in Applied Mechanics and Engineering December 17, 2015

ated with the adjoint of the deformation gradient tensor is incorporated in the proposed variational electro-mechanical framework, leading to insightful representations of otherwise complex algebraic expressions. Finally, under a characteristic experimental set up in dielectric elastomers, the behaviour of a convex multi-variable constitutive model capturing some intrinsic nonlinear effects such as electrostriction, is numerically studied.

Keywords: Dielectric elastomers, Nonlinear electro-elasticity, Large strains, material stability, Mixed variational principles, polyconvexity

1. Introduction

The actuator and harvesting capabilities of the early piezoelectric crystals and ceramics were not very long ago eclipsed by those of Electro Active Polymers (EAP). This heterogeneous group can be divided into two further subgroups, namely Electronic Electro Active Polymers (EEAP) and Ionic Electro Active Polymers (IEAP) [4]. Within the first subgroup, Dielectric Elastomers (DE) and electrostrictive relaxor ferroelectric polymers or simply Piezoelectric Polymers (PP), have become increasingly relevant. The second subgroup includes ionic gels, Ionic Polymer Metal Composites (IPMC) and carbon nanotubes.

The present manuscript focuses mainly on DEs and PPs. The elastomer VHB 4910 and the highly popular PolyVinylidene DiFlouride (PVDF) are the most representative examples of both groups, respectively. However, DEs are becoming specially attractive due to their outstanding actuation properties [5–8]. For instance, a voltage induced area expansion of 1980% on a DE membrane film has been recently reported by Li et al. [9]. In this specific case, the electromechanical instability is harnessed as a means for obtaining these electrically induced massive deformations with potential applications in soft robots, adaptive optics, balloon catheters and Braille displays [9], among others. Moreover, these materials have been successfully applied as generators to harvest energy from renewable sources as human movements and ocean waves [10].

With the emergence of these highly deformable materials, a variational framework for nonlinear electro-elasticity was developed by different authors [11–21]. Within that framework, as customary in nonlinear continuum mechanics, the constitutive behaviour of the material is encoded in an energy functional which depends typically upon appropriate strain measures, a Lagrangian electric variable and, if dissipative effects are considered, upon an electromechanical internal variable.

Several authors have proposed alternative representations of the energy functional in terms of electromechanical invariants [12–17]. However, some restrictions need to be imposed on the invariant representation if physically admissible behaviours are expected to occur. Bustamante and Merodio [22] considered classical constitutive inequalities, namely: the Baker-Ericksen inequality, the pressure-compression inequality, the traction-extension inequality and the ordered forces inequality. The objective was to study under what conditions a specific invariant representation of the energy functional for magneto-sensitive elastomers would violate the previous inequalities for very specific deformation scenarios.

The most well accepted constitutive inequality is ellipticity, also known as the Legendre-Hadamard condition [2, 23]. This inequality has important physical implications. In particular, it guarantees positive definiteness of the generalised electromechanical acoustic tensor [24] and hence, existence of real wave speeds in the material in the vicinity of an equilibrium configuration. Several authors have also studied under what conditions positive definiteness of the generalised electromechanical acoustic tensor is compromised for a specific invariant representation of the energy functional [24–26]. Recently, a material stability criterion based on an incremental quasi-convexity condition of the energy functional has been introduced by Miehe et al. [27].

In nonlinear elasticity, polyconvexity [1, 2, 23, 28–34, 34–45] of the (strain) energy functional, namely, convexity with respect to the components of the deformation gradient tensor $\boldsymbol{F}$, the components of its adjoint or cofactor $\boldsymbol{H}$ and its determinant J, automatically implies the ellipticity condition. Following the work of Rogers [46], the present manuscript presents an extension of the concept of polyconvexity to the field of nonlinear electro-elasticity based on a new convex multi-variable definition of the energy functional. Notice that the focus of this paper is on material stability and not on the existence of minimisers. The latter would also require the study of the sequentially weak lower semicontinuity and the coercivity of the energy functional.

A new electro-kinematic variable set is introduced including the deformation gradient $\boldsymbol{F}$, its adjoint $\boldsymbol{H}$, its determinant J, the Lagrangian electric displacement field $\boldsymbol{D}_0$ and an additional spatial or Eulerian vector $\boldsymbol{d}$ computed as the product between the deformation gradient tensor and the Lagrangian electric displacement field. The resulting energy functional is called the internal energy and as presented in Reference [47], convexity of the internal energy functional with respect to the elements of the new extended set permits an extension of the concept of ellipticity [23], not only to the entire range of deformations but to any applied electric field as well.

The extended set of variables $\mathcal{V} = \{\boldsymbol{F}, \boldsymbol{H}, J, \boldsymbol{D}_0, \boldsymbol{d}\}$ enables the introduction of another new set of work conjugate variables $\Sigma_{\mathcal{V}} = \{\boldsymbol{\Sigma}_{\boldsymbol{F}}, \boldsymbol{\Sigma}_{\boldsymbol{H}}, \Sigma_J, \boldsymbol{\Sigma}_{\boldsymbol{D}_0}, \boldsymbol{\Sigma}_{\boldsymbol{d}}\}$ [48]. Convexity of the internal energy with respect to $\boldsymbol{\mathcal{V}}$ guarantees that the relationship between both sets of variables is one to one and invertible. In addition, convexity of the internal energy enables three additional energy functionals to be defined (at least implicitly) by making appropriate use of the Legendre transform[2].

From the computational standpoint, the scientific community typically resorts to a discretisation of a displacement-electric potential based variational principle via the Finite Element Method [11, 49–52]. Bustamante [14] presents alternative variational principles in which the unknown variables are displacements and the Lagrangian electric displacement field and the vector potential. Moreover, the authors in Reference [53] present a series of mixed variational principles for electro-elasticity. In our case, the new extended set of electro-kinematic variables associated to the proposed definition of multi-variable convexity, their work conjugates and the four new different types of energy functionals enable new mixed variational principles to be defined. The present manuscript presents extended Hu-Washizu type of variational principles [39, 54–56, 56–61, 61–67] which open up new interesting possibilities in terms of using various interpolation spaces for different variables, leading to enhanced type of formulations [36, 68–73]. A Finite Element implementation of these new variational principles has been presented in Reference [74].

This paper is organised as follows. Section 2 revises the fundamental concepts of large strain kinematics with the help of the tensor cross product notation re-introduced by Bonet et al. [1]. Section 3 summarises key aspects of nonlinear elasticity in the context of polyconvexity as presented by the authors in recent papers [1, 75]. Section 4 presents the extension of the concept of polyconvexity to nonlinear electro-elasticity, where the more appropriate term multi-variable convexity has been used instead. An extended set of electro-kinematic variables and its work conjugate counterpart

[2]Two partial Legendre transforms can be obtained by fixing either purely mechanical or purely electrical variables of the extended set. A total Legendre transform of the internal energy would render the third energy functional in terms of the elements of the extended set of work conjugate variables

are presented for the first time. Moreover, different energy functionals are derived via appropriate application of the Legendre transform over the convex multi-variable internal energy functional. Based on the new extended set of electro-kinematic variables and their work conjugate counterpart, Section 5 presents new interesting Hu-Washizu type of mixed variational principles. Section 6 presents simple (convexification or stabilisation) strategies which permit to create convex multi-variable electromechanical invariants by adding simple modifications to a priori non-convex ones.

A simple convex multi-variable constitutive model able to capture non-linear constitutive features inherent to Dielectric Elastomers, namely, electrostriction and electric saturation, is presented in Section 7. The material parameters of the proposed constitutive model are adjusted to reproduce the electrostrictive behaviour reported by Zhao et al [76] in DE films. Moreover, the effect of electrostriction and saturation on the behaviour of the DE films subjected to a specific experimental set up is investigated numerically. Section 8 provides some concluding remarks and a summary of the key contributions of this paper.

Three appendices have been included for the sake of completeness. Appendix A summarises the algebra associated to the tensor cross product operation [1, 75]. Appendix B expands on the developments of Section 6 including some tedious algebraic manipulations. Finally, Appendix C details the necessary steps required in order to carry out a realistic material characterisation at the origin.

2. Motion and deformation

Let us consider the motion of an electro active polymer which in its initial or material configuration is defined by a domain V of boundary ∂V with outward unit normal $\boldsymbol{N}$, which is embedded within a truncated continuum V_∞ with inner boundary ∂V (with outward unit normal $-\boldsymbol{N}$) and outer boundary $\partial_\infty V_\infty$. Let $\partial_\infty V_\infty$ be ideally located in a region infinitely far from the electro active polymer such that the deformation can be assumed to vanish. After the motion, the electro active polymer occupies a spatial configuration defined by a domain v of boundary ∂v with outward unit normal $\boldsymbol{n}$, whilst the deformed truncated continuum is defined by v_∞ with boundaries ∂v (with outward unit normal $-\boldsymbol{n}$) and $\partial_\infty v_\infty \equiv \partial_\infty V_\infty$ (refer to Figure 1).

The motion of the electro active polymer V (extended to also include that of the surrounding truncated continuum V_∞) is defined by a pseudo-time t

dependent mapping field $\boldsymbol{\phi}$ which links a material particle from material configuration $\boldsymbol{X}$ to spatial configuration $\boldsymbol{x}$ according to $\boldsymbol{x} = \boldsymbol{\phi}(\boldsymbol{X}, t)$, where displacement boundary conditions can be defined as $\boldsymbol{x} = (\boldsymbol{\phi})_{\partial_u V}$ on the boundary $\partial_u V \subset \partial V$, where the notation $(\bullet)_{\partial_u V}$ is used to indicate the *given* value of a variable $\bullet$ ion the boundary $\partial_u V$.

The two-point deformation gradient tensor or fibre-map $\boldsymbol{F}$, which relates a fibre of differential length from the material configuration $d\boldsymbol{X}$ to the spatial configuration $d\boldsymbol{x}$, namely $d\boldsymbol{x} = \boldsymbol{F} d\boldsymbol{x}$, is defined as the material gradient $\boldsymbol{\nabla}_0$ of the spatial configuration [2, 23, 28–30, 67, 77–80]

$$\boldsymbol{F} = \boldsymbol{\nabla}_0 \boldsymbol{x} = \frac{\partial \boldsymbol{\phi}(\boldsymbol{X}, t)}{\partial \boldsymbol{X}}. \tag{1}$$

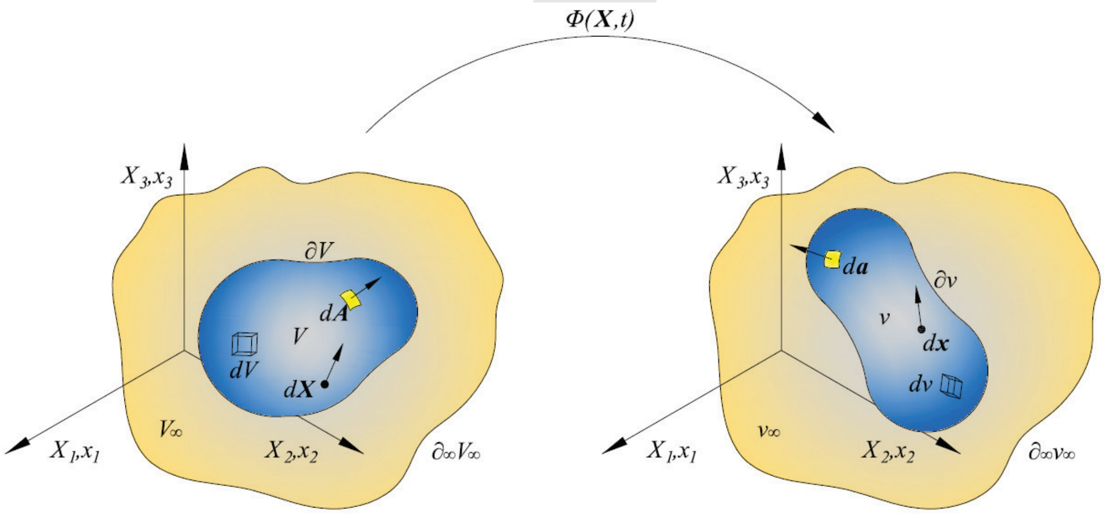

Figure 1: Electro active polymer and surrounding truncated domain in initial (undeformed) and final (deformed) configurations.

In addition, $J = \det \boldsymbol{F}$ represents the Jacobian or volume-map of the deformation, which relates differential volume elements in the material configuration dV and the spatial configuration dv as $dv = JdV$. Finally, the element area vector is mapped from initial $d\boldsymbol{A}$ (colinear with $\boldsymbol{N}$) to final $d\boldsymbol{a}$

(colinear with $\boldsymbol{n}$) configuration by means of the two-point co-factor or adjoint tensor $\boldsymbol{H}$ as $d\boldsymbol{a} = \boldsymbol{H} d\boldsymbol{A}$, which is related to the deformation gradient via the so-called Nanson's rule [67]

$$\boldsymbol{H} = J\boldsymbol{F}^{-T}. \tag{2}$$

Figure 1 depicts the deformation process as well the three kinematic maps, that is, $\boldsymbol{F}$, $\boldsymbol{H}$ and J. With the help of the definition of the tensor cross product $\times$ presented in [3], rediscovered in [1] and included in Appendix A for completeness, it is possible to re-write the area $\boldsymbol{H}$ and volume J maps in tensor and indicial notation as follows

$$\boldsymbol{H} = \frac{1}{2}\boldsymbol{F} \times \boldsymbol{F}; \qquad H_{iI} = \frac{1}{2}\mathcal{E}_{ijk}\mathcal{E}_{IJK}F_{jJ}F_{kK}; \tag{3a}$$

$$J = \frac{1}{3}\boldsymbol{H} : \boldsymbol{F}; \qquad J = \frac{1}{3}H_{iI}F_{iI}, \tag{3b}$$

where $\mathcal{E}_{ijk}$ (or $\mathcal{E}_{IJK}$) symbolises the third order alternating tensor components[3] and the use of repeated indices implies summation, unless otherwise stated.

In addition, throughout the paper, the symbol $(\cdot)$ is used to indicate the scalar product or contraction of a single index $\boldsymbol{a} \cdot \boldsymbol{b} = a_i b_i$; the symbol $(:)$ is used to indicate double contraction of two indices $\boldsymbol{A} : \boldsymbol{B} = A_{ij}B_{ij}$; the symbol $(\times)$ is used to indicate the cross product between vectors $[\boldsymbol{a} \times \boldsymbol{b}]_i = \mathcal{E}_{ijk}a_j b_k$ and the symbol $(\otimes)$ is used to indicate the outer or dyadic product $[\boldsymbol{a} \otimes \boldsymbol{b}]_{ij} = a_i b_j$.

For a smooth deformation mapping $\boldsymbol{\phi}$, it can be shown from equations (1) and (3) that the material divergence of the co-factor $\boldsymbol{H}$ as well as the material CURL of the deformation gradient $\boldsymbol{F}$ vanish, that is [81]:

$$\text{DIV}\boldsymbol{H} = \boldsymbol{0}; \qquad [\text{DIV}\boldsymbol{H}]_i = \frac{\partial H_{iI}}{\partial X_I} = 0; \tag{4a}$$

$$\text{CURL}\boldsymbol{F} = \boldsymbol{0}; \qquad [\text{CURL}\boldsymbol{F}]_{iI} = \mathcal{E}_{IJK}\frac{\partial F_{iK}}{\partial X_J} = 0. \tag{4b}$$

In general, it is possible to consider a subdivision of the domain V so that $V = \cup_{i=1}^{i=n} V_i$, with interfaces $\partial V_i \cap \partial V_j, i \neq j$. The deformation mapping $\boldsymbol{\phi}$

[3] Lower case indices $\{i, j, k\}$ will be used to represent the spatial configuration whereas capital case indices $\{I, J, K\}$ will be used to represent the material description.

is considered to be sufficiently regular in every subdomain V_i and in the surrounding truncated domain V_∞ but not necessarily smooth across interfaces. In this case, equations (4) apply to V_i and V_∞, whilst suitable boundary and jump conditions can be introduced as follows

$$\boldsymbol{\phi} = (\boldsymbol{\phi})_{\partial_u V} \qquad \text{on } \partial_u V; \tag{5a}$$
$$\boldsymbol{\phi} = \mathbf{0} \qquad \text{on } \partial_\infty V_\infty; \tag{5b}$$
$$[\![\boldsymbol{\phi}]\!] = \mathbf{0} \qquad \text{on } (\partial V_i \cap \partial V_j) \cup \partial V; \tag{5c}$$
$$\boldsymbol{F} \times \boldsymbol{N} = (\boldsymbol{F} \times \boldsymbol{N})_{\partial_u V} \qquad \text{on } \partial_u V; \tag{5d}$$
$$[\![\boldsymbol{F}]\!] \times \boldsymbol{N}|_{\partial V_i} = \mathbf{0} \qquad \text{on } (\partial V_i \cap \partial V_j) \cup \partial V; \tag{5e}$$
$$\boldsymbol{H}\boldsymbol{N} = (\boldsymbol{H}\boldsymbol{N})_{\partial_u V} \qquad \text{on } \partial_u V; \tag{5f}$$
$$[\![\boldsymbol{H}]\!]\, \boldsymbol{N}|_{\partial V_i} = \mathbf{0} \qquad \text{on } (\partial V_i \cap \partial V_j) \cup \partial V, \tag{5g}$$

where $[\![\varphi]\!] = (\varphi^i - \varphi^j)$ denotes the jump of a variable φ across an interface $\partial V_i \cap \partial V_j$ with associated unit outward normal $\boldsymbol{N}|_{\partial V_i}$.

Let us define $\delta\boldsymbol{u}$ and $\boldsymbol{u}$ as virtual and incremental variations of $\boldsymbol{x}$, respectively, where it will be assumed that $\delta\boldsymbol{u}$ and $\boldsymbol{u}$ satisfy compatible homogeneous displacement based boundary conditions that vanishes on $\partial_u V$ and $\partial_\infty V_\infty$. Following the notation of [67] and making use of the tensor cross product $\times$ introduced above, the first and second directional derivatives of the co-factor $\boldsymbol{H}$ with respect to virtual and incremental variations of the geometry are easily evaluated as

$$D\boldsymbol{H}\,[\delta\boldsymbol{u}] = \boldsymbol{F} \times D\boldsymbol{F}\,[\delta\boldsymbol{u}] = \boldsymbol{F} \times \boldsymbol{\nabla}_0 \delta\boldsymbol{u}; \tag{6a}$$
$$D^2\boldsymbol{H}\,[\delta\boldsymbol{u}; \boldsymbol{u}] = D\boldsymbol{F}\,[\boldsymbol{u}] \times D\boldsymbol{F}\,[\delta\boldsymbol{u}] = \boldsymbol{\nabla}_0 \delta\boldsymbol{u} \times \boldsymbol{\nabla}_0 \boldsymbol{u}. \tag{6b}$$

Similarly, the directional derivatives of the Jacobian J with respect to virtual and incremental variations of the geometry can be obtained as

$$DJ\,[\delta\boldsymbol{u}] = \boldsymbol{H} : \boldsymbol{\nabla}_0 \delta\boldsymbol{u}; \tag{7a}$$
$$D^2 J\,[\delta\boldsymbol{u}; \boldsymbol{u}] = \boldsymbol{F} : (\boldsymbol{\nabla}_0 \delta\boldsymbol{u} \times \boldsymbol{\nabla}_0 \boldsymbol{u}). \tag{7b}$$

A stated in [1], the directional derivatives (6)-(7) are greatly simplified when using the new tensor cross product $\times$ [4].

[4] As an example and for comparison purposes, the classical way [67] to compute expression (6a) results in the cumbersome expression $D\boldsymbol{H}\,[\delta\boldsymbol{u}] = \left(J\boldsymbol{F}^{-T} : \boldsymbol{\nabla}_0 \delta\boldsymbol{u}\right) \boldsymbol{F}^{-T} - J\boldsymbol{F}^{-T} (\boldsymbol{\nabla}_0 \delta\boldsymbol{u})^T \boldsymbol{F}^{-T}$.

3. Equilibrium and constitutive law in nonlinear continuum mechanics

In this section, the translational and rotational equilibrium equations are presented. Moreover, the internal energy and the concept of polyconvexity in the context of nonlinear elasticity (electric effects are not considered in this section) are also introduced.

3.1. Translational and rotational equilibrium

Let us assume that the domain defined by the electro active polymer is subjected to a body force per unit of undeformed volume $\boldsymbol{f}_0$ and a traction force per unit of undeformed area $\boldsymbol{t}_0$ applied on $\partial_t V \subset \partial V$, such that $\partial_t V \cup \partial_u V = \partial V$ and $\partial_t V \cap \partial_u V = \emptyset$. The global conservation of linear momentum leads to the integral translational equilibrium equations as [67, 80]

$$\int_{\partial_t V} \boldsymbol{t}_0 dA + \int_V \boldsymbol{f}_0 dV = \boldsymbol{0}. \tag{8}$$

From above equation (8), the local (strong form) translational equilibrium equations and the associated boundary and jump conditions can be expressed as

$$\begin{aligned} \text{DIV}\boldsymbol{P} + \boldsymbol{f}_0 &= \boldsymbol{0} && \text{in } V_i,\ i = 1 \dots n; && \text{(9a)} \\ \boldsymbol{P}\boldsymbol{N} &= \boldsymbol{t}_0 && \text{on } \partial_t V; && \text{(9b)} \\ [\![\boldsymbol{P}]\!]\, \boldsymbol{N}|_{\partial V_i} &= \boldsymbol{0} && \text{on } \partial V_i \cap \partial V_j. && \text{(9c)} \end{aligned}$$

where $\boldsymbol{P}$ represents the first Piola-Kirchoff two-point stress tensor. Furthermore, satisfaction of rotational equilibrium leads to the well-known tensor condition $\boldsymbol{P}\boldsymbol{F}^T = \boldsymbol{F}\boldsymbol{P}^T$.

3.2. The internal energy density: polyconvex elasticity

For the closure of the system of equations defined by (5) and (9), an additional constitutive law is needed relating deformation and stresses in both the continuum and the surrounding medium. In the case of reversible elasticity, where thermal effects and any other possible state variables (i.e. accumulated plastic deformation) are disregarded, the internal energy density e per unit of undeformed volume can be solely defined in terms of the deformation, namely $e = e(\boldsymbol{\nabla}_0 \boldsymbol{x})$. In this case, combination of (9) and the first law of thermodynamics yields

$$De[\delta \boldsymbol{u}] = \boldsymbol{P} : \boldsymbol{\nabla}_0 \delta \boldsymbol{u}; \qquad \boldsymbol{P} = \left. \frac{\partial e(\boldsymbol{F})}{\partial \boldsymbol{F}} \right|_{\boldsymbol{F}=\boldsymbol{\nabla}_0 \boldsymbol{x}}. \tag{10}$$

The concept of polyconvexity was introduced by Ball [2, 28, 30] in order to establish sufficient conditions for the existence of solutions in nonlinear elasticity. It is recognised these days [1, 23, 29, 39] that polyconvexity is a useful mathematical requirement that can be used to ensure the well-posedness of the equations in the large strain regime. Moreover, polyconvexity implies ellipticity (or rank-one convexity) [31], guaranteeing the existence of real wave speeds [1, 2, 23, 28–30, 34, 81]. Essentially, the internal energy density e must be a function of the deformation gradient $\boldsymbol{\nabla}_0 \boldsymbol{x}$ via a convex multi-variable density functional W as

$$e\left(\boldsymbol{\nabla}_0 \boldsymbol{x}\right) = W\left(\boldsymbol{F}, \boldsymbol{H}, J\right), \tag{11}$$

where W is convex with respect to its 19 variables, namely, J and the 3×3 components of $\boldsymbol{F}$ and $\boldsymbol{H}$. In addition, the requirement for objectivity or material frame indifference (i.e. invariance with respect to rotations in the material configuration) implies that W must be independent of the rotational components of $\boldsymbol{F}$ and $\boldsymbol{H}$ and hence a function of these tensors via symmetric tensors such as the right Cauchy-Green strain tensor $\boldsymbol{C} = \boldsymbol{F}^T \boldsymbol{F}$ or $\boldsymbol{G} = \boldsymbol{H}^T \boldsymbol{H}$[5].

3.3. Conjugate stresses, the first Piola-Kirchhoff and Cauchy stress tensors

The fibre, area and volume mappings $\boldsymbol{F}$, $\boldsymbol{H}$ and J, respectively, have work conjugate stresses $\boldsymbol{\Sigma}_{\boldsymbol{F}}$, $\boldsymbol{\Sigma}_{\boldsymbol{H}}$ and Σ_J defined by [1]:

$$\boldsymbol{\Sigma}_{\boldsymbol{F}} = \frac{\partial W}{\partial \boldsymbol{F}}; \qquad \boldsymbol{\Sigma}_{\boldsymbol{H}} = \frac{\partial W}{\partial \boldsymbol{H}}; \qquad \Sigma_J = \frac{\partial W}{\partial J}. \tag{12}$$

For notational convenience, the following sets to be used in subsequent sections are defined

$$\mathcal{V}^m = \{\boldsymbol{F}, \boldsymbol{H}, J\}; \qquad \Sigma^m_{\mathcal{V}} = \{\boldsymbol{\Sigma}_{\boldsymbol{F}}, \boldsymbol{\Sigma}_{\boldsymbol{H}}, \Sigma_J\}, \tag{13}$$

[5]Notice that using equation (3), it is easy to show that $\boldsymbol{G}$ is related to the right Cauchy-Green strain tensor $\boldsymbol{C}$ as $\boldsymbol{G} = J^2 \boldsymbol{C}^{-1} = \frac{1}{2} \boldsymbol{C} \times \boldsymbol{C}$.

where the superscript m denotes the mechanical set of variables, that will be extended later with electric components. By using equation (12), it is therefore possible to evaluate the directional derivative of the internal energy density e as:

$$\begin{aligned} De[\delta\boldsymbol{u}] &= DW[D\boldsymbol{F}[\delta\boldsymbol{u}], D\boldsymbol{H}[\delta\boldsymbol{u}], DJ[\delta\boldsymbol{u}]] \\ &= \boldsymbol{\Sigma_F} : D\boldsymbol{F}[\delta\boldsymbol{u}] + \boldsymbol{\Sigma_H} : D\boldsymbol{H}[\delta\boldsymbol{u}] + \Sigma_J DJ[\delta\boldsymbol{u}] \\ &= \boldsymbol{\Sigma_F} : \boldsymbol{\nabla}_0\delta\boldsymbol{u} + \boldsymbol{\Sigma_H} : (\boldsymbol{F} \times \boldsymbol{\nabla}_0\delta\boldsymbol{u}) + \Sigma_J(\boldsymbol{H} : \boldsymbol{\nabla}_0\delta\boldsymbol{u}) \\ &= (\boldsymbol{\Sigma_F} + \boldsymbol{\Sigma_H} \times \boldsymbol{F} + \Sigma_J\boldsymbol{H}) : \boldsymbol{\nabla}_0\delta\boldsymbol{u}. \end{aligned} \tag{14}$$

Comparison of (10) with above equation (14), leads to the evaluation of the first Piola-Kirchhoff tensor as

$$\boldsymbol{P} = \boldsymbol{\Sigma_F} + \boldsymbol{\Sigma_H} \times \boldsymbol{F} + \Sigma_J\boldsymbol{H}. \tag{15}$$

In addition to the first Piola-Kirchhoff stress, it is necessary to derive expressions for the Cauchy $\boldsymbol{\sigma}$ and Kirchhoff $\boldsymbol{\tau}$ stress tensors, as often these stresses are needed in order to display solution results at a post-processing stage (e.g. visualisation). Such expressions can be derived from the standard push forward relationship between these tensors [67], namely $J\boldsymbol{\sigma} = \boldsymbol{\tau} = \boldsymbol{P}\boldsymbol{F}^T$. Following a similar procedure to that presented in [1, 81], an expression for the Kirchhoff stress tensor emerges as

$$J\boldsymbol{\sigma} = \boldsymbol{\tau} = \boldsymbol{\tau_F} + \boldsymbol{\tau_H} \times \boldsymbol{I} + \tau_J\boldsymbol{I}. \tag{16}$$

where $\boldsymbol{I}$ denotes the second order identity tensor and with

$$\boldsymbol{\tau_F} = \boldsymbol{\Sigma_F}\boldsymbol{F}^T; \qquad \boldsymbol{\tau_H} = \boldsymbol{\Sigma_H}\boldsymbol{H}^T; \qquad \tau_J = J\Sigma_J. \tag{17}$$

3.4. Tangent elasticity operator

With a Newton-Raphson type of solution process in mind, it is useful to derive the tangent elasticity operator. This is typically evaluated in terms of a fourth order tangent elasticity tensor $\boldsymbol{\mathcal{C}}$ defined by

$$D^2e[\delta\boldsymbol{u};\boldsymbol{u}] = \boldsymbol{\nabla}_0\delta\boldsymbol{u} : D\boldsymbol{P}[\boldsymbol{u}] = \boldsymbol{\nabla}_0\delta\boldsymbol{u} : \boldsymbol{\mathcal{C}} : \boldsymbol{\nabla}_0\boldsymbol{u}, \tag{18}$$

where

$$\boldsymbol{\mathcal{C}} := \left.\frac{\partial\boldsymbol{P}}{\partial\boldsymbol{F}}\right|_{\boldsymbol{F}=\boldsymbol{\nabla}_0\boldsymbol{x}} = \left.\frac{\partial^2 e(\boldsymbol{F})}{\partial\boldsymbol{F}\partial\boldsymbol{F}}\right|_{\boldsymbol{F}=\boldsymbol{\nabla}_0\boldsymbol{x}}. \tag{19}$$

Using equation (15) for the first Piola-Kirchhoff tensor and following a chain rule derivation similar to that in equation (14) (refer to [1]), a more physically insightful representation of the tangent elasticity operator (18) is

$$D^2 e\,[\delta \boldsymbol{u}; \boldsymbol{u}] = \left[\mathbb{S}_\delta\right]^T [\mathbb{H}_W] \left[\mathbb{S}_\Delta\right] + (\boldsymbol{\Sigma}_{\boldsymbol{H}} + \Sigma_J \boldsymbol{F}) : (\boldsymbol{\nabla}_0 \delta \boldsymbol{u} \times \boldsymbol{\nabla}_0 \boldsymbol{u})\,, \tag{20}$$

where

$$\left[\mathbb{S}_\delta\right]^T = \left[(\boldsymbol{\nabla}_0 \delta \boldsymbol{u}) : \quad (\boldsymbol{\nabla}_0 \delta \boldsymbol{u} \times \boldsymbol{F}) : \quad (\boldsymbol{\nabla}_0 \delta \boldsymbol{u} : \boldsymbol{H})\right];\ \left[\mathbb{S}_\Delta\right] = \begin{bmatrix} : (\boldsymbol{\nabla}_0 \boldsymbol{u}) \\ : (\boldsymbol{F} \times \boldsymbol{\nabla}_0 \boldsymbol{u}) \\ (\boldsymbol{H} : \boldsymbol{\nabla}_0 \boldsymbol{u}) \end{bmatrix}, \tag{21}$$

and with the Hessian operator $[\mathbb{H}_W]$ denoting the symmetric positive definite operator containing the second derivatives of $W(\boldsymbol{F}, \boldsymbol{H}, J)$ as

$$[\mathbb{H}_W] = \begin{bmatrix} W_{\boldsymbol{FF}} & W_{\boldsymbol{FH}} & W_{\boldsymbol{F}J} \\ W_{\boldsymbol{HF}} & W_{\boldsymbol{HH}} & W_{\boldsymbol{H}J} \\ W_{J\boldsymbol{F}} & W_{J\boldsymbol{H}} & W_{JJ} \end{bmatrix}, \tag{22}$$

where $W_{\boldsymbol{AB}} = \frac{\partial^2 W}{\partial \boldsymbol{A} \partial \boldsymbol{B}}$. As discussed in [1], polyconvexity dictates that the first (constitutive) term on the right hand side of equation (20) is necessarily positive for a virtual field $\delta \boldsymbol{u}$ satisfying $\delta \boldsymbol{u} = \boldsymbol{u}$ and thus, buckling can only be induced by the second (geometrical) term. As presented in reference [75], the alternative representation of the tangent operator in equation (20) enables to easily see the relationship between polyconvexity and ellipticity (rank-one convexity).

3.5. Material characterisation in the reference configuration

As an example, one of the simplest isotropic polyconvex energy functionals is that representing a compressible Mooney-Rivlin material, which can be described as

$$W_{MR}(\boldsymbol{F}, \boldsymbol{H}, J) = \alpha II_{\boldsymbol{F}} + \beta II_{\boldsymbol{H}} + f(J)\,; \quad II_{\boldsymbol{F}} = \boldsymbol{F} : \boldsymbol{F}; \quad II_{\boldsymbol{H}} = \boldsymbol{H} : \boldsymbol{H}; \tag{23}$$

where α and β are positive material parameters and f denotes a convex function of J and $II_{(\bullet)}$ denotes the squared of the L_2 norm of the entity $(\bullet)$.

For the Mooney-Rivlin energy functional in (23), the first Piola-Kirchhoff stress tensor becomes (refer to equation (15)):

$$\boldsymbol{P} = 2\alpha\boldsymbol{F} + 2\beta\boldsymbol{H} \times \boldsymbol{F} + f'(J)\,\boldsymbol{H}. \tag{24}$$

For this particular constitutive model, the Hessian operator $[\mathbb{H}_W]$ (22) contained in the tangent operator of the internal energy defined in (20) becomes

$$[\mathbb{H}_W] = \begin{bmatrix} 2\alpha\boldsymbol{\mathcal{I}} & \boldsymbol{0} & \boldsymbol{0} \\ \boldsymbol{0} & 2\beta\boldsymbol{\mathcal{I}} & \boldsymbol{0} \\ \boldsymbol{0} & \boldsymbol{0} & f''(J) \end{bmatrix}, \tag{25}$$

where $\boldsymbol{\mathcal{I}}$ denotes the identity fourth order tensor, defined as $\mathcal{I}_{iIjJ} = \delta_{ij}\delta_{IJ}$. It is interesting to observe the positive definite nature of the above Hessian operator provided that the constants α and β are positive and that the function $f(J)$ is convex. Appropriate values for α and β and suitable functions $f(J)$ must be such that, at the initial configuration, the stress vanishes. Moreover, the typical linear elasticity relation between stresses and strains through the classical forth order linear elasticity tensor in terms of the Lamé coefficients λ and μ must be recovered [1]. Material characterisation in the reference configuration (obtention of α and β in terms of λ and μ) of a simple isotropic Mooney-Rivlin model with strain energy as that of equation (23) has been described in Bonet et al. [1].

Remark 1. The case $\beta = 0$ gives the simpler compressible Neo-Hookean model W_{NH}, which is convex in $\boldsymbol{F}$ and J alone without the need to introduce $\boldsymbol{H}$ as a separate independent variable or its conjugate stress $\boldsymbol{\Sigma_H}$.

---

4. Nonlinear continuum electromechanics

4.1. Governing equations in nonlinear electromechanics

In this section, the entire set of governing equations in nonlinear electromechanics is presented. First, the Faraday and Gauss laws are introduced in a global and local manner. Then, the translational and rotational equilibrium equations are revisited. Moreover, the internal energy and the concept of multi-variable convexity (notice that in the context pure elasticity in Section 3.2 the term polyconvexity was used instead) in the context of nonlinear electromechanics are introduced in this section.

4.1.1. Faraday and Gauss laws

Maxwell's equations, when neglecting time dependent effects and in the absence of magnetic fields and electric currents, can be used to describe the behaviour of electrostatic fields. Let us recall the electro active polymer introduced in Section 2 surrounded by a medium which, without loss of generality in the present manuscript, will be the vacuum or free space. Moreover, let ρ_0^e denote an applied electric charge per unit of undeformed volume. The electric charge per unit of undeformed volume V_∞ is typically neglected in the particular case in which V_∞ corresponds to the vacuum. Let ω_0^e be an electric charge per unit of undeformed area applied on $\partial_\omega V \subset \partial V$. The integral version of the Gauss law can be written in a Lagrangian format as

$$\int_{\partial_\omega V} \omega_0^e \, dA + \int_V \rho_0^e \, dV = 0. \tag{26}$$

The local version of equation (26) and the associated boundary and jump conditions can be written as

$$\begin{aligned}
\text{DIV}\boldsymbol{D}_0 &= \rho_0 && \text{in } V_i, \; i = 1 \dots n; && (27a)\\
\text{DIV}\boldsymbol{D}_0 &= 0 && \text{in } V_\infty; && (27b)\\
[\![\boldsymbol{D}_0]\!] \cdot \boldsymbol{N} &= \omega_0 && \text{on } \partial_\omega V; && (27c)\\
[\![\boldsymbol{D}_0]\!] \cdot \boldsymbol{N} &= 0 && \text{on } \partial_\varphi V; && (27d)\\
[\![\boldsymbol{D}_0]\!] \cdot \boldsymbol{N}|_{\partial V_i} &= 0 && \text{on } \partial V_i \cap \partial V_j && (27e)
\end{aligned}$$

where $\boldsymbol{D}_0$ is the Lagrangian electric displacement field [12, 13]. Notice that equations (27a) and (27b) represent the local Gauss law in the dielectric and the vacuum, respectively. In addition, in the case of equations (27c)-(27d), the term $[\![\boldsymbol{D}_0]\!]$ represents the jump of electric displacement between the domain defined by the dielectric V and the surrounding vacuum V_∞. Equations (27) could alternatively be presented in a spatial description in terms of the Eulerian electric displacement $\boldsymbol{D}$ field[6], which is related to its

[6]Note that the computation of the Eulerian electric displacement $\boldsymbol{D}$ is also important at a post-processing stage when computing or visualising final results.

Lagrangian counterpart $\boldsymbol{D}_0$ through the standard Piola (area) transformation as $\boldsymbol{D}_0 = \boldsymbol{H}^T\boldsymbol{D}$ [12, 13].

Analogously, the integral version of the static Faraday law can be written in a Lagrangian format for a closed curve $\mathcal{C}$ embedded in $V \cup \partial V$ as

$$\oint_{\mathcal{C}} \boldsymbol{E}_0 \cdot d\boldsymbol{X} = 0, \tag{28}$$

where $\boldsymbol{E}_0$ is the Lagrangian electric field vector. The local version of equation (28) and the associated boundary and jump conditions can be expressed as

$$\begin{aligned}
\boldsymbol{E}_0 &= -\boldsymbol{\nabla}_0\varphi && \text{in } V_i,\; i = 1\ldots n; && \text{(29a)}\\
\boldsymbol{E}_0 &= -\boldsymbol{\nabla}_0\varphi && \text{in } V_\infty; && \text{(29b)}\\
\varphi &= (\varphi)_{\partial_\varphi V} && \text{on } \partial_\varphi V; && \text{(29c)}\\
\varphi &= 0 && \text{on } \partial_\infty V_\infty; && \text{(29d)}\\
[\![\boldsymbol{E}_0]\!] \times \boldsymbol{N} &= \boldsymbol{0} && \text{on } \partial_\omega V; && \text{(29e)}\\
[\![\boldsymbol{E}_0]\!] \times \boldsymbol{N}|_{\partial V_i} &= \boldsymbol{0} && \text{on } \partial V_i \cap \partial V_j, && \text{(29f)}
\end{aligned}$$

where φ is an electric potential field that can be introduced in the case of a contractible domain[7]. Typically, the origin of electric potential field is defined on $\partial_\infty V_\infty$. This is mathematically stated in equation (29d). In equation (29c), $\partial_\varphi V \subset \partial V$ represents the part of the boundary subjected to electric potential boundary conditions, such that $\partial_\omega V \cup \partial_\varphi V = \partial V$ and $\partial_\omega V \cap \partial_\varphi V = \emptyset$. As above equations (27), equations (29) could alternatively be presented in a spatial description in terms of the Eulerian electric field $\boldsymbol{E}$, which is related to its Lagrangian counterpart $\boldsymbol{E}_0$ through the standard fibre transformation $\boldsymbol{E}_0 = \boldsymbol{F}^T\boldsymbol{E}$ [12, 13].

4.1.2. Translational and rotational equilibrium

The existence of an electric field leads to a modification of the translational equilibrium equations of the dielectric to account for the presence of coupled electromechanical stresses and vacuum effects. Specifically, this leads to the modification of the local form of translational equilibrium and

[7]Alternatively, equation (29a) could be replaced by the more general condition $\text{CURL}\boldsymbol{E}_0 = \boldsymbol{0}$ and equation (29c) by $\boldsymbol{E}_0 \times \boldsymbol{N} = (\boldsymbol{E}_0 \times \boldsymbol{N})_{\partial_\varphi V}$.

its associated boundary and jump conditions in (9) as

$$\mathrm{DIV}\boldsymbol{P} + \boldsymbol{f}_0 = \boldsymbol{0} \qquad \text{in } V_i,\ i = 1\ldots n; \tag{30a}$$
$$\mathrm{DIV}\boldsymbol{P} = \boldsymbol{0} \qquad \text{in } V_\infty; \tag{30b}$$
$$[\![\boldsymbol{P}]\!]\boldsymbol{N} = \boldsymbol{t}_0 \qquad \text{on } \partial_t V; \tag{30c}$$
$$[\![\boldsymbol{P}]\!]\boldsymbol{N} = \boldsymbol{0} \qquad \text{on } \partial_u V; \tag{30d}$$
$$[\![\boldsymbol{P}]\!]\, \boldsymbol{N}|_{\partial V_i} = \boldsymbol{0} \qquad \text{on } \partial V_i \cap \partial V_j. \tag{30e}$$

In this case, the stress tensor $\boldsymbol{P}$ includes both deformation and electrical components. As pointed out in [14], as there are no experiments that can separate the mechanical from the electrical contributions in $\boldsymbol{P}$, it is preferred to work with the overall coupled stress tensor and not with its individual (deformation and electrical) components.

Notice that equations (30a) and (30b) represent the local translational equilibrium in the dielectric and the vacuum, respectively. Moreover, in the case of equations (30c)-(30d), $[\![\boldsymbol{P}]\!]$ represents the jump in the first Piola-Kirchhoff stress tensor between that of the domain defined by the dielectric V and that of the surrounding vacuum, the latter known as Maxwell stress tensor [14, 19, 50]. Once again, satisfaction of rotational equilibrium leads to the condition $\boldsymbol{P}\boldsymbol{F}^T = \boldsymbol{F}\boldsymbol{P}^T$ imposed on the coupled electromechanical stress tensor [12], and not on its individual deformation and electrical contributions.

Remark 2. When the surrounding truncated medium corresponds to vacuum, a distribution of stress (typically known as the Maxwell stress) due to the surrounding electric field arises. The Maxwell stress is divergence free and hence, we can conclude that $\boldsymbol{f}_0 = \boldsymbol{0}$ in V_∞, which is stated in equation (30b).

4.2. The internal energy in nonlinear electro-elasticity: multi-variable convexity

For the closure of the system of equations defined by (5), (27), (29), (30) and (34), an additional constitutive law is needed relating deformation and electric displacement with stresses and electric field in the domain defined by the dielectric. In the case of reversible electro-elasticity, where thermal effects and any other possible state variables (i.e. accumulated plastic deformation or electrical relaxation) are disregarded, the internal energy density e per unit of undeformed volume can be defined in terms of the deformation and the electric displacement, namely $e = e(\boldsymbol{\nabla}_0\boldsymbol{x}, \boldsymbol{D}_0)$. In addition, let us consider $\delta\boldsymbol{D}_0$ and $\Delta\boldsymbol{D}_0$ to denote virtual and incremental variations of $\boldsymbol{D}_0$, respectively, satisfying compatible homogeneous electric displacement based boundary conditions on $\partial_\omega V$. In this case, combination of (27) and (30) and the first law of thermodynamics yields

$$De[\delta\boldsymbol{u}, \delta\boldsymbol{D}_0] = \boldsymbol{P} : \boldsymbol{\nabla}_0\delta\boldsymbol{u} + \boldsymbol{E}_0 \cdot \delta\boldsymbol{D}_0, \tag{31}$$

or alternatively,

$$\boldsymbol{P} = \left.\frac{\partial e(\boldsymbol{F}, \boldsymbol{D}_0)}{\partial \boldsymbol{F}}\right|_{\boldsymbol{F}=\boldsymbol{\nabla}_0\boldsymbol{x}}; \qquad \boldsymbol{E}_0 = \left.\frac{\partial e(\boldsymbol{F}, \boldsymbol{D}_0)}{\partial \boldsymbol{D_0}}\right|_{\boldsymbol{F}=\boldsymbol{\nabla}_0\boldsymbol{x}}. \tag{32}$$

As an example, the internal energy functional of a very popular material is that of an ideal isotropic dielectric elastomer, which is defined based on the additive decomposition of a purely mechanical component $e_m(\boldsymbol{\nabla}_0\boldsymbol{x})$ and an electromechanical component which is proportional to the internal energy of the vacuum e_0, namely

$$\begin{aligned} e_{\text{ideal}}(\boldsymbol{\nabla}_0\boldsymbol{x}, \boldsymbol{D}_0) &= e_m(\boldsymbol{\nabla}_0\boldsymbol{x}) + \frac{1}{\varepsilon_r} e_0(\boldsymbol{\nabla}_0\boldsymbol{x}, \boldsymbol{D}_0); \\ e_0(\boldsymbol{\nabla}_0\boldsymbol{x}, \boldsymbol{D}_0) &= \frac{1}{2\varepsilon_0 J} II_{\boldsymbol{d}}; \qquad \boldsymbol{d} = \boldsymbol{F}\boldsymbol{D}_0 = J\boldsymbol{D}; \qquad II_{\boldsymbol{d}} = \boldsymbol{d} \cdot \boldsymbol{d}; \end{aligned} \tag{33}$$

where ε_r is a dimensionless constant representing the relative permittivity of the dielectric and ε_0, the electric permittivity of the vacuum, with $\varepsilon_0 \approx 8.854 \times 10^{-12} A^2 s^4 kg^{-1} m^{-3}$. For the particular case of the vacuum, equation (32) enables to obtain the Maxwell stress tensor and the relationship between the electric field and the electric displacement field based on the internal energy $W_0(\boldsymbol{x}, \boldsymbol{D}_0)$ defined in equation (33) as

$$\begin{aligned} \boldsymbol{P} &= \frac{1}{\varepsilon_0 J} \boldsymbol{d} \otimes \boldsymbol{D}_0 - \frac{1}{2\varepsilon_0 J^2} II_{\boldsymbol{d}} \boldsymbol{H} \qquad &\text{in } V_\infty; \\ \boldsymbol{E}_0 &= \frac{1}{\varepsilon_0 J} \boldsymbol{F}^T \boldsymbol{d} \qquad &\text{in } V_\infty. \end{aligned} \tag{34}$$

These expressions can be pushed forward to the Eulerian configuration using the standard Piola transformation $\boldsymbol{\sigma} = J^{-1}\boldsymbol{P}\boldsymbol{F}^T$ and $\boldsymbol{E} = \boldsymbol{F}^{-T}\boldsymbol{E}_0$ to give after simple algebra the Cauchy stress tensor in the vacuum and the corresponding electric field as

$$\begin{aligned} \boldsymbol{\sigma} &= \frac{1}{\varepsilon_0}\boldsymbol{D}\otimes\boldsymbol{D} - \frac{1}{2\varepsilon_0} II_{\boldsymbol{D}}\boldsymbol{I} && \text{in } V_\infty; \\ \boldsymbol{E} &= \frac{1}{\varepsilon_0}\boldsymbol{D} && \text{in } V_\infty. \end{aligned} \tag{35}$$

In this paper, a generalisation of expression (11) for the internal energy density functional e including electromechanical contributions is postulated as[8]

$$e\left(\boldsymbol{\nabla}_0\boldsymbol{x}, \boldsymbol{D}_0\right) = W\left(\boldsymbol{F}, \boldsymbol{H}, J, \boldsymbol{D}_0, \boldsymbol{d}\right), \tag{37}$$

where W represents a convex multi-variable functional in terms of its extended set of arguments $\mathcal{V} = \{\boldsymbol{F}, \boldsymbol{H}, J, \boldsymbol{D}_0, \boldsymbol{d}\}$ and with $\boldsymbol{d}$ defined in equation (33). Objectivity or material frame indifference implies that $W(\boldsymbol{F}, \boldsymbol{H}, J, \boldsymbol{D}_0, \boldsymbol{F}\boldsymbol{D}_0)$ must be independent of the rotational components of $\boldsymbol{F}$ and $\boldsymbol{H}$ via symmetric tensors such as the right Cauchy-Green strain tensor $\boldsymbol{C} = \boldsymbol{F}^T\boldsymbol{F}$ or $\boldsymbol{G} = \boldsymbol{H}^T\boldsymbol{H}$.

Remark 3. It would be tempting to postulate W as a convex function of $\{\boldsymbol{F}, \boldsymbol{H}, J, \boldsymbol{D}_0\}$ [21], excluding the vector $\boldsymbol{d}$. However, it is easy to show that this leads to a non-convex representation of the energy function describing the vacuum (33) and hence, that for a ideal dielectric elastomer. In other words, as the invariant $\boldsymbol{F}\boldsymbol{D}_0 \cdot \boldsymbol{F}\boldsymbol{D}_0$ is not convex with respect to arguments $\{\boldsymbol{F}, \boldsymbol{D}_0\}$, this would preclude its use in the sense of material stability. However, as this invariant is convex with respect to $\boldsymbol{d}$, its use can still be incorporated into our framework, hence including the electro-mechanical energy of both vacuum and ideal dielectric elastomers as a valid degenerate case of our formulation.

---

[8] Note that extension of the definition of multi-variable convexity in equation (37) to electro-magneto-elasticity is simply obtained through a definition of the internal energy as

$$e\left(\boldsymbol{\nabla}_0\boldsymbol{x}, \boldsymbol{D}_0, \boldsymbol{B}_0\right) = W\left(\boldsymbol{F}, \boldsymbol{H}, J, \boldsymbol{D}_0, \boldsymbol{B}_0, \boldsymbol{d}, \boldsymbol{b}\right); \quad \boldsymbol{d} = \boldsymbol{F}\boldsymbol{D}_0 = J\boldsymbol{D}; \quad \boldsymbol{b} = \boldsymbol{F}\boldsymbol{B}_0 = J\boldsymbol{B}, \tag{36}$$

where W represents a convex multi-variable functional in terms of its extended set of arguments, namely $\{\boldsymbol{F}, \boldsymbol{H}, J, \boldsymbol{D}_0, \boldsymbol{B}_0, \boldsymbol{d}, \boldsymbol{b}\}$ and $\boldsymbol{B}$, the spatial counterpart of $\boldsymbol{B}_0$, defined through the classical area transformation $\boldsymbol{B}_0 = \boldsymbol{H}^T\boldsymbol{B}$.

4.3. Work conjugate variables

The definition of multi-variable convexity in equation (37) enables the introduction of a set of work conjugate variables $\Sigma_{\mathcal{V}} = \{\boldsymbol{\Sigma}_{\boldsymbol{F}}, \boldsymbol{\Sigma}_{\boldsymbol{H}}, \Sigma_J, \boldsymbol{\Sigma}_{\boldsymbol{D}_0}, \boldsymbol{\Sigma}_{\boldsymbol{d}}\}$ to those in the set $\mathcal{V}$ defined as

$$\boldsymbol{\Sigma}_{\boldsymbol{F}} = \frac{\partial W}{\partial \boldsymbol{F}}; \quad \boldsymbol{\Sigma}_{\boldsymbol{H}} = \frac{\partial W}{\partial \boldsymbol{H}}; \quad \Sigma_J = \frac{\partial W}{\partial J}; \quad \boldsymbol{\Sigma}_{\boldsymbol{D}_0} = \frac{\partial W}{\partial \boldsymbol{D}_0}; \quad \boldsymbol{\Sigma}_{\boldsymbol{d}} = \frac{\partial W}{\partial \boldsymbol{d}}. \tag{38}$$

For notational convenience, in addition to the sets $\mathcal{V}^m$ and $\Sigma_{\mathcal{V}}^m$ defined in equation (13), two new sets which contain the electrical variables, namely $\mathcal{V}^e$ and $\Sigma_{\mathcal{V}}^e$, used in subsequent sections are defined as,

$$\mathcal{V}^e = \{\boldsymbol{D}_0, \boldsymbol{d}\}; \qquad \Sigma_{\mathcal{V}}^e = \{\boldsymbol{\Sigma}_{\boldsymbol{D}_0}, \boldsymbol{\Sigma}_{\boldsymbol{d}}\}. \tag{39}$$

Following a similar procedure to that of equation (14), the directional derivative of the internal energy e with respect to virtual changes in the geometry is obtained as

$$\begin{aligned} De\,[\delta\boldsymbol{u}] &= DW\,[D\boldsymbol{F}\,[\delta\boldsymbol{u}]\,, D\boldsymbol{H}\,[\delta\boldsymbol{u}]\,, DJ\,[\delta\boldsymbol{u}]\,, D\boldsymbol{d}\,[\delta\boldsymbol{u}]] \\ &= \boldsymbol{\Sigma}_{\boldsymbol{F}} : D\boldsymbol{F}\,[\delta\boldsymbol{u}] + \boldsymbol{\Sigma}_{\boldsymbol{H}} : D\boldsymbol{H}\,[\delta\boldsymbol{u}] + \Sigma_J DJ\,[\delta\boldsymbol{u}] + \boldsymbol{\Sigma}_{\boldsymbol{d}} \cdot D\boldsymbol{d}\,[\delta\boldsymbol{u}] \\ &= \boldsymbol{\Sigma}_{\boldsymbol{F}} : \boldsymbol{\nabla}_0\delta\boldsymbol{u} + \boldsymbol{\Sigma}_{\boldsymbol{H}} : (\boldsymbol{F} \times \boldsymbol{\nabla}_0\delta\boldsymbol{u}) + \Sigma_J\,(\boldsymbol{H} : \boldsymbol{\nabla}_0\delta\boldsymbol{u}) + (\boldsymbol{\Sigma}_{\boldsymbol{d}} \otimes \boldsymbol{D}_0) : \boldsymbol{\nabla}_0\delta\boldsymbol{u} \\ &= (\boldsymbol{\Sigma}_{\boldsymbol{F}} + \boldsymbol{\Sigma}_{\boldsymbol{H}} \times \boldsymbol{F} + \Sigma_J\boldsymbol{H} + \boldsymbol{\Sigma}_{\boldsymbol{d}} \otimes \boldsymbol{D}_0) : \boldsymbol{\nabla}_0\delta\boldsymbol{u}, \end{aligned} \tag{40}$$

where the relationship $D\boldsymbol{d}[\delta\boldsymbol{u}] = (\boldsymbol{\nabla}_0\delta\boldsymbol{u})\boldsymbol{D}_0$ emanating from the relationship $\boldsymbol{d} = \boldsymbol{F}\boldsymbol{D}_0$ has been used. Similarly, the first directional derivative of the internal energy with respect to virtual variations of the electric displacement field is obtained as

$$\begin{aligned} De\,[\delta\boldsymbol{D}_0] &= DW\,[\delta\boldsymbol{D}_0, \boldsymbol{F}\delta\boldsymbol{D}_0] = \boldsymbol{\Sigma}_{\boldsymbol{D}_0} \cdot \delta\boldsymbol{D}_0 + \boldsymbol{\Sigma}_{\boldsymbol{d}} \cdot \boldsymbol{F}\delta\boldsymbol{D}_0 \\ &= \left(\boldsymbol{\Sigma}_{\boldsymbol{D}_0} + \boldsymbol{F}^T\boldsymbol{\Sigma}_{\boldsymbol{d}}\right) \cdot \delta\boldsymbol{D}_0. \end{aligned} \tag{41}$$

Comparison of equations (40) and (41) against (31), enables the first Piola-Kirchhoff stress tensor and the material electric displacement field to be expressed in terms of the elements of both sets $\mathcal{V}$ and $\Sigma_{\mathcal{V}}$ as

$$\boldsymbol{P} = \boldsymbol{\Sigma}_{\boldsymbol{F}} + \boldsymbol{\Sigma}_{\boldsymbol{H}} \times \boldsymbol{F} + \Sigma_J\boldsymbol{H} + \boldsymbol{\Sigma}_{\boldsymbol{d}} \otimes \boldsymbol{D}_0; \quad \boldsymbol{E}_0 = \boldsymbol{\Sigma}_{\boldsymbol{D}_0} + \boldsymbol{F}^T\boldsymbol{\Sigma}_{\boldsymbol{d}}. \tag{42}$$

An expression for the Kirchhoff stress tensor [1] and the spatial electric field emerges based upon the relations $\boldsymbol{\tau} = \boldsymbol{P}\boldsymbol{F}^T$ and $\boldsymbol{E} = \boldsymbol{F}^{-T}\boldsymbol{E}_0$ as

$$\begin{aligned} \boldsymbol{\tau} &= \boldsymbol{\Sigma}_{\boldsymbol{F}}\boldsymbol{F}^T + \left(\boldsymbol{\Sigma}_{\boldsymbol{H}}\boldsymbol{H}^T\right) \times \boldsymbol{I} + J\Sigma_J\boldsymbol{I} + \boldsymbol{\Sigma}_{\boldsymbol{d}} \otimes \boldsymbol{d}; \\ \boldsymbol{E} &= \boldsymbol{F}^{-T}\left(\boldsymbol{\Sigma}_{\boldsymbol{D}_0} + \boldsymbol{F}^T\boldsymbol{\Sigma}_{\boldsymbol{d}}\right) = \boldsymbol{F}^{-T}\boldsymbol{\Sigma}_{\boldsymbol{D}_0} + \boldsymbol{\Sigma}_{\boldsymbol{d}}. \end{aligned} \tag{43}$$

4.4. Tangent electromechanics operator for the internal energy

With a Newton-Raphson type of solution process in mind, the internal energy $e = e(\boldsymbol{\nabla}_0\boldsymbol{x}, \boldsymbol{D}_0)$ can be further linearised leading to a tangent operator defined as follows

$$D^2e\,[\delta\boldsymbol{u}, \delta\boldsymbol{D}_0; \boldsymbol{u}, \Delta\boldsymbol{D}_0] = \begin{bmatrix} \boldsymbol{\nabla}_0\delta\boldsymbol{u} : & \delta\boldsymbol{D}_0\cdot \end{bmatrix} \begin{bmatrix} \boldsymbol{\mathcal{C}} & \boldsymbol{\mathcal{Q}}^T \\ \boldsymbol{\mathcal{Q}} & \boldsymbol{\theta} \end{bmatrix} \begin{bmatrix} :\boldsymbol{\nabla}_0\boldsymbol{u} \\ \Delta\boldsymbol{D}_0 \end{bmatrix}, \quad (44)$$

with the fourth order tensor $\boldsymbol{\mathcal{C}}$, the third order tensor $\boldsymbol{\mathcal{Q}}$ and the second order tensor $\boldsymbol{\theta}$ defined as

$$\boldsymbol{\mathcal{C}} = \left.\frac{\partial^2 e(\boldsymbol{F}, \boldsymbol{D}_0)}{\partial\boldsymbol{F}\partial\boldsymbol{F}}\right|_{\boldsymbol{F}=\boldsymbol{\nabla}_0\boldsymbol{x}}; \; \boldsymbol{\mathcal{Q}} = \left.\frac{\partial^2 e(\boldsymbol{F}, \boldsymbol{D}_0)}{\partial\boldsymbol{D}_0\partial\boldsymbol{F}}\right|_{\boldsymbol{F}=\boldsymbol{\nabla}_0\boldsymbol{x}}; \; \boldsymbol{\theta} = \left.\frac{\partial^2 e(\boldsymbol{F}, \boldsymbol{D}_0)}{\partial\boldsymbol{D}_0\partial\boldsymbol{D}_0}\right|_{\boldsymbol{F}=\boldsymbol{\nabla}_0\boldsymbol{x}}. \quad (45)$$

Following a similar procedure to that presented in Section 3.4, with the additional relationships $D^2\boldsymbol{d}[\delta\boldsymbol{u}, \Delta\boldsymbol{D}_0] = (\boldsymbol{\nabla}_0\delta\boldsymbol{u})\Delta\boldsymbol{D}_0$ and $D^2\boldsymbol{d}[\delta\boldsymbol{D}_0, \boldsymbol{u}] = (\boldsymbol{\nabla}_0\boldsymbol{u})\delta\boldsymbol{D}_0$, a more physically insightful representation of the tangent operator (44) is

$$\begin{aligned} D^2e\,[\delta\boldsymbol{u}, \delta\boldsymbol{D}_0; \boldsymbol{u}, \Delta\boldsymbol{D}_0] &= [\mathbb{S}_\delta]^T\,[\mathbb{H}_W]\,[\mathbb{S}_\Delta] + (\boldsymbol{\Sigma}_{\boldsymbol{H}} + \Sigma_J\boldsymbol{F}) : (\boldsymbol{\nabla}_0\delta\boldsymbol{u} \times \boldsymbol{\nabla}_0\boldsymbol{u}) \\ &\quad + \boldsymbol{\Sigma}_{\boldsymbol{d}} \cdot ((\boldsymbol{\nabla}_0\delta\boldsymbol{u})\Delta\boldsymbol{D}_0 + (\boldsymbol{\nabla}_0\boldsymbol{u})\delta\boldsymbol{D}_0)\,, \end{aligned} \quad (46)$$

where

$$[\mathbb{S}_\delta]^T = \begin{bmatrix} (\boldsymbol{\nabla}_0\delta\boldsymbol{u}) : & (\boldsymbol{\nabla}_0\delta\boldsymbol{u} \times \boldsymbol{F}) : & (\boldsymbol{\nabla}_0\delta\boldsymbol{u} : \boldsymbol{H}) & \delta\boldsymbol{D}_0\cdot & ((\boldsymbol{\nabla}_0\delta\boldsymbol{u})\boldsymbol{D}_0 + \boldsymbol{F}\delta\boldsymbol{D}_0)\cdot \end{bmatrix};$$
$$[\mathbb{S}_\Delta] = \begin{bmatrix} :(\boldsymbol{\nabla}_0\boldsymbol{u}) \\ :(\boldsymbol{F} \times \boldsymbol{\nabla}_0\boldsymbol{u}) \\ (\boldsymbol{H} : \boldsymbol{\nabla}_0\boldsymbol{u}) \\ \Delta\boldsymbol{D}_0 \\ (\boldsymbol{\nabla}_0\boldsymbol{u})\boldsymbol{D}_0 + \boldsymbol{F}\Delta\boldsymbol{D}_0 \end{bmatrix}, \quad (47)$$

and with the extended Hessian operator $[\mathbb{H}_W]$ denoting the symmetric positive definite operator containing the second derivatives of $W(\boldsymbol{F}, \boldsymbol{H}, J, \boldsymbol{D}_0, \boldsymbol{d})$

as

$$[\mathbb{H}_W] = \begin{bmatrix} W_{\boldsymbol{FF}} & W_{\boldsymbol{FH}} & W_{\boldsymbol{F}J} & W_{\boldsymbol{FD}_0} & W_{\boldsymbol{Fd}} \\ W_{\boldsymbol{HF}} & W_{\boldsymbol{HH}} & W_{\boldsymbol{H}J} & W_{\boldsymbol{HD}_0} & W_{\boldsymbol{Hd}} \\ W_{J\boldsymbol{F}} & W_{J\boldsymbol{H}} & W_{JJ} & W_{J\boldsymbol{D}_0} & W_{J\boldsymbol{d}} \\ W_{\boldsymbol{D}_0\boldsymbol{F}} & W_{\boldsymbol{D}_0\boldsymbol{H}} & W_{\boldsymbol{D}_0 J} & W_{\boldsymbol{D}_0\boldsymbol{D}_0} & W_{\boldsymbol{D}_0\boldsymbol{d}} \\ W_{\boldsymbol{dF}} & W_{\boldsymbol{dH}} & W_{\boldsymbol{d}J} & W_{\boldsymbol{dD}_0} & W_{\boldsymbol{dd}} \end{bmatrix}. \tag{48}$$

It is important to emphasise that this additive decomposition of the tangent operator is not merely technical but, extremely useful, as the multi-physics of the problem is completely captured in the first term on the right hand side of equation (46), whilst geometrically nonlinear terms are collected on the second and third terms.

Multi-variable convexity dictates that the first term on the right hand side of equation (46) is necessarily positive for virtual fields $\{\delta\boldsymbol{u}, \delta\boldsymbol{D}_0\}$ satisfying $\{\delta\boldsymbol{u} = \boldsymbol{u}, \delta\boldsymbol{D}_0 = \Delta\boldsymbol{D}_0\}$ and thus, buckling can only be induced by the second and third (geometrically-based) terms.

Remark 4. Equation (46) makes it possible to highlight the relationship between multi-variable convexity and ellipticity in the case of electromechanics. Taking rank-one equal virtual and incremental displacement gradient tensors $\boldsymbol{\nabla}_0\delta\boldsymbol{u} = \boldsymbol{\nabla}_0\boldsymbol{u} = \boldsymbol{v}\otimes\boldsymbol{V}$ and $\Delta\boldsymbol{D}_0 = \delta\boldsymbol{D}_0 = \boldsymbol{V}_\perp$ (where $\boldsymbol{V}_\perp$ represents any orthogonal vector to $\boldsymbol{V}$) [47] in equation (46) makes the initial stress term vanish since,

$$\begin{aligned} &\boldsymbol{\nabla}_0\delta\boldsymbol{u}\times\boldsymbol{\nabla}_0\boldsymbol{u} = (\boldsymbol{v}\otimes\boldsymbol{V})\times(\boldsymbol{v}\otimes\boldsymbol{V}) = (\boldsymbol{v}\times\boldsymbol{v})\otimes(\boldsymbol{V}\times\boldsymbol{V}) = \boldsymbol{0};\\ &\boldsymbol{\Sigma}_{\boldsymbol{d}}\cdot((\boldsymbol{\nabla}_0\delta\boldsymbol{u})\Delta\boldsymbol{D}_0 + (\boldsymbol{\nabla}_0\boldsymbol{u})\delta\boldsymbol{D}_0) = 2\,(\boldsymbol{v}\cdot\boldsymbol{\Sigma}_{\boldsymbol{d}})\,(\boldsymbol{V}\cdot\boldsymbol{V}_\perp) = 0. \end{aligned} \tag{49}$$

This leaves only the contribution from the first positive definite term in equation (46), leading to (refer to equation (44)),

$$\begin{bmatrix} \boldsymbol{u}\otimes\boldsymbol{V} : & \boldsymbol{V}_\perp\cdot \end{bmatrix} \begin{bmatrix} \boldsymbol{\mathcal{C}} & \boldsymbol{\mathcal{Q}}^T \\ \boldsymbol{\mathcal{Q}} & \boldsymbol{\theta} \end{bmatrix} \begin{bmatrix} :\boldsymbol{u}\otimes\boldsymbol{V} \\ \boldsymbol{V}_\perp \end{bmatrix} > 0. \tag{50}$$

Equation (50) is a generalisation of the concept of ellipticity to the case of electromechanics[9].

[9]In the context of elasticity, ellipticity is equivalent to rank-one convexity and requires

---

4.5. A simple convex multi-variable electromechanical constitutive model

As an example, a simple internal energy functional which complies with the definition of multi-variable convexity in (37) can be defined as

$$W_1 = \mu_1 II_{\boldsymbol{F}} + \mu_2 II_{\boldsymbol{H}} + f(J) + \frac{1}{2\varepsilon_1 J} II_{\boldsymbol{d}} + \frac{1}{2\varepsilon_2} II_{\boldsymbol{D}_0}, \tag{51}$$

where a possible definition of the function $f(J)$ in equation (51) could be

$$f(J) = -2(\mu_1 + 2\mu_2) \ln J + \frac{\kappa}{2}(J-1)^2. \tag{52}$$

The work conjugates in (38) for the internal energy functional in (51) are obtained as

$$\boldsymbol{\Sigma}_{\boldsymbol{F}} = 2\mu_1 \boldsymbol{F}; \quad \boldsymbol{\Sigma}_{\boldsymbol{H}} = 2\mu_2 \boldsymbol{H}; \quad \Sigma_J = f'(J) - \frac{1}{2\varepsilon_1 J^2} II_{\boldsymbol{d}}; \quad \boldsymbol{\Sigma}_{\boldsymbol{D}_0} = \frac{1}{\varepsilon_2}\boldsymbol{D}_0; \quad \boldsymbol{\Sigma}_{\boldsymbol{d}} = \frac{1}{\varepsilon_1 J}\boldsymbol{d}. \tag{53}$$

For the particular constitutive model defined in equation (51), the first Piola-Kirchhoff stress tensor and the material electric field are obtained according to equation (42) as

$$\begin{aligned} \boldsymbol{P} &= 2\mu_1 \boldsymbol{F} + 2\mu_2 \boldsymbol{H} \times \boldsymbol{F} + \left(f'(J) - \frac{1}{2\varepsilon_1 J^2} II_{\boldsymbol{d}}\right)\boldsymbol{H} + \frac{1}{\varepsilon_1}\boldsymbol{d} \otimes \boldsymbol{D}_0; \\ \boldsymbol{E}_0 &= \frac{1}{\varepsilon_2}\boldsymbol{D}_0 + \frac{1}{\varepsilon_1 J}\boldsymbol{F}^T \boldsymbol{d}. \end{aligned} \tag{54}$$

Substitution of the relationship $\boldsymbol{d} = \boldsymbol{F}\boldsymbol{D}_0$ enables the last equation to be re-written as

$$\boldsymbol{E}_0 = \left(\frac{1}{\varepsilon_2}\boldsymbol{I} + \frac{1}{\varepsilon_1}\boldsymbol{C}\right)\boldsymbol{D}_0, \tag{55}$$

where $\boldsymbol{C}$ is the right Cauchy-Green deformation tensor defined above. For the particular constitutive model defined in equation (51), the Hessian operator

---

that the double contraction of the elasticity tensor by an arbitrary rank-one tensor $\boldsymbol{v} \otimes \boldsymbol{V}$ should be positive.

becomes:

$$[\mathbb{H}_W] = \begin{bmatrix} 2\mu_1\boldsymbol{\mathcal{I}} & \boldsymbol{0} & \boldsymbol{0} & \boldsymbol{0} & \boldsymbol{0} \\ \boldsymbol{0} & 2\mu_2\boldsymbol{\mathcal{I}} & \boldsymbol{0} & \boldsymbol{0} & \boldsymbol{0} \\ \boldsymbol{0} & \boldsymbol{0} & f''(J) + \frac{1}{\varepsilon_1 J^3} II_{\boldsymbol{d}} & \boldsymbol{0} & -\frac{1}{\varepsilon_1 J^2}\boldsymbol{d} \\ \boldsymbol{0} & \boldsymbol{0} & \boldsymbol{0} & \frac{1}{\varepsilon_2}\boldsymbol{I} & \boldsymbol{0} \\ \boldsymbol{0} & \boldsymbol{0} & -\frac{1}{\varepsilon_1 J^2}\boldsymbol{d} & \boldsymbol{0} & \frac{1}{\varepsilon_1 J}\boldsymbol{I} \end{bmatrix}. \tag{56}$$

It is interesting to observe the positive definite nature of the above Hessian operator provided that the constants μ_1, μ_2, ε_1 and ε_2 are positive and that the function $f(J)$ is convex.

Remark 5. Similarly to Remark 1 in the case of nonlinear elasticity, the degenerate case $\varepsilon_2 = \infty$ results in the ideal dielectric model in equation (33), which is convex in $\{\boldsymbol{F}, \boldsymbol{H}, J, \boldsymbol{d}\}$ alone without the need to introduce $\boldsymbol{D}_0$ as a separate independent variable. Moreover, for $\mu_1 = \mu_2 = 0$ and $f(J) = 0$, the energy of the vacuum is retrieved, which is convex in the reduced set $\{J, \boldsymbol{d}\}$.

It is important to emphasise that the energy of an ideal dielectric (vacuum) cannot be expressed as a convex multi-variable function of $\{\boldsymbol{F}, \boldsymbol{H}, J, \boldsymbol{D}_0\}$ ($\{J, \boldsymbol{D}_0\}$). That is the reason behind the definition of the extended set $\mathcal{V}$ including the spatial vector $\boldsymbol{d}$ among its variables. Crucially, this enables to consider the vacuum as a degenerate case of the formulation presented in this paper.

4.6. Alternative energy density functionals

Multi-variable convexity of the internal energy guarantees that the relationship between both sets of variables $\mathcal{V}$ and $\Sigma_{\mathcal{V}}$ is one to one and invertible. This enables the definition of alternative energy functionals established via appropriate Legendre transforms applied to the internal energy $W(\mathcal{V})$ as

$$\Upsilon\left(\Sigma_{\mathcal{V}}\right) = \sup_{\mathcal{V}} \left\{T^m + T^e - W\left(\mathcal{V}\right)\right\}; \tag{57a}$$

$$\Psi\left(\Sigma_{\mathcal{V}}^m, \mathcal{V}^e\right) = \sup_{\mathcal{V}^m} \left\{T^m - W\left(\mathcal{V}\right)\right\}; \tag{57b}$$

$$\Phi\left(\mathcal{V}^m, \Sigma_{\mathcal{V}}^e\right) = -\sup_{\mathcal{V}^e} \left\{T^e - W\left(\mathcal{V}\right)\right\}, \tag{57c}$$

with the sets $\mathcal{V}^m$, $\mathcal{V}^e$, $\Sigma_{\mathcal{V}}^m$ and $\Sigma_{\mathcal{V}}^e$ defined in equations (13) and (39) and with

$$T^m = \boldsymbol{\Sigma}_{\boldsymbol{F}} : \boldsymbol{F} + \boldsymbol{\Sigma}_{\boldsymbol{H}} : \boldsymbol{H} + \Sigma_J J; \qquad T^e = \boldsymbol{\Sigma}_{\boldsymbol{D_0}} \cdot \boldsymbol{D}_0 + \boldsymbol{\Sigma}_{\boldsymbol{d}} \cdot \boldsymbol{d}. \tag{58}$$

In equation (57), $\Upsilon(\Sigma_{\mathcal{V}})$ represents an extended Gibbs' energy density, $\Psi(\Sigma_{\mathcal{V}}^m, \mathcal{V}^e)$, an extended enthalpy energy density and $\Phi(\mathcal{V}, \Sigma_{\mathcal{V}}^e)$, an extended Helmholtz's energy density[10]. Expressions relating strain, stress and electric fields, in terms of the different energy densities, follow naturally as

$$\boldsymbol{F} = \frac{\partial \Upsilon}{\partial \boldsymbol{\Sigma}_{\boldsymbol{F}}}; \quad \boldsymbol{H} = \frac{\partial \Upsilon}{\partial \boldsymbol{\Sigma}_{\boldsymbol{H}}}; \quad J = \frac{\partial \Upsilon}{\partial \Sigma_J}; \quad \boldsymbol{D}_0 = \frac{\partial \Upsilon}{\partial \boldsymbol{\Sigma}_{\boldsymbol{D}_0}}; \quad \boldsymbol{d} = \frac{\partial \Upsilon}{\partial \boldsymbol{\Sigma}_{\boldsymbol{d}}}; \tag{59a}$$

$$\boldsymbol{F} = \frac{\partial \Psi}{\partial \boldsymbol{\Sigma}_{\boldsymbol{F}}}; \quad \boldsymbol{H} = \frac{\partial \Psi}{\partial \boldsymbol{\Sigma}_{\boldsymbol{H}}}; \quad J = \frac{\partial \Psi}{\partial \Sigma_J}; \quad \boldsymbol{\Sigma}_{\boldsymbol{D}_0} = -\frac{\partial \Psi}{\partial \boldsymbol{D}_0}; \quad \boldsymbol{\Sigma}_{\boldsymbol{d}} = -\frac{\partial \Psi}{\partial \boldsymbol{d}}; \tag{59b}$$

$$\boldsymbol{\Sigma}_{\boldsymbol{F}} = \frac{\partial \Phi}{\partial \boldsymbol{F}}; \quad \boldsymbol{\Sigma}_{\boldsymbol{H}} = \frac{\partial \Phi}{\partial \boldsymbol{H}}; \quad \Sigma_J = \frac{\partial \Phi}{\partial J}; \quad \boldsymbol{D}_0 = -\frac{\partial \Phi}{\partial \boldsymbol{\Sigma}_{\boldsymbol{D}_0}}; \quad \boldsymbol{d} = -\frac{\partial \Phi}{\partial \boldsymbol{\Sigma}_{\boldsymbol{d}}}. \tag{59c}$$

[10]The terminology adopted here matches that of classical Thermodynamics, where the electric displacement (electric field) plays the same role as the entropy (temperature) of the system.

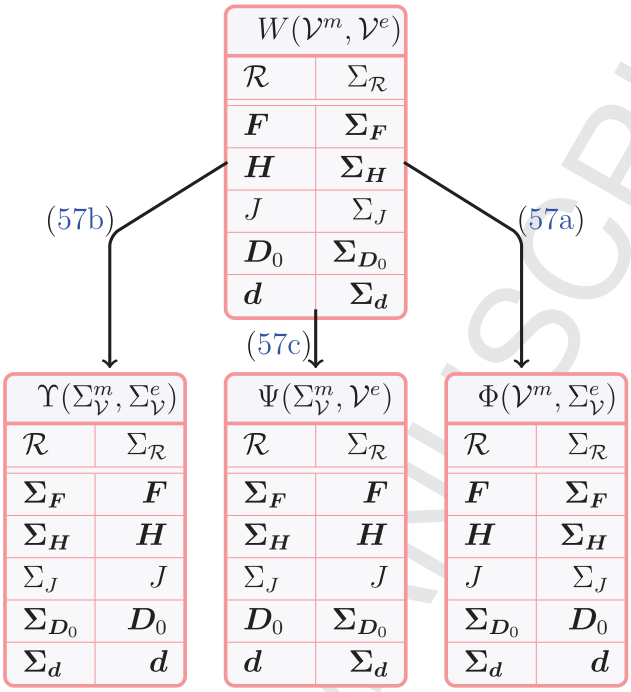

Figure 2: The arguments ($\mathcal{R}$) of the internal $W(\mathcal{V})$ (37), Gibbs's $\Upsilon(\Sigma_{\mathcal{V}})$ (57a), Enthalpy $\Psi(\Sigma_{\mathcal{V}}^m, \mathcal{V}^e)$ (57b) and Helmtholz's $\Phi(\mathcal{V}^m, \Sigma_{\mathcal{V}}^e)$ (57c) energy functionals and their respective set of work conjugates ($\Sigma_{\mathcal{R}}$). Relation between $W(\mathcal{V})$ and the remaining energy functionals according to the Legendre transforms defined in equation (57).

Figure 2 summarises the set of arguments (denoted as $\mathcal{R}$) for the different extended energy functionals defined, namely the internal, Gibbs's, Enthalpy and Helmtholz's energy functionals and their respective set of work conjugates (denoted as $\Sigma_{\mathcal{R}}$).

Remark 6. Notice that the definition of multi-variable convexity in (37) ensures a one to one relationship between the pairs $\{\boldsymbol{D}_0, \boldsymbol{d}\}$ and $\{\boldsymbol{\Sigma}_{\boldsymbol{D}_0}, \boldsymbol{\Sigma}_{\boldsymbol{d}}\}$, respectively. Moreover, consideration of the definition of the spatial vector $\boldsymbol{d} = \boldsymbol{\nabla}_0 \boldsymbol{x} \boldsymbol{D}_0$ and the definition of the material electric field $-\boldsymbol{\nabla}_0\varphi$ in terms of the work conjugates $\{\boldsymbol{\Sigma}_{\boldsymbol{D}_0}, \boldsymbol{\Sigma}_{\boldsymbol{d}}\}$ in (42), results in turn in a one to one relationship between the variables $\boldsymbol{D}_0$ and $-\boldsymbol{\nabla}_0\varphi$.

In this case, it is possible to define an alternative energy functional to $e = e(\boldsymbol{\nabla}_0\boldsymbol{x}, \boldsymbol{D}_0)$ by making use of the Legendre transform. This might be a computationally convenient approach in the case of pursuing a standard semi-discrete variational implementation via the Finite Element Method, where the scalar electric potential is preferred as an unknown over the electric displacement field vector. For instance, the Helmholtz's energy density $\mathit{\Phi} = \mathit{\Phi}(\boldsymbol{\nabla}_0\boldsymbol{x}, -\boldsymbol{\nabla}_0\varphi)$ can be defined as[11]

$$\mathit{\Phi}\left(\boldsymbol{\nabla}_0\boldsymbol{x}, -\boldsymbol{\nabla}_0\varphi\right) = -\sup_{\boldsymbol{D}_0}\left\{-\boldsymbol{\nabla}_0\varphi\cdot\boldsymbol{D}_0 - e\left(\boldsymbol{\nabla}_0\boldsymbol{x}, \boldsymbol{D}_0\right)\right\}, \tag{60}$$

leading to an alternative definition to that of (32) for the stress and electric fields as

$$\boldsymbol{P} = \left.\frac{\partial\mathit{\Phi}(\boldsymbol{F}, \boldsymbol{E}_0)}{\partial\boldsymbol{F}}\right|_{\substack{\boldsymbol{F}=\boldsymbol{\nabla}_0\boldsymbol{x}\\ \boldsymbol{E}_0=-\boldsymbol{\nabla}_0\varphi}}; \qquad \boldsymbol{D}_0 = -\left.\frac{\partial\mathit{\Phi}(\boldsymbol{F}, \boldsymbol{E}_0)}{\partial\boldsymbol{E}_0}\right|_{\substack{\boldsymbol{F}=\boldsymbol{\nabla}_0\boldsymbol{x}\\ \boldsymbol{E}_0=-\boldsymbol{\nabla}_0\varphi}}. \tag{61}$$

---

5. Variational formulations

This section presents several possible variational principles in nonlinear electro-elasticity. Initially, a revision of the standard displacement and electric potential based variational principle [14, 49] is presented for completeness. Exploiting the convex multi-variable properties of the internal energy $e(\boldsymbol{\nabla}_0\boldsymbol{x}, \boldsymbol{D}_0)$, new interesting mixed variational principles in terms of the extended energy functionals $W(\mathcal{V})$ (37), $\Phi(\mathcal{V}^m, \Sigma^e_{\mathcal{V}})$ (57c), $\Psi(\Sigma^m_{\mathcal{V}}, \mathcal{V}^e)$ (57b) and $\Upsilon(\Sigma_{\mathcal{V}})$ (57a) emerge. In particular, two new mixed variational principles based upon the extended energy functionals $\Phi(\mathcal{V}^m, \Sigma^e_{\mathcal{V}})$ (57c) and $W(\mathcal{V})$ (37) are presented in Sections 5.3 and 5.2 respectively, for the first time in the context of nonlinear electro-elasticity.

These new mixed variational principles belong to the general class of Franjs-de-Veubeke-Hu-Washizu (FdVHW) type variational principles, which were developed with the purpose of enhancing the numerical solution obtained though Finite Element based variational principles. Finite element implementation of the two mixed variational principles presented has been carried out in Reference [74].

[11] Alternatively, an equivalent definition of the Legendre transform in equation (60) can be defined as $\mathit{\Phi}\left(\boldsymbol{\nabla}_0\boldsymbol{x}, -\boldsymbol{\nabla}_0\varphi\right) = \inf_{\boldsymbol{D}_0}\left\{\boldsymbol{\nabla}_0\varphi\cdot\boldsymbol{D}_0 + e\left(\boldsymbol{\nabla}_0\boldsymbol{x}, \boldsymbol{D}_0\right)\right\}$

5.1. Standard displacement and electric potential based variational principle

A first variational principle can be established by the total energy minimisation defined in terms of the internal energy of the system $e(\boldsymbol{\nabla}_0\boldsymbol{x}, \boldsymbol{D}_0)$. The principle applies to the space occupied by both the electro active polymer and the surrounding truncated domain, namely $V \cup V_\infty$, as [14]

$$\hat{\Pi}_e(\boldsymbol{x}^*, \boldsymbol{D}_0^*) = \inf_{\boldsymbol{x}, \boldsymbol{D}_0} \left\{ \int_{V \cup V_\infty} e(\boldsymbol{\nabla}_0\boldsymbol{x}, \boldsymbol{D}_0) dV - \Pi_{ext}^m(\boldsymbol{x}) \right\}; \\ \text{s.t.} \begin{cases} \textbf{DIV}\boldsymbol{D}_0 = \rho_0^e & \text{in } V \cup V_\infty \\ [\![\boldsymbol{D}_0]\!] \cdot \boldsymbol{N} = \omega_0^e & \text{on } \partial_\omega V \end{cases}; \tag{62}$$

where $\{\boldsymbol{x}^*, \boldsymbol{D}_0^*\}$ denotes the exact solution and

$$\Pi_{ext}^m(\boldsymbol{x}) = \int_V \boldsymbol{f}_0 \cdot \boldsymbol{x} dV + \int_{\partial_t V} \boldsymbol{t}_0 \cdot \boldsymbol{x} dA, \tag{63}$$

represents the total external work due to the action of external mechanical forces. Using a standard Lagrange multiplier approach to enforce the constraints defined by the Gauss' law, a new variational principle defined by a new energy potential $\Pi_e(\boldsymbol{x}^*, \varphi^*, \boldsymbol{D}_0^*)$ emerges as

$$\Pi_e(\boldsymbol{x}^*, \varphi^*, \boldsymbol{D}_0^*) = \inf_{\boldsymbol{x}, \boldsymbol{D}_0} \sup_{\varphi} \left\{ \int_{V \cup V_\infty} e(\boldsymbol{\nabla}_0\boldsymbol{x}, \boldsymbol{D}_0) dV - \Pi_{ext}^m(\boldsymbol{x}) \right. \\ \left. + \int_{V \cup V_\infty} \varphi \left(\rho_0^e - \textbf{DIV}\boldsymbol{D}_0\right) dV + \int_{\partial_\omega V} \varphi \left(\omega_0^e - [\![\boldsymbol{D}_0]\!] \cdot \boldsymbol{N}\right) dA \right\}, \tag{64}$$

where the electric potential φ acts as the Lagrange multiplier needed to enforce the constraints. Application of the Gauss divergence theorem to above equation (64) yields an alternative representation of the variational principle as

$$\Pi_e(\boldsymbol{x}^*, \varphi^*, \boldsymbol{D}_0^*) = \inf_{\boldsymbol{x}, \boldsymbol{D}_0} \sup_{\varphi} \left\{ \int_{V \cup V_\infty} e(\boldsymbol{\nabla}_0\boldsymbol{x}, \boldsymbol{D}_0) dV + \int_{V \cup V_\infty} \boldsymbol{\nabla}_0\varphi \cdot \boldsymbol{D}_0 dV - \Pi_{ext}(\boldsymbol{x}, \varphi) \right\}, \tag{65}$$

with

$$\Pi_{ext}(\boldsymbol{x},\varphi) = \Pi^m_{ext}(\boldsymbol{x}) + \Pi^e_{ext}(\varphi); \qquad \Pi^e_{ext}(\varphi) = -\int_V \rho^e_0 \varphi dV - \int_{\partial_\omega V} \omega^e_0 \varphi dA, \tag{66}$$

where a new external work contribution, that is $\Pi^e_{ext}(\varphi)$, appears due to electrical effects. Provided that a one to one relationship between $\boldsymbol{D}_0$ and $-\boldsymbol{\nabla}_0\varphi$ exists (refer to Remark 5), application of the Legendre transform (60) enables above variational principle (65) to be reformulated as

$$\Pi_{\Phi}(\boldsymbol{x}^*,\varphi^*) = \inf_{\boldsymbol{x}} \sup_{\varphi} \left\{ \int_{V\cup V_\infty} \Phi(\boldsymbol{\nabla}_0\boldsymbol{x}, -\boldsymbol{\nabla}_0\varphi) dV - \Pi_{ext}(\boldsymbol{x},\varphi) \right\}. \tag{67}$$

Traditional Finite Element based implementations resort to this variational principle, where the geometry and the electrical potential are the only unknowns of the problem [49, 50]. The stationary condition of this functional with respect to changes in the geometry leads to the principle of virtual work (or power), written as

$$D\Pi_{\Phi}[\delta\boldsymbol{u}] = \int_{V\cup V_\infty} \boldsymbol{P}_{\boldsymbol{x}} : \boldsymbol{\nabla}_0\delta\boldsymbol{u} dV - D\Pi_{ext}[\delta\boldsymbol{v}], \tag{68}$$

where the term $\boldsymbol{P}_{\boldsymbol{x}}$ represents the first Piola-Kirchhoff stress tensor evaluated in the standard fashion (15) in terms of the gradient of the geometry and the electric potential, namely, by using $\{\boldsymbol{F}_{\boldsymbol{x}}, \boldsymbol{H}_{\boldsymbol{x}}, J_{\boldsymbol{x}}, -\boldsymbol{\nabla}_0\varphi\}$, where

$$\boldsymbol{F}_{\boldsymbol{x}} = \boldsymbol{\nabla}_0\boldsymbol{x}; \qquad \boldsymbol{H}_{\boldsymbol{x}} = \frac{1}{2}\boldsymbol{\nabla}_0\boldsymbol{x} \times \boldsymbol{\nabla}_0\boldsymbol{x}; \qquad J_{\boldsymbol{x}} = \det \boldsymbol{\nabla}_0\boldsymbol{x}. \tag{69}$$

Explicitly, the computation can be carried out from equation $(61)_a$. Analogously, the stationary point with respect to changes in the electric potential leads to the variational statement for the Gauss' law as

$$D\Pi_{\Phi}[\delta\varphi] = \int_{V\cup V_\infty} \boldsymbol{D}_{0,\varphi} \cdot \boldsymbol{\nabla}_0\delta\varphi dV - D\Pi_{ext}[\delta\varphi], \tag{70}$$

where the term $\boldsymbol{D}_{0,\varphi}$ represents the electric displacement evaluated from $(61)_b$ by using $\{\boldsymbol{F}_{\boldsymbol{x}}, \boldsymbol{H}_{\boldsymbol{x}}, J_{\boldsymbol{x}}, -\boldsymbol{\nabla}_0\varphi\}$.

5.2. A new mixed variational principle in terms of the extended internal energy functional W

In the case of an electromechanical convex multi-variable energy functional, an equivalent representation of the total variational principle Π_e in equation (65) is

$$\Pi_e(\boldsymbol{x}^*, \varphi^*, \boldsymbol{D}_0^*) = \inf_{\boldsymbol{x},\boldsymbol{D}_0} \sup_{\varphi} \left\{ \int_{V\cup V_\infty} W(\mathcal{V})\, dV + \int_{V\cup V_\infty} \boldsymbol{D}_0 \cdot \boldsymbol{\nabla}_0\varphi \, dV - \Pi_{ext}(\boldsymbol{x},\varphi) \right\};$$
$$\text{s.t. } \left\{ \boldsymbol{F} = \boldsymbol{F}_{\boldsymbol{x}}; \quad \boldsymbol{H} = \boldsymbol{H}_{\boldsymbol{x}}; \quad J = J_{\boldsymbol{x}}; \quad \boldsymbol{d} = \boldsymbol{F}_x \boldsymbol{D}_0 \quad \text{in } V \cup V_\infty \right. \tag{71}$$

Using a standard Lagrange multiplier approach to enforce the compatibility constraints in (71) yields a new variational principle which can be represented as

$$\begin{aligned}
&\Pi_W(\boldsymbol{x}^*, \boldsymbol{F}^*, \boldsymbol{H}^*, J^*, \boldsymbol{\Sigma}_{\boldsymbol{F}}^*, \boldsymbol{\Sigma}_{\boldsymbol{H}}^*, \Sigma_J^*, \varphi^*, \boldsymbol{D}_0^*, \boldsymbol{d}^*, \boldsymbol{\Sigma}_{\boldsymbol{d}}^*)\\
&= \inf_{\boldsymbol{x},\boldsymbol{F},\boldsymbol{H},J,\boldsymbol{D}_0,\boldsymbol{d}} \ \sup_{\boldsymbol{\Sigma}_{\boldsymbol{F}},\boldsymbol{\Sigma}_{\boldsymbol{H}},\Sigma_J,\varphi,\boldsymbol{\Sigma}_{\boldsymbol{d}}} \left\{ \int_{V\cup V_\infty} W(\mathcal{V})\, dV + \int_{V\cup V_\infty} \boldsymbol{D}_0 \cdot \boldsymbol{\nabla}_0\varphi\, dV \right.\\
&+ \int_{V\cup V_\infty} [\boldsymbol{\Sigma}_{\boldsymbol{F}} : (\boldsymbol{F}_{\boldsymbol{x}} - \boldsymbol{F}) + \boldsymbol{\Sigma}_{\boldsymbol{H}} : (\boldsymbol{H}_{\boldsymbol{x}} - \boldsymbol{H}) + \Sigma_J (J_{\boldsymbol{x}} - J)\\
&\left. + \boldsymbol{\Sigma}_{\boldsymbol{d}} \cdot (\boldsymbol{F}_{\boldsymbol{x}} \boldsymbol{D}_0 - \boldsymbol{d})]\, dV - \Pi_{ext}(\boldsymbol{x},\varphi) \right\}.
\end{aligned} \tag{72}$$

For notational convenience, the following sets of variables are introduced

$$\mathcal{W} = \{\boldsymbol{F}, \boldsymbol{H}, J, \boldsymbol{d}\}; \qquad \Sigma_{\mathcal{W}} = \{\boldsymbol{\Sigma}_{\boldsymbol{F}}, \boldsymbol{\Sigma}_{\boldsymbol{H}}, \Sigma_J, \boldsymbol{\Sigma}_{\boldsymbol{d}}\}. \tag{73}$$

Virtual and incremental variations of the elements in the sets $\mathcal{W}$ and $\Sigma_{\mathcal{W}}$ in above equation (73) are denoted as

$$\begin{aligned}
\delta\mathcal{W} &= \{\delta\boldsymbol{F}, \delta\boldsymbol{H}, \delta J, \delta\boldsymbol{\Sigma}_{\boldsymbol{D}_0}\}; \qquad & \delta\Sigma_{\mathcal{W}} &= \{\delta\boldsymbol{\Sigma}_{\boldsymbol{F}}, \delta\boldsymbol{\Sigma}_{\boldsymbol{H}}, \delta\Sigma_J, \delta\boldsymbol{\Sigma}_{\boldsymbol{d}}\};\\
\Delta\mathcal{W} &= \{\Delta\boldsymbol{F}, \Delta\boldsymbol{H}, \Delta J, \Delta\boldsymbol{\Sigma}_{\boldsymbol{d}}\}; \qquad & \Delta\Sigma_{\mathcal{W}} &= \{\Delta\boldsymbol{\Sigma}_{\boldsymbol{F}}, \Delta\boldsymbol{\Sigma}_{\boldsymbol{H}}, \Delta\Sigma_J, \Delta\boldsymbol{\Sigma}_{\boldsymbol{d}}\}.
\end{aligned} \tag{74}$$

The stationary point of the above variational principle (81) with respect to virtual changes of the geometry leads to the principle of virtual work (power) as

$$D_1\Pi_W[\delta\boldsymbol{u}] = \int_{V\cup V_\infty} \boldsymbol{P}_W : \boldsymbol{\nabla}_0\delta\boldsymbol{u}\, dV - D\Pi_{ext}[\delta\boldsymbol{v}], \tag{75}$$

where the first Piola-Kirchoff stress tensor is now evaluated as

$$\boldsymbol{P}_W = \boldsymbol{\Sigma}_{\boldsymbol{F}} + \boldsymbol{\Sigma}_{\boldsymbol{H}} \times \boldsymbol{F}_{\boldsymbol{x}} + \Sigma_J \boldsymbol{H}_{\boldsymbol{x}} + \boldsymbol{\Sigma}_{\boldsymbol{d}} \otimes \boldsymbol{D}_0. \tag{76}$$

Similarly, the stationary point of (81) with respect to the electric potential yields

$$D_8\Pi_W[\delta\varphi] = \int_{V\cup V_\infty} \boldsymbol{D}_0 \cdot \boldsymbol{\nabla}_0 \delta\varphi \, dV - D\Pi_{ext}[\delta\varphi]. \tag{77}$$

The directional derivative with respect to the elements in the set $\mathcal{W}$ (73) and with respect to the electric displacement field results in the constitutive relationships formulated in a weak (variational) sense

$$\begin{aligned} D_{2,3,4,10,9}\Pi_W[\delta\mathcal{W}, \delta\boldsymbol{D}_0] = & \int_{V\cup V_\infty} \left(\frac{\partial W}{\partial \boldsymbol{F}} - \boldsymbol{\Sigma}_{\boldsymbol{F}} \right) : \delta\boldsymbol{F} \, dV + \int_{V\cup V_\infty} \left(\frac{\partial W}{\partial \boldsymbol{H}} - \boldsymbol{\Sigma}_{\boldsymbol{H}} \right) : \delta\boldsymbol{H} \, dV \\ & + \int_{V\cup V_\infty} \left(\frac{\partial W}{\partial J} - \Sigma_J \right) \delta J \, dV + \int_{V\cup V_\infty} \left(\frac{\partial W}{\partial \boldsymbol{D}_0} + \boldsymbol{\nabla}_0\varphi + \boldsymbol{F}_{\boldsymbol{x}}{}^T \boldsymbol{\Sigma}_{\boldsymbol{d}} \right) \cdot \delta\boldsymbol{D}_0 \, dV \\ & + \int_{V\cup V_\infty} \left(\frac{\partial W}{\partial \boldsymbol{d}} - \boldsymbol{\Sigma}_{\boldsymbol{d}} \right) \cdot \delta\boldsymbol{d} \, dV. \end{aligned} \tag{78}$$

The directional derivative with respect to the elements of the set $\Sigma_{\mathcal{W}}$ (73) results in the electro-kinematic constraints as follows

$$\begin{aligned} D_{5,6,7,11}\Pi_W[\delta\Sigma_{\mathcal{W}}] = & \int_{V\cup V_\infty} (\boldsymbol{F}_{\boldsymbol{x}} - \boldsymbol{F}) : \delta\boldsymbol{\Sigma}_{\boldsymbol{F}} \, dV + \int_{V\cup V_\infty} (\boldsymbol{H}_{\boldsymbol{x}} - \boldsymbol{H}) : \delta\boldsymbol{\Sigma}_{\boldsymbol{H}} \, dV \\ & + \int_{V\cup V_\infty} (J_{\boldsymbol{x}} - J) \, \delta\Sigma_J \, dV + \int_{V\cup V_\infty} (\boldsymbol{F}_{\boldsymbol{x}}\boldsymbol{D}_0 - \boldsymbol{d}) \cdot \delta\boldsymbol{\Sigma}_{\boldsymbol{d}} \, dV. \end{aligned} \tag{79}$$

5.3. A new mixed variational principle in terms of the extended Helmholtz' energy functional Φ

In order to derive a variational principle in terms of the extended Helmholtz's energy (57c), recall first the mixed variational principle Π_W in (72) with a different ordering of terms and where addition of subtraction of the term $\boldsymbol{\Sigma}_{\boldsymbol{D}_0} \cdot \boldsymbol{D}_0$ has been carried out, namely

$$\Pi_W(\boldsymbol{x}^*, \boldsymbol{F}^*, \boldsymbol{H}^*, J^*, \boldsymbol{\Sigma}^*_{\boldsymbol{F}}, \boldsymbol{\Sigma}^*_{\boldsymbol{H}}, \Sigma^*_J, \varphi^*, \boldsymbol{D}^*_0, \boldsymbol{d}^*, \boldsymbol{\Sigma}^*_{\boldsymbol{d}})$$
$$= - \inf_{\boldsymbol{x},\boldsymbol{F},\boldsymbol{H},J,\boldsymbol{D}_0,\boldsymbol{d}} \sup_{\boldsymbol{\Sigma}_{\boldsymbol{F}},\boldsymbol{\Sigma}_{\boldsymbol{H}},\Sigma_J,\varphi,\boldsymbol{\Sigma}_{\boldsymbol{d}}} \left\{ \int_{V\cup V_\infty} [T^e - W(\mathcal{V})]\, dV + \int_{V\cup V_\infty} \boldsymbol{D}_0 \cdot \boldsymbol{\nabla}_0\varphi \, dV \right.$$
$$+ \int_{V\cup V_\infty} [\boldsymbol{\Sigma}_{\boldsymbol{F}} : (\boldsymbol{F}_{\boldsymbol{x}} - \boldsymbol{F}) + \boldsymbol{\Sigma}_{\boldsymbol{H}} : (\boldsymbol{H}_{\boldsymbol{x}} - \boldsymbol{H}) + \Sigma_J(J_{\boldsymbol{x}} - J)$$
$$\left. + \boldsymbol{\Sigma}_{\boldsymbol{d}} \cdot \boldsymbol{F}_{\boldsymbol{x}}\boldsymbol{D}_0 + \boldsymbol{\Sigma}_{\boldsymbol{D}_0} \cdot \boldsymbol{D}_0]\, dV - \Pi_{ext}(\boldsymbol{x}, \varphi) \right\}. \tag{80}$$

where T^e has been defined in equation (58). Comparing the term in brackets in the first integral in above equation with the definition of the extended Helmholtz's energy functional in (57c) enables to obtain an equivalent representation of the above variational principle as

$$\begin{aligned} &\Pi_\Phi(\boldsymbol{x}^*, \boldsymbol{F}^*, \boldsymbol{H}^*, J^*, \boldsymbol{\Sigma}^*_{\boldsymbol{F}}, \boldsymbol{\Sigma}^*_{\boldsymbol{H}}, \Sigma^*_J, \varphi^*, \boldsymbol{D}^*_0, \boldsymbol{\Sigma}^*_{\boldsymbol{D}_0}, \boldsymbol{\Sigma}_{\boldsymbol{d}}{}^*) \\ &= \inf_{\boldsymbol{x},\boldsymbol{F},\boldsymbol{H},J,\boldsymbol{D}_0} \sup_{\boldsymbol{\Sigma}_{\boldsymbol{F}},\boldsymbol{\Sigma}_{\boldsymbol{H}},\Sigma_J,\varphi,\boldsymbol{\Sigma}_{\boldsymbol{D}_0},\boldsymbol{\Sigma}_{\boldsymbol{d}}} \left\{ \int_{V\cup V_\infty} \Phi(\mathcal{V}^m, \Sigma^e_{\mathcal{V}}) dV \right. \\ &+ \int_{V\cup V_\infty} [\boldsymbol{\Sigma}_{\boldsymbol{F}} : (\boldsymbol{F}_{\boldsymbol{x}} - \boldsymbol{F}) + \boldsymbol{\Sigma}_{\boldsymbol{H}} : (\boldsymbol{H}_{\boldsymbol{x}} - \boldsymbol{H}) + \Sigma_J(J_{\boldsymbol{x}} - J) \\ &\left. + \boldsymbol{D}_0 \cdot (\boldsymbol{\Sigma}_{\boldsymbol{D}_0} + \boldsymbol{\nabla}_0\varphi) + \boldsymbol{\Sigma}_{\boldsymbol{d}} \cdot \boldsymbol{F}_{\boldsymbol{x}}\boldsymbol{D}_0]\, dV - \Pi_{ext}(\boldsymbol{x}, \varphi) \right\}. \end{aligned} \tag{81}$$

For notational convenience, the following sets are introduced,

$$\mathcal{D} = \{\boldsymbol{F}, \boldsymbol{H}, J, \boldsymbol{\Sigma}_{\boldsymbol{D}_0}\}; \qquad \Sigma_{\mathcal{D}} = \{\boldsymbol{\Sigma}_{\boldsymbol{F}}, \boldsymbol{\Sigma}_{\boldsymbol{H}}, \Sigma_J, \boldsymbol{D}_0\}. \tag{82}$$

Virtual and incremental variations of the elements in the sets $\mathcal{D}$ and $\Sigma_{\mathcal{D}}$ in above equation (82) are denoted as

$$\begin{aligned} \delta\mathcal{D} &= \{\delta\boldsymbol{F}, \delta\boldsymbol{H}, \delta J, \delta\boldsymbol{\Sigma}_{\boldsymbol{D}_0}\}; & \delta\Sigma_{\mathcal{D}} &= \{\delta\boldsymbol{\Sigma}_{\boldsymbol{F}}, \delta\boldsymbol{\Sigma}_{\boldsymbol{H}}, \delta\Sigma_J, \delta\boldsymbol{D}_0\}; \\ \Delta\mathcal{D} &= \{\Delta\boldsymbol{F}, \Delta\boldsymbol{H}, \Delta J, \Delta\boldsymbol{\Sigma}_{\boldsymbol{D}_0}\}; & \Delta\Sigma_{\mathcal{D}} &= \{\Delta\boldsymbol{\Sigma}_{\boldsymbol{F}}, \Delta\boldsymbol{\Sigma}_{\boldsymbol{H}}, \Delta\Sigma_J, \Delta\boldsymbol{D}_0\}. \end{aligned} \tag{83}$$

The directional derivative of above variational principle in (72) with respect to virtual changes of the geometry and electrical potential leads to identical expressions to those for Π_Φ in (75) and (77) as

$$D_1\Pi_\Phi[\delta\boldsymbol{u}] = D_1\Pi_W[\delta\boldsymbol{u}]; \qquad D_8\Pi_\Phi[\delta\varphi] = D_8\Pi_W[\delta\varphi]. \tag{84}$$

The stationary conditions with respect to the elements in the set $\mathcal{D}$ (82) and $\boldsymbol{\Sigma_d}$ results in the constitutive relationships formulated in a weak (variational) sense as

$$D_{2,3,4,10,11}\Pi_\Phi[\delta\mathcal{D},\delta\boldsymbol{\Sigma_d}] = \int_{V\cup V_\infty}\left(\frac{\partial\Phi}{\partial\boldsymbol{F}} - \boldsymbol{\Sigma_F}\right):\delta\boldsymbol{F}\,dV + \int_{V\cup V_\infty}\left(\frac{\partial\Phi}{\partial\boldsymbol{H}} - \boldsymbol{\Sigma_H}\right):\delta\boldsymbol{H}\,dV$$
$$+ \int_{V\cup V_\infty}\left(\frac{\partial\Phi}{\partial J} - \Sigma_J\right)\delta J\,dV + \int_{V\cup V_\infty}\left(\frac{\partial\Phi}{\partial\boldsymbol{\Sigma_{D_0}}} + \boldsymbol{D}_0\right)\cdot\delta\boldsymbol{\Sigma_{D_0}}\,dV$$
$$+ \int_{V\cup V_\infty}\left(\frac{\partial\Phi}{\partial\boldsymbol{\Sigma_d}} + \boldsymbol{F_x}\boldsymbol{D}_0\right)\cdot\delta\boldsymbol{\Sigma_d}\,dV. \tag{85}$$

The stationary conditions with respect to the elements of the set $\Sigma_\mathcal{D}$ (82) results in the kinematic constraints and Faraday's law as follows

$$D_{5,6,7,9}\Pi_\Phi[\delta\Sigma_\mathcal{D}] = \int_{V\cup V_\infty}(\boldsymbol{F_x} - \boldsymbol{F}):\delta\boldsymbol{\Sigma_F}\,dV + \int_{V\cup V_\infty}(\boldsymbol{H_x} - \boldsymbol{H}):\delta\boldsymbol{\Sigma_H}\,dV$$
$$+ \int_{V\cup V_\infty}(J_{\boldsymbol{x}} - J)\,\delta\Sigma_J\,dV + \int_{V\cup V_\infty}\left(\boldsymbol{\Sigma_{D_0}} + \boldsymbol{F_x}^T\boldsymbol{\Sigma_d} + \boldsymbol{\nabla}_0\varphi\right)\cdot\delta\boldsymbol{D}_0\,dV. \tag{86}$$

6. Convexification (stabilisation) of materially unstable invariants

For isotropic materials, the internal energy e is typically represented [12, 13, 16] as

$$e(\boldsymbol{\nabla}_0\boldsymbol{x},\boldsymbol{D}_0) = \hat{e}(II_{\boldsymbol{F}}, II_{\boldsymbol{H}}, J, II_{\boldsymbol{D}_0}, II_{\boldsymbol{d}}, II_{\boldsymbol{h}}), \tag{87}$$

where $\boldsymbol{h} = \boldsymbol{H}\boldsymbol{D}_0$. Unfortunately, since $\boldsymbol{h}$ is not included in the extended set $\mathcal{V}$, the invariant $II_{\boldsymbol{h}}$ is not convex multi-variable itself. Furthermore, not every possible combination of the remaining convex multi-variable invariants in (87), namely $II_{\boldsymbol{F}}$, $II_{\boldsymbol{H}}$, J, $II_{\boldsymbol{D}_0}$ and $II_{\boldsymbol{d}}$ will result in a convex multi-variable energy functional according to (37) [12].

Nevertheless, appropriate modifications of a non-convex multi-variable invariant can yield an invariant convex multi-variable according to (37). The

[12]For instance, the purely mechanical invariant Ψ_m defined as $\Psi_m(\boldsymbol{F},\boldsymbol{H}) = II_{\boldsymbol{F}}II_{\boldsymbol{H}}$ is not convex in its arguments, i.e, $\boldsymbol{F}$ and $\boldsymbol{H}$.

obtention of convex multi-variable invariants through suitable modifications of non-convex multi-variable invariants is denoted in the present manuscript as convexification or stabilisation. In particular, two simple examples of stabilisation of a priori non-convex multi-variable invariants will be shown.

6.1. Stabilisation example 1

In this section, the following non-convex multi-variable invariants will be considered

$$W_1 = II_{\boldsymbol{F}} II_{\boldsymbol{D_0}}; \qquad W_2 = II_{\boldsymbol{H}} II_{\boldsymbol{D_0}}. \tag{88}$$

The one-dimensional representation of the invariant W_1 in above equation (88) is expressed in terms of the stretch λ and the sole component of the electric displacement D_0 as $W_1(\lambda, D_0) = \lambda^2 D_0^2$. The Hessian of $W_1(\lambda, D_0)$ is simply obtained as

$$[\mathbb{H}_{W_1}] = \begin{bmatrix} \frac{\partial^2 W}{\partial\lambda\partial\lambda} & \frac{\partial^2 W}{\partial\lambda\partial D_0} \\ \frac{\partial^2 W}{\partial D_0\partial\lambda} & \frac{\partial^2 W}{\partial D_0\partial D_0} \end{bmatrix} = \begin{bmatrix} 2D_0^2 & 4\lambda D_0 \\ 4\lambda D_0 & 2\lambda^2 \end{bmatrix}. \tag{89}$$

Clearly, the one dimensional representation of the invariant W_1 and hence, its three-dimensional counterpart, is not convex multi-variable as $\det[\mathbb{H}_{W_1}] \leq 0$. Alternatively, the invariant $W_1(\lambda, D_0)$ could be stabilised by adding two convex functions of λ and D_0 as

$$W_{1,mod}(\lambda, D_0) = (\lambda^2 + D_0^2)^2 = 2W_1(\lambda, D_0) + \lambda^4 + D_0^4. \tag{90}$$

The Hessian of the resulting invariant $W_{1,mod}(\lambda, D_0)$ in above equation (90) is obtained as

$$\left[\mathbb{H}_{W_{1,mod}}\right] = \begin{bmatrix} \frac{\partial^2 W_{1,mod}}{\partial\lambda\partial\lambda} & \frac{\partial^2 W_{1,mod}}{\partial\lambda\partial D_0} \\ \frac{\partial^2 W_{1,mod}}{\partial D_0\partial\lambda} & \frac{\partial^2 W_{1,mod}}{\partial D_0\partial D_0} \end{bmatrix} = \begin{bmatrix} 12\lambda^2 + 4D_0^2 & 8\lambda D_0 \\ 8\lambda D_0 & 12D_0^2 + 4\lambda^2 \end{bmatrix}. \tag{91}$$

Clearly, $W_{1,mod}(\lambda, D_0)$ is convex in its arguments $\{\lambda, D_0\}$ since $\det[\mathbb{H}_{W1,mod}] \geq 0$. Based on the stabilisation procedure in equation (90) for the one-dimensional representations of $W_1(\lambda, D_0)$, a convex multi-variable three-dimensional energy functional including the stabilised version of the non-convex multi-variable invariants $W_1(\boldsymbol{F}, \boldsymbol{D}_0)$ and $W_2(\boldsymbol{H}, \boldsymbol{D}_0)$ in (88) could be defined as

$$W(\boldsymbol{F}, \boldsymbol{H}, J, \boldsymbol{D}_0, \boldsymbol{d}) = \alpha \underbrace{\left(II_{\boldsymbol{F}} + \gamma^2 II_{\boldsymbol{D_0}}\right)^2}_{W_{\boldsymbol{F}\boldsymbol{D}_0}(\boldsymbol{F}, \boldsymbol{D}_0)} + \beta \underbrace{\left(II_{\boldsymbol{H}} + \gamma^2 II_{\boldsymbol{D_0}}\right)^2}_{W_{\boldsymbol{H}\boldsymbol{D}_0}(\boldsymbol{H}, \boldsymbol{D}_0)} + f(\boldsymbol{F}, \boldsymbol{H}, J, \boldsymbol{D}_0, \boldsymbol{d}), \tag{92}$$

with α, β and γ[13] positive material parameters and $f(\boldsymbol{F}, \boldsymbol{H}, J, \boldsymbol{D}_0, \boldsymbol{d})$, a convex function of the elements of the extended set $\mathcal{V}$. Appropriate values for α, β and γ and suitable functions f must be such that, at the initial configuration, the stress vanishes, the Hessian operator (48) is positive definite and material characterisation can be carried out against available data. Since f is convex multi-variable and α and β are positive material parameters, sufficient conditions to ensure the multi-variable convexity of the functional (92) are the convexity of the energy contributions $W_{\boldsymbol{F}\boldsymbol{D}_0}$ with respect to its arguments $\{\boldsymbol{F}, \boldsymbol{D}_0\}$ and $W_{\boldsymbol{H}\boldsymbol{D}_0}$ with respect to its arguments $\{\boldsymbol{H}, \boldsymbol{D}_0\}$ (refer to equation (92)). Proof of convexity of $W_{\boldsymbol{F}\boldsymbol{D}_0}$ with respect to $\{\boldsymbol{F}, \boldsymbol{D}_0\}$ can be found in Appendix B.1. Similar procedure can be applied to prove convexity of $W_{\boldsymbol{H}\boldsymbol{D}_0}$ with respect to $\{\boldsymbol{H}, \boldsymbol{D}_0\}$.

6.2. Stabilisation example 2

Following a similar stabilisation procedure to that presented in Section 6.1 for invariants W_1 and W_2 (88), an energy functional including the stabilised version of the non-convex multi-variable invariant $II_{\boldsymbol{h}}$ could be defined as

$$W(\boldsymbol{F}, \boldsymbol{H}, J, \boldsymbol{D}_0, \boldsymbol{d}) = \alpha \underbrace{\left[II_{\boldsymbol{H}}^2 + \gamma^2 II_{\boldsymbol{h}} + \gamma^4 II_{\boldsymbol{D_0}}^2 \right]}_{\hat{W}_{\boldsymbol{H}\boldsymbol{D}_0}(\boldsymbol{H}, \boldsymbol{D}_0)}, + f(\boldsymbol{F}, \boldsymbol{H}, J, \boldsymbol{D}_0, \boldsymbol{d}), \tag{93}$$

with α, β and γ[14] positive material parameters and f a convex multi-variable function. Therefore, a sufficient condition to ensure the multi-variable convexity of the functional (93) is the convexity of the energy contribution $\hat{W}_{\boldsymbol{H}\boldsymbol{D}_0}$ with respect to its arguments $\{\boldsymbol{H}, \boldsymbol{D}_0\}$ (refer to equation (93)). Proof of convexity of $\hat{W}_{\boldsymbol{H}\boldsymbol{D}_0}$ with respect to $\{\boldsymbol{H}, \boldsymbol{D}_0\}$ can be found in Appendix B.2.

7. Numerical examples

The objective of this section is to present well posed constitutive models via definition of internal energy density functionals $e(\boldsymbol{\nabla}_0 \boldsymbol{x}, \boldsymbol{D}_0)$ complying with the multi-variable convexity condition in equation (37). Without loss of generality, convex multi-variable internal energy functionals suitable for a reliable description of the constitutive behaviour of isotropic dielectric elastomers will be presented.

[13]The material parameter γ is employed for re-scaling purposes.
[14]The material parameter γ is employed for re-scaling purposes.

Two examples will be presented. The objective of the first example, in Section 7.1, is to present a convex multi-variable constitutive model which captures the electrostrictive behaviour of dielectric elastomers measured typically for a small value of the electric field, which can be considered in practice as zero. The objective of the second example, in Section 7.2, is to study the effect of two additional material parameters necessary for the stabilisation of the constitutive model. These material parameters do not intervene in the characterisation of electrostriction at low values of the electric field. However, modification of these parameters might alter significantly the response of the material, showing an additional nonlinearity which manifests in dielectric elastomers, namely electric saturation, which manifests at high values of the electric field.

7.1. Incorporation of electrostriction in convex multi-variable constitutive models for dielectric elastomers

It is customary to define the internal energy for ideal dielectric elastomers (recall the definition of the internal energy $e_{\text{ideal}}(\boldsymbol{\nabla}_0\boldsymbol{x}, \boldsymbol{D}_0)$ in equation (33)) via an additive decomposition of a purely mechanical component and an additional contribution proportional to the internal energy of the vacuum, as

$$W_{\text{ideal}} = W_m(\boldsymbol{F}, \boldsymbol{H}, J) + \frac{1}{\varepsilon_r} W_0(J, \boldsymbol{d}); \qquad W_0(J, \boldsymbol{d}) = \frac{1}{2\varepsilon_0 J} II_{\boldsymbol{d}};$$
$$W_m(\boldsymbol{F}, \boldsymbol{H}, J) = \mu_{1,0} II_{\boldsymbol{F}} + \mu_{2,0} II_{\boldsymbol{H}} + f(J), \tag{94}$$

where $f(J)$ is defined as in equation (52) by replacing the constants μ_1, μ_2 and κ with $\mu_{1,0}$, $\mu_{2,0}$ and κ_0, respectively. In addition, the elastic parameters $\mu_{1,0}$, $\mu_{2,0}$ and κ_0 and the relative electric permittivity ε_r in (94) match the material properties of the dielectric elastomer in the reference configuration, namely the shear modulus μ, the first Lamé parameter $\hat{\lambda}$ and the electric permittivity ϵ if the following relationships are imposed

$$\mu = 2\mu_{1,0} + 2\mu_{2,0}; \qquad \hat{\lambda} = \kappa_0 + 4\mu_{2,0}; \qquad \varepsilon = \varepsilon_r \varepsilon_0. \tag{95}$$

A constitutive model defined as in equation (94) is termed ideal because it neglects physical nonlinearities which are inherent to dielectric elastomers. In particular, electrostriction [76] and saturation [82] are not captured in a model like that in (94). It has been reported in the experimental literature [5, 76] that the spatial electric permittivity of dielectric elastomers, namely ε, is a function of the deformation gradient tensor. This phenomenon is called electrostrictive effect [76]. Moreover, the spatial electric permittivity exhibits a nonlinear dependence with respect to the electric field. In general, as the electric field increases, the value of ε decreases until a stagnation scenario is reached. In this situation, the electric displacement field would not exhibit any further variation irrespectively of the increment in the applied electric field. This asymptotic behaviour is denoted as saturation [82].

For the particular constitutive model in equation (94), tensor $\boldsymbol{\theta}$ in equation (44) (inverse of the dielectric tensor) can be obtained by using equation (C.8), leading to the following expression

$$\boldsymbol{\theta} = \frac{1}{\varepsilon J}\boldsymbol{F}^T\boldsymbol{F}. \tag{96}$$

Equation (96) and the push forward relation $\boldsymbol{\varepsilon}^{-1} = J\boldsymbol{F}^{-T}\boldsymbol{\theta}\boldsymbol{F}^{-1}$ between the tensor $\boldsymbol{\theta}$ and its spatial counterpart $\boldsymbol{\varepsilon}^{-1}$ enables the following expression for the spatial dielectric tensor $\boldsymbol{\varepsilon}$ to be obtained as

$$\boldsymbol{\varepsilon} = \varepsilon\boldsymbol{I}. \tag{97}$$

Since the electric permittivity tensor $\boldsymbol{\varepsilon}$ in equation (97) is constant, electrostriction and saturation cannot be incorporated using a constitutive model defined as that defined in equation (94).

The authors in Reference [76] have proposed constitutive models for dielectric elastomers incorporating the electrostrictive behaviour based on experimental observations. These authors focused on the particular experimental set up depicted in Figure 3. In this set up, a thin film of an incompressible dielectric elastomer is subjected to an electric field applied across its thickness, namely, in direction OX_3. Consequently, a uniform deformation in the plane of the film (perpendicular to the axis OX_3) characterised by the stretch λ, is observed. Moreover, the incompressibility constraint enables the deformation gradient in the film to be expressed as

$$\boldsymbol{F} = \begin{bmatrix} \lambda & 0 & 0 \\ 0 & \lambda & 0 \\ 0 & 0 & 1/\lambda^2 \end{bmatrix}. \tag{98}$$

Under this particular experimental set up, the internal electromechanical energy of the vacuum, namely W_0 (94) can be expressed in terms of the stretch λ and the only component of the material electric displacement field D_0 as

$$W_0(\lambda, D_0) = \frac{D_0^2}{2\varepsilon_r\varepsilon_0\lambda^4}. \tag{99}$$

The authors in Reference [76] incorporate the electrostrictive effect by modifying the internal energy in equation (94) as

$$W_{\text{Zhao}} = W_m(\lambda) + \frac{1}{\varepsilon_{r,\text{Zhao}}(\lambda)} W_0(\lambda, D_0), \tag{100}$$

with $W_0(\lambda, D_0)$ defined in (99). For different levels of pre-stretch λ, the spatial electric permittivity was measured as a function of the stretch (at a fixed value of the electric field). Then, Zhao et al. propose an expression for $\varepsilon_{r,\text{Zhao}}(\lambda)$ as

$$\varepsilon_{r,\text{Zhao}}(\lambda) = 4.68\,(1 - 0.106(\lambda - 1))\,. \tag{101}$$

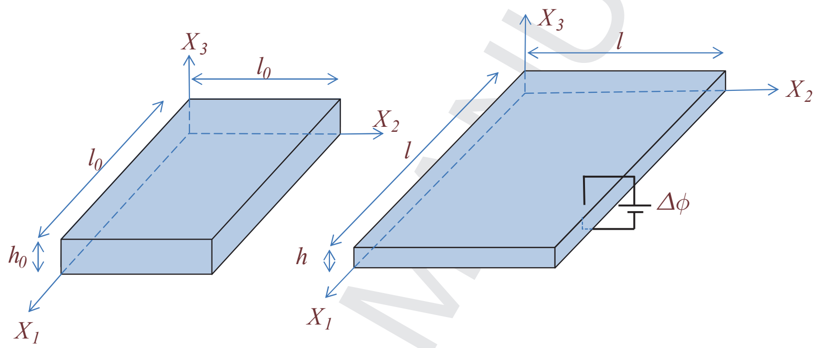

Figure 3: Experimental set up. The application of a uniform electric potential gradient across the thickness of the incompressible dielectric elastomer film (parallel to the axis OX_3) of initial length and thickness l_0 and h_0 respectively, leads to a uniform biaxial expansion of the film with final length $l = \lambda l_0$ and final thickness $h = 1/\lambda^2 h_0$, with λ the stretch in the dielectric elastomer.

The spatial electric permittivity in the reference configuration, namely ε, of the dielectric elastomer studied by Zhao et al is $\varepsilon = \varepsilon_{r,\text{Zhao}}|_{\lambda=1}\,\varepsilon_0 = 4.68\varepsilon_0$. Notice that the electric permittivity associated to the constitutive model proposed by Zhao et al. [76] in equations (100) and (101) does not depend on the electric displacement, and hence, on the electric field. Therefore, this model cannot capture the saturation effect. Alternatively, a generalised three-dimensional[15] convex multi-variable constitutive model incorporating

[15]The proposed constitutive model can be applied to more general scenarios than that for the experimental set up depicted in Figure 3.

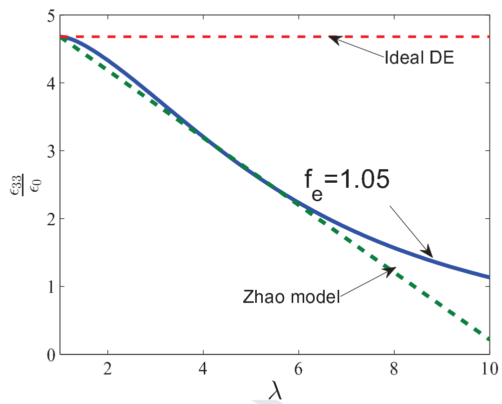

Figure 4: Prediction of electrostrictive effect in a dielectric elastomer film subjected to different levels of pre-stretch and at a fixed value of the electric field of $E = 0$. The green dashed line corresponds to the constitutive model proposed by Zhao et al. (101). The blue line corresponds to the convex multi-variable constitutive model in equation (102) with $\mu_1 = 2\mu_2$, $f_s = 0.1$, $\varepsilon_2 = \infty$, $\varepsilon_e = 252\varepsilon$ and $f_e = 1.05$, consistent with $\varepsilon_r = 4.68$, $\mu = 7.5 \times 10^4\ N/m^2$ and $\lambda = 10^6\ N/m^2$ in the reference configuration.

electrostriction and, moreover, saturation, can be defined through and extended convex multi-variable function as follows

$$W_{el,1} = \mu_1 II_{\boldsymbol{F}} + \mu_2 II_{\boldsymbol{H}} + \frac{1}{2J\varepsilon_1} II_{\boldsymbol{d}} + \mu_e \underbrace{\left(II_{\boldsymbol{F}}^2 + \frac{2}{\mu_e \varepsilon_e} II_{\boldsymbol{F}} II_{\boldsymbol{d}} + \frac{1}{\mu_e^2 \varepsilon_e^2} II_{\boldsymbol{d}}^2 \right)}_{\text{Stabilised electrostrictive invariant } W_{\boldsymbol{Fd}}(\boldsymbol{F}, \boldsymbol{d})}$$
$$+ \frac{1}{2\varepsilon_2} II_{\boldsymbol{D}_0} - (2\mu_1 + 4\mu_2 + 12\mu_e) \ln J + \frac{\kappa}{2}(J-1)^2. \tag{102}$$

Material characterisation in the reference configuration enables the material parameters μ_1, μ_2, μ_e, ε_1, ε_2 and ε_e in above (102) to be expressed in terms of the material properties in the reference configuration, namely μ, $\hat{\lambda}$ and ε as

$$\mu = 2\mu_1 + 2\mu_2 + 12\mu_e; \qquad \hat{\lambda} = \kappa + 8\mu_e + 4\mu_2; \qquad \frac{1}{\varepsilon} = \frac{1}{\varepsilon_1} + \frac{1}{\varepsilon_2} + \frac{12}{\varepsilon_e}. \tag{103}$$

The amount of electrostriction in the constitutive model $W_{el,1}$ (102) is controlled by an additional electrostrictive parameter f_e, defined as

$$\varepsilon_1 = f_e \varepsilon, \tag{104}$$

where $f_e \geq 1$ in order to ensure positiveness of ε_2 and ε_e. High values of the parameter f_e are associated to highly electrostrictive materials (for a constant value of ε_2) leading to a high value of $\frac{12}{\varepsilon_e}$ in detriment of $\frac{1}{\varepsilon_1}$ (103). An additional stiffening parameter can be introduced for the convex multi-variable constitutive model $W_{el,1}$ (102), defined as

$$12\mu_e = f_s \mu. \tag{105}$$

High values of the stiffening parameter f_s lead to mechanically stiffer constitutive models. Notice that the energy functional $W_{el,1}$ in above equation (102) contains the invariant $W_{\boldsymbol{Fd}}$. This invariant results after stabilising the non-convex multi-variable invariant $II_{\boldsymbol{F}} II_{\boldsymbol{d}}$, where the same stabilisation procedure as that for $W_{\boldsymbol{F}\boldsymbol{D}_0}$ and $W_{\boldsymbol{H}\boldsymbol{D}_0}$ in equation (92) has been utilised (refer to Section 6). Following the same procedure as that for the constitutive model in (94), the spatial dielectric tensor is obtained as

$$\begin{aligned}\boldsymbol{\varepsilon}(\boldsymbol{F},\boldsymbol{d}) &= \left(\frac{1}{\varepsilon_1}\boldsymbol{I} + \frac{4J}{\varepsilon_e}II_{\boldsymbol{F}}\boldsymbol{I} + \hat{\boldsymbol{\varepsilon}}^{-1}(J,\boldsymbol{F},\boldsymbol{d})\right)^{-1};\\ \hat{\boldsymbol{\varepsilon}}^{-1}(\boldsymbol{F},\boldsymbol{d}) &= \frac{4J}{\varepsilon_e^2\mu_e}II_{\boldsymbol{d}}\boldsymbol{b}^{-1} + \frac{8J}{\varepsilon_e^2\mu_e}\boldsymbol{d}\otimes\boldsymbol{d} + \frac{J\boldsymbol{b}^{-1}}{\varepsilon_2},\end{aligned} \tag{106}$$

where $\boldsymbol{b}$ is the left Cauchy-Green deformation tensor, defined as $\boldsymbol{b} = \boldsymbol{F}\boldsymbol{F}^T$. Evaluation of the expression for $\boldsymbol{\varepsilon}$ in above (106) for a vanishing electric displacement field, namely $\boldsymbol{D}_0 = \boldsymbol{0}$ leads to the following expression for $\boldsymbol{\varepsilon}(\boldsymbol{F},\boldsymbol{0})$

$$\boldsymbol{\varepsilon}(\boldsymbol{F},\boldsymbol{0}) = \left(\frac{1}{\varepsilon_1}\boldsymbol{I} + \frac{4J}{\varepsilon_e}II_{\boldsymbol{F}}\boldsymbol{I} + \frac{J}{\varepsilon_2}\boldsymbol{b}^{-1}\right)^{-1}. \tag{107}$$

Particularisation of the kinematical restrictions of the experimental set up described in equation (98) enables a diagonal representation of the above electric permittivity tensor as

$$\boldsymbol{\varepsilon} = \begin{bmatrix}\varepsilon_{11} & 0 & 0\\ 0 & \varepsilon_{11} & 0\\ 0 & 0 & \varepsilon_{33}\end{bmatrix}, \tag{108}$$

where an expression for the component ε_{33} can be obtained in terms of the stretch λ as

$$\varepsilon_{33}(\lambda,0) = \left(\frac{1}{\varepsilon_1} + \frac{4}{\varepsilon_e}f(\lambda) + \frac{1}{\varepsilon_2}\lambda^4\right)^{-1}; \qquad f(\lambda) = 2\lambda^2 + \frac{1}{\lambda^4}. \tag{109}$$

For the shake of simplicity, the material parameter ε_2 is prescribed as $\varepsilon_2 = \infty$. Notice that the resulting energy functional would be convex in a reduced set $\{\boldsymbol{F},\boldsymbol{H},J,\boldsymbol{d}\} \subset \mathcal{V}$. Choosing the extreme values of the deformation in the experiment considered in reference [76], namely $\lambda_1 = 1$ and $\lambda_2 = 6$, the following system of equations is obtained

$$\left(\frac{1}{\varepsilon_1} + \frac{1}{\varepsilon_e}f(\lambda_1)\right)^{-1} = \varepsilon_{r,\text{Zhao}}(\lambda_1)\varepsilon_0; \qquad \left(\frac{1}{\varepsilon_1} + \frac{1}{\varepsilon_e}f(\lambda_2)\right)^{-1} = \varepsilon_{r,\text{Zhao}}(\lambda_2)\varepsilon_0 \tag{110}$$

The above system of equations in (110) enables ε_1 and ε_e to be determined as

$$\varepsilon_1 = 1.05\varepsilon \Rightarrow f_e = 1.05; \qquad \varepsilon_e = 252\varepsilon. \tag{111}$$

Figure 4 shows the good agreement between the predicted spatial permittivity for the constitutive model proposed by Zhao et al. [76] and for the convex multi-variable (with electric material parameters chosen as in (111)) constitutive models in equations (102), for the range of deformations considered in the experiment, i.e $1 \leq \lambda \leq 6$ and for the particular scenario for which $\boldsymbol{D}_0 = \mathbf{0}$. Notice that in the material characterisation carried out to predict the electrostrictive behaviour of the constitutive model in equation (102), the elastic parameter μ_e did not have any influence. This characterisation was performed at the specific scenario for which $\boldsymbol{D}_0 = \mathbf{0}$. In the more general case, i.e. $\boldsymbol{D}_0 \neq \mathbf{0}$, the parameter μ_e introduces a further nonlinear dependence of the spatial electric permittivity upon the material electric displacement field which, for extreme values of the electric field, resembles the physical behaviour known as electric saturation. This nonlinear effect will be observed in the following section.

7.2. Numerical experiment

In this section, in addition to the constitutive models W_{ideal} and $W_{el,1}$ in equations (94) and (102), respectively, a non-convex multi-variable internal energy functional very similar to the convex multi-variable model in (102) containing the invariant $II_{\boldsymbol{F}} II_{\boldsymbol{d}}$ without the additional stabilising invariants will be defined as

$$\begin{aligned} W_{el,2} =& \hat{\mu}_1 II_{\boldsymbol{F}} + \hat{\mu}_2 II_{\boldsymbol{H}} + \frac{1}{2J\hat{\varepsilon}_1} II_{\boldsymbol{d}} + \underbrace{\frac{2}{\hat{\varepsilon}_e} II_{\boldsymbol{F}} II_{\boldsymbol{d}}}_{\text{Non-convex multi-variable invariant}} \\ &+ \frac{1}{2\hat{\varepsilon}_2} II_{\boldsymbol{D}_0} - (2\hat{\mu}_1 + 4\hat{\mu}_2)\ln J + \frac{\hat{\kappa}}{2}(J-1)^2. \end{aligned} \tag{112}$$

Equivalence in the reference configuration between the convex multi-variable constitutive model in equation (102)-(103) and the non-convex multi-variable model in above (112) is guaranteed if the parameters $\hat{\mu}_1$, $\hat{\mu}_2$, $\hat{\varepsilon}_e$, $\hat{\varepsilon}_2$ and $\hat{\kappa}$ are related to the material properties of the material in the reference configuration, namely μ, κ and ε as

$$\mu = \hat{2}\mu_1 + 2\hat{\mu}_2; \qquad \hat{\lambda} = \hat{\kappa} + 4\hat{\mu}_2; \qquad \frac{1}{\varepsilon} = \frac{1}{\hat{\varepsilon}_1} + \frac{1}{\hat{\varepsilon}_2} + \frac{12}{\hat{\varepsilon}_e}. \tag{113}$$

An electrostrictive parameter similar to that in equation (104) can be defined for the constitutive model in above equation (112) as

$$\hat{\varepsilon}_1 = \hat{f}_e \varepsilon. \tag{114}$$

Notice that the following choice of material parameters, i.e,

$$\hat{\varepsilon}_1 = 1.05\varepsilon \Rightarrow \hat{f}_e = 1.05; \qquad \hat{\varepsilon}_e = 252\varepsilon, \tag{115}$$

would replicate the electrostrictive behaviour (variation of the spatial electric permittivity with the deformation for $\boldsymbol{D}_0 = \boldsymbol{0}$) of the model in (102) with the particular choice of electric material parameters ε_1, c_1 and c_2 in equation (115).

The objective of this section is to study the behaviour of the convex multi-variable and non-convex multi-variable constitutive models in equations (102) and (112) respectively, for the experimental set up depicted in Figure 3 under a more general scenario where $\boldsymbol{D}_0 \neq \boldsymbol{0}$. For a given value of the only component of the material electric field, i.e, E_0, the stretch λ and the only component of the material electric displacement field, namely D_0 are obtained via minimisation of an energy functional per unit undeformed volume $\pi(\lambda, D_0)$ defined as

$$\pi(\lambda, D_0) = \min_{\lambda, D_0} \left\{ W(\boldsymbol{F}(\lambda), \boldsymbol{D}_0(D_0)) - E_0 D_0 \right\}. \tag{116}$$

The stationary conditions of the energy functional $\pi(\lambda, D_0)$ in above (116) are obtained as

$$\begin{aligned} D\pi(\lambda, D_0)[\delta\lambda] &= \frac{\partial W}{\partial \boldsymbol{F}} : \frac{\partial \boldsymbol{F}}{\partial \lambda} \delta\lambda = 0; \\ D\pi(\lambda, D_0)[\delta D_0] &= \left(\frac{\partial W}{\partial \boldsymbol{D}_0} \cdot \frac{\partial \boldsymbol{D}_0}{\partial D_0} - E_0 \right) \delta D_0 = 0. \end{aligned} \tag{117}$$

Since equation (117) must hold for any arbitrary virtual variations $\{\delta\lambda, \delta D_0\}$, the final system of nonlinear equations is obtained

$$\boldsymbol{\mathcal{R}}(\lambda, D_0) = \boldsymbol{0}; \qquad \boldsymbol{\mathcal{R}}(\lambda, D_0) = \begin{bmatrix} \mathcal{R}_\lambda(\lambda, D_0) \\ \mathcal{R}_{D_0}(\lambda, D_0) \end{bmatrix}, \tag{118}$$

with

$$\mathcal{R}_\lambda(\lambda, D_0) = \frac{\partial W}{\partial \boldsymbol{F}} : \frac{\partial \boldsymbol{F}}{\partial \lambda}; \qquad \mathcal{R}_{D_0}(\lambda, D_0) = \frac{\partial W}{\partial \boldsymbol{D}_0} \cdot \frac{\partial \boldsymbol{D}_0}{\partial D_0} - E_0. \tag{119}$$

For the particular experimental set up described in Section 7.1, where the deformation gradient tensor $\boldsymbol{F}$ is defined as in equation (98) and where the material electric displacement field is defined as $\boldsymbol{D}_0 = \begin{bmatrix} 0 & 0 & D_0 \end{bmatrix}^T$, the derivatives $\frac{\partial \boldsymbol{F}}{\partial \lambda}$ and $\frac{\partial \boldsymbol{D}_0}{\partial D_0}$ featuring in equations (117) and (119) are obtained as

$$\frac{\partial \boldsymbol{F}}{\partial \lambda} = \begin{bmatrix} 1 & 0 & 0 \\ 0 & 1 & 0 \\ 0 & 0 & -2\lambda^{-3} \end{bmatrix}; \qquad \frac{\partial \boldsymbol{D}_0}{\partial D_0} = \begin{bmatrix} 0 & 0 & 1 \end{bmatrix}. \tag{120}$$

A combined Newton-Raphson/arc length algorithm has been applied to solve the above system of nonlinear equations in (118)-(119). Figure 5 shows the result of the nonlinear equations (118) replicating the experimental set up in Figure 3. The predicted behaviour of the dielectric elastomer film considering the convex multi-variable constitutive model in equation (102) (where different values of the stiffening parameter f_e (refer to equation (105)) have been considered), the non-convex multi-variable constitutive model in (112) and the ideal dielectric elastomer model in (94) has been studied. The three models considered have identical material properties in the reference configuration, namely μ, $\hat{\lambda}$ and ε. As it can observed from Figure 5(b), a constitutive model with a low value of the stiffening parameter f_s is more prone to develop electric saturation. In other words, a highly nonlinear behaviour of the curve relating $\boldsymbol{E}$ and $\boldsymbol{D}$ occurs, which in the ideal case, would tend to a stagnation scenario.

Additionally, Figure 6 studies the influence of the electrostrictive electric parameter f_e on the convex multi-variable constitutive model in equation (102). Notice that in this case, unlike that one depicted in Figure 5 (for which the stiffening parameter f_s is changed), the electrostrictive behaviour of the convex multi-variable constitutive model for $\boldsymbol{D}_0 = \boldsymbol{0}$ is not the same for different values of f_e, since f_e (refer to equation (111)) takes place in the definition of electrostriction for $\boldsymbol{D}_0 = \boldsymbol{0}$, as shown in equation (109). A comparison of the response of the convex multi-variable constitutive model in equation (102) for different values of the electrostrictive parameter f_e for a fixed value of f_s is carried out against that of the non-convex multi-variable constitutive model in equation (112) (with $\hat{f}_e$ chosen according to equation (115)) and the ideal dielectric elastomer model in equation (94). As it can be observed from Figure 6(b), a constitutive model with a high value of the electrostrictive parameter f_e is also more prone to develop electric saturation.

Finally, Figure 7 shows the graphical visualisation of the inverse of the La-

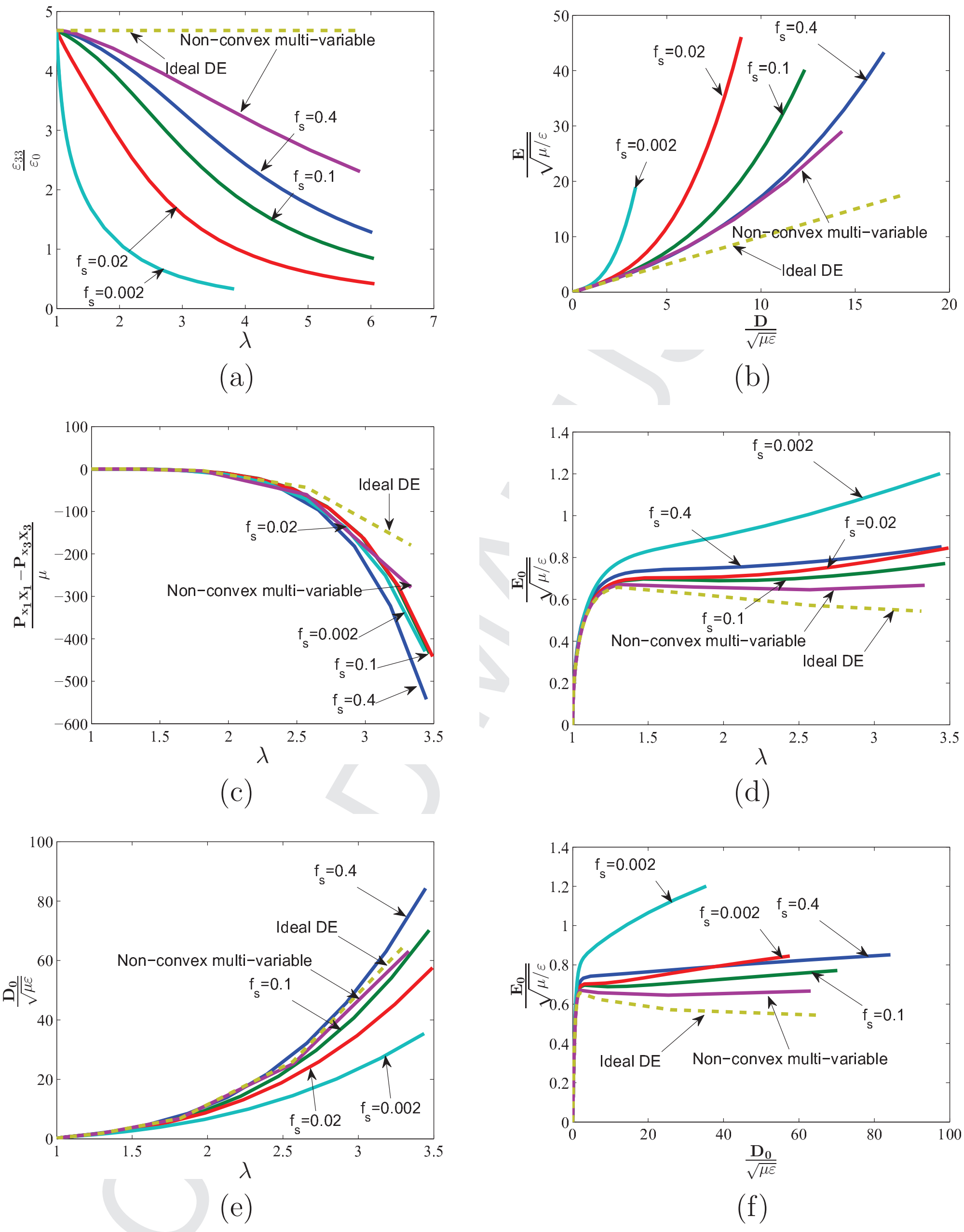

Figure 5: Relation between (a) ε_3 and λ, (b) E and D, (c) $\boldsymbol{P}_{x_1X_1} - \boldsymbol{P}_{x_3X_3}$ and λ, (d) E_0 and λ, (e) D_0 and λ and (f) E_0 and D_0 for the convex multi-variable model in equation (102) (for different values of the stiffening parameter f_s), the non-convex multi-variable model in (112) and an ideal dielectric elastomer (94). Material parameters: $f_e = 1.05$, $\varepsilon_2 = \infty$, $\varepsilon_2 = 252\varepsilon$ and $\mu_1 = 2\mu_2$ for the convex multi-variable model and with $\hat{f}_e = 1.05$, $\hat{\varepsilon}_2 = \infty$ and $\hat{\mu}_1 = 2\hat{\mu}_2$ for the non-convex multi-variable model. $\varepsilon_r = 4.68$, $\mu = 7.5 \times 10^4\ N/m^2$ and $\lambda = 10^6\ N/m^2$.

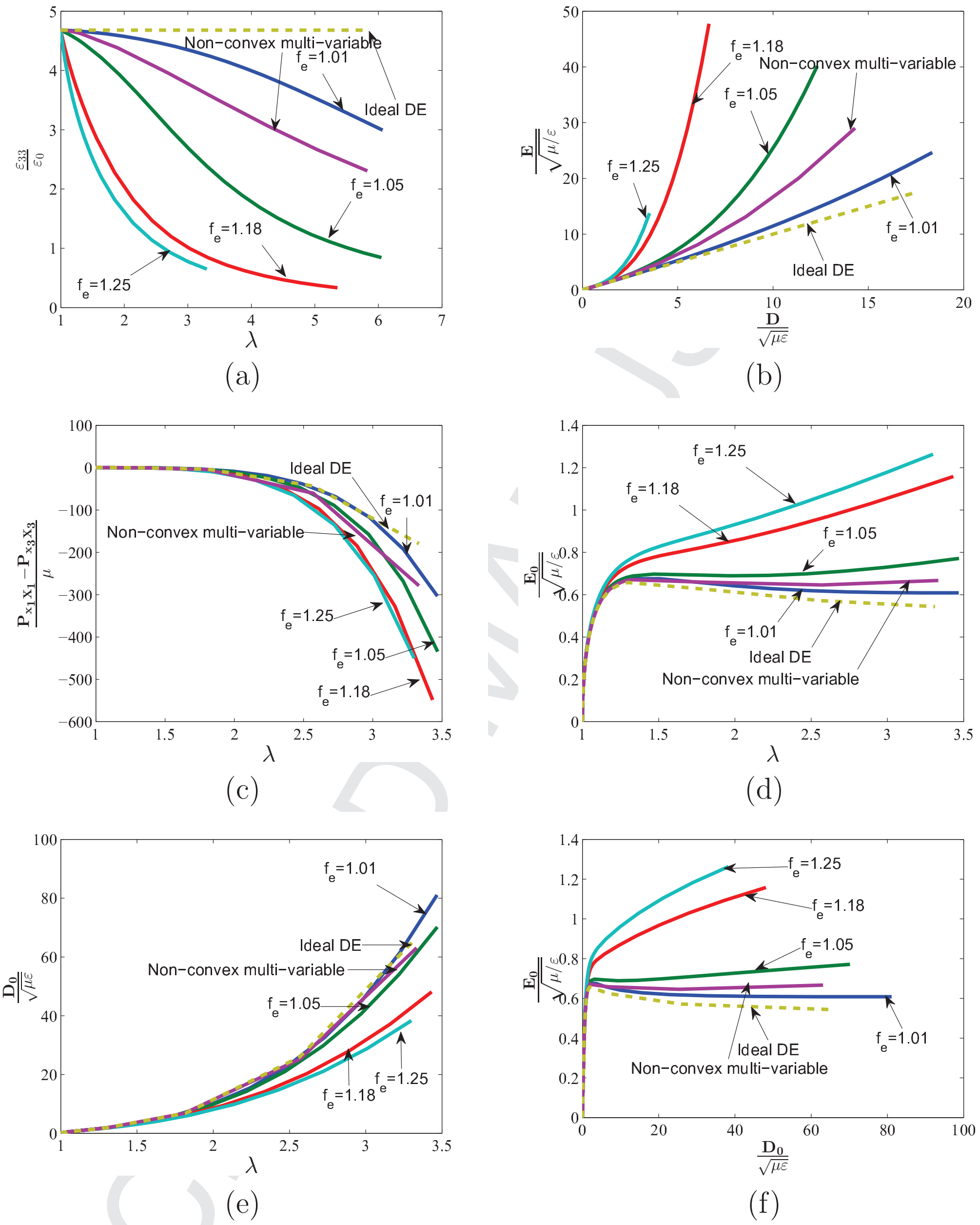

Figure 6: Relations between (a) ε_3 and λ, (b) E and D, (c) $\boldsymbol{P}_{x_1X_1} - \boldsymbol{P}_{x_3X_3}$ and λ, (d) E_0 and λ, (e) D_0 and λ and (f) E_0 and D_0 for the convex multi-variable model in equation (102) (for different values of ε_e), the non-convex multi-variable model in (112) and an ideal dielectric elastomer (94). Material parameters: $\varepsilon_2 = \infty$, $f_s = 0.1$ and $\mu_1 = 2\mu_2$ for the convex multi-variable model and with $\hat{\varepsilon}_2 = \infty$ and $\hat{\mu}_1 = 2\hat{\mu}_2$ for the non-convex multi-variable model. $\varepsilon_r = 4.68$, $\mu = 7.5 \times 10^4\ N/m^2$ and $\lambda = 10^6\ N/m^2$.

grangian dielectric tensor $\boldsymbol{\theta}$, the piezoelectric tensor $\boldsymbol{\mathcal{Q}}^T$, and the Lagrangian electrostrictive tensor $\boldsymbol{\mathcal{B}}$ computed according to equations (C.8), (C.5) and (C.10), respectively, for the convex multi-variable constitutive model in equation (102), the non-convex multi-variable constitutive model in (112) and the ideal dielectric elastomer model (94), having the three models the same material properties in the reference configuration, namely, μ, $\hat{\lambda}$ and ε. For the visualisation of these tensors, their associated moduli $\frac{1}{\tilde{\varepsilon}}$, $\widetilde{\mathcal{Q}}$, and $\widetilde{\mathcal{B}}_\mu$ are defined via a spherical parametrisation of the arbitrary direction $\boldsymbol{n}$ as in [83][16]:

$$\frac{1}{\tilde{\varepsilon}} = \boldsymbol{n} \cdot \boldsymbol{\theta} \boldsymbol{n}; \qquad \widetilde{\mathcal{Q}} = \boldsymbol{\mathcal{Q}} : (\boldsymbol{n} \otimes \boldsymbol{n} \otimes \boldsymbol{n}); \qquad \widetilde{\mathcal{B}}_\mu = (\boldsymbol{n} \otimes \boldsymbol{n}) : \boldsymbol{\mathcal{B}} : (\boldsymbol{n} \otimes \boldsymbol{n}). \tag{121}$$

As predicted from Figures 5 and 6, for increasing values of the dimensionless electric field $\boldsymbol{E}/\sqrt{\mu/\varepsilon}$, the differences in the three constitutive tensors between the three constitutive models involved increase.

8. Concluding remarks

This paper has proposed a new variational framework to formulate large strain/large electric field electro-elasticity. This work extends for the first time the ideas presented by Bonet et al. [1] in the field of polyconvex elasticity to nonlinear electro-elasticity. With that in mind, a new internal energy density functional has been introduced in the form of a convex multi-variable function with respect to an extended set of electromechanical variables $\mathcal{V} = \{\boldsymbol{F}, \boldsymbol{H}, J, \boldsymbol{D}_0, \boldsymbol{d}\}$, which enables the ellipticity condition and hence, material stability to be satisfied for the entire range of deformations and electric fields. Notice that the focus of this paper is on material stability and not on the existence of minimisers. The latter would also require the study of the sequentially weak lower semicontinuity and the coercivity of the energy functional.

The introduction of the spatial vector $\boldsymbol{d}$ as an element of the set $\mathcal{V}$ proves to be extremely relevant since it permits the electromechanical energy of the vacuum and hence, that of ideal dielectric elastomers, to be considered as a degenerate case of a convex multi-variable functional. Furthermore, the

[16]An additional modulus can be associated to the forth order tensor $\boldsymbol{\mathcal{B}}$, namely $\widetilde{\mathcal{B}}_\kappa = \frac{1}{3}\boldsymbol{I} : \boldsymbol{\mathcal{B}} : \boldsymbol{n} \otimes \boldsymbol{n}$., resembling both $\widetilde{\mathcal{B}}_\mu$ and $\widetilde{\mathcal{B}}_\kappa$ the shear $\widetilde{\mathcal{C}}_\mu$ an volumetric $\widetilde{\mathcal{C}}_\kappa$ counterparts of the elasticity tensor $\boldsymbol{\mathcal{C}}$ (C.2).

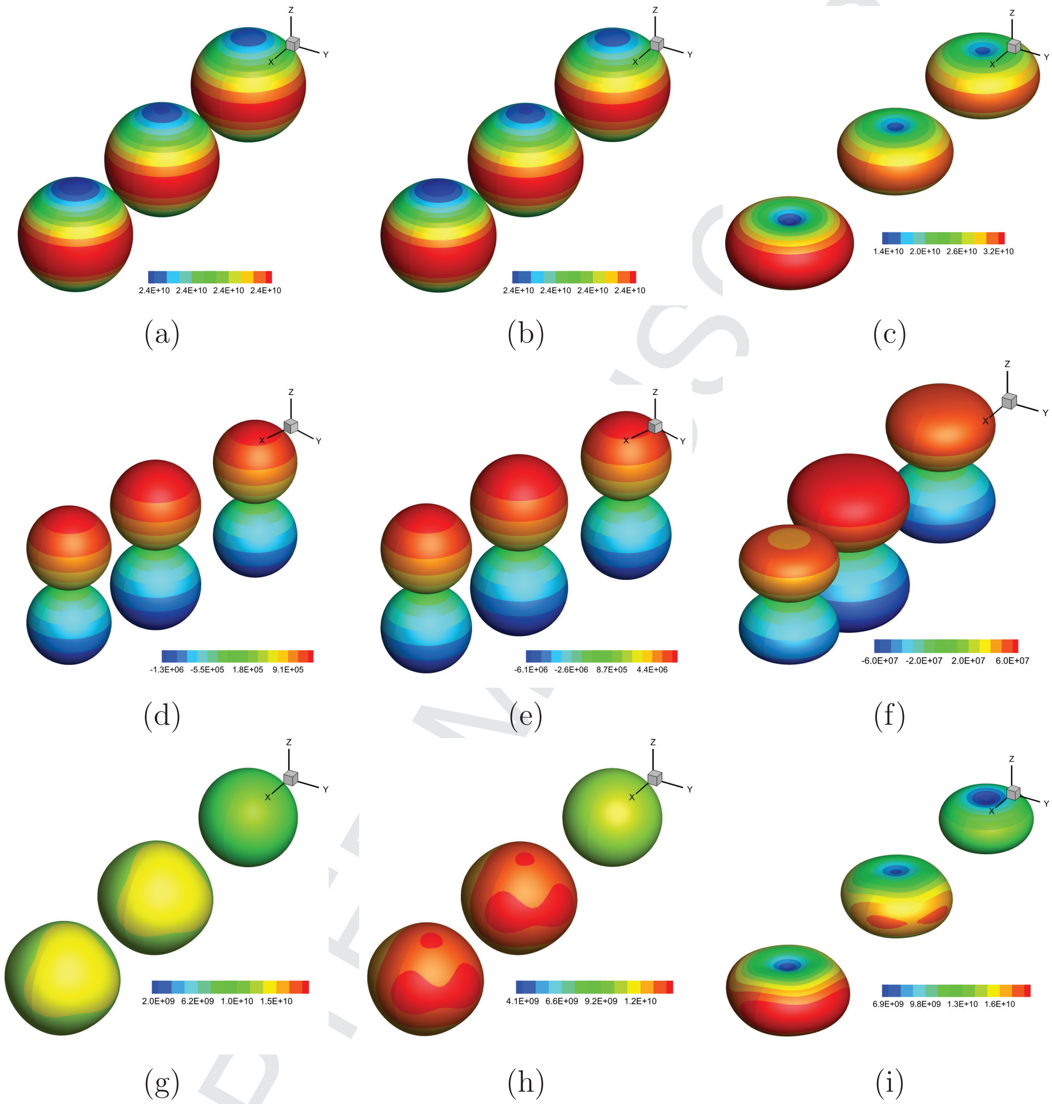

Figure 7: Numerical experiment for the experimental set up in Figure 3. From left to right: convex multi-variable constitutive model in equation (102); non-convex multi-variable constitutive model in (112); ideal dielectric elastomer (94). Graphical representation of $1/\widetilde{\varepsilon}$ $(121)_a$ for (a) $E/\sqrt{\mu/\varepsilon} = 0.028$, (b) $E/\sqrt{\mu/\varepsilon} = 0.14$ and (c) $E/\sqrt{\mu/\varepsilon} = 2.35$. Graphical representation of $\widetilde{\mathcal{Q}}$ $(121)_b$ for (d) $E/\sqrt{\mu/\varepsilon} = 0.028$, (e) $E/\sqrt{\mu/\varepsilon} = 0.14$ and (f) $E/\sqrt{\mu/\varepsilon} = 2.35$. Graphical representation of $\widetilde{\mathcal{B}}_\mu$ $(121)_c$ for (g) $E/\sqrt{\mu/\varepsilon} = 0.028$, (h) $E/\sqrt{\mu/\varepsilon} = 0.14$ and (i) $E/\sqrt{\mu/\varepsilon} = 2.35$. Material parameters: $f_e = 1.05\varepsilon$, $\varepsilon_2 = \infty$, $\varepsilon_e = 252\varepsilon$ and $\mu_1 = 2\mu_2$ for the convex multi-variable model in (102) and $\hat{f}_e = 1.05$, $\hat{\varepsilon}_2 = \infty$ and $\hat{\mu}_1 = 2\hat{\mu}_2$ for the non-convex multi-variable model in (112). $\varepsilon_r = 4.68$, $\mu = 7.5 \times 10^4\ N/m^2$ and $\lambda = 10^6\ N/m^2$.

authors show simple techniques, denoted as convexification or stabilisation, which enable to create convex multi-variable electromechanical invariants by modifying a priori non-convex multi-variable invariants.

An additional set of variables $\Sigma_{\mathcal{V}} = \{\boldsymbol{\Sigma_F}, \boldsymbol{\Sigma_H}, \Sigma_J, \boldsymbol{\Sigma_{D_0}}, \boldsymbol{\Sigma_d}\}$, dual (work conjugate) to those in $\mathcal{V}$ is presented for the first time in the context of nonlinear electro-elasticity. Very remarkably, the one to one relationship between both sets $\mathcal{V}$ and $\Sigma_{\mathcal{V}}$, enable the definition of new interesting extended Hu-Washizu type of mixed variational principles which are presented. The use of a tensor cross product [1, 3, 75] operation and its associated algebra, greatly facilitates the algebraic manipulations of expressions involving the adjoint of the deformation gradient and its derivatives.

The Finite Element implementation of some of the mixed variational principles presented in this paper as well as the development of a general conservation law system (along with the analysis of its hyperbolicity) will be the next steps of our work.

Acknowledgements

The first author would like to acknowledge the financial support received through "The Leverhulme Prize" awarded by The Leverhulme Trust, United Kingdom. Both authors acknowledge the financial support provided by the Sêr Cymru National Research Network for Advanced Engineering and Materials.

Appendix A. Cross product tensor product

The left cross product of a vector $\boldsymbol{v}$ and a second order tensor $\boldsymbol{A}$ to give a second order tensor denoted $\boldsymbol{v} \times \boldsymbol{A}$ is defined so that when applied to a general vector $\boldsymbol{w}$ gives:

$$(\boldsymbol{v} \times \boldsymbol{A})\, \boldsymbol{w} = \boldsymbol{v} \times (\boldsymbol{A}\boldsymbol{w})\, ; \quad (\boldsymbol{v} \times \boldsymbol{A})_{ij} = \mathcal{E}_{ikl} v_k A_{lj}, \tag{A.1}$$

where $\mathcal{E}_{ikl}$ denotes the components of the standard third order alternating tensor and $\times$ is the standard vector cross product. The right cross product of a second order tensor $\boldsymbol{A}$ by a vector $\boldsymbol{v}$ to give a second order tensor denoted $\boldsymbol{A} \times \boldsymbol{v}$ is defined so that for every vector $\boldsymbol{w}$:

$$(\boldsymbol{A} \times \boldsymbol{v})\, \boldsymbol{w} = \boldsymbol{A}\,(\boldsymbol{v} \times \boldsymbol{w})\, ; \quad (\boldsymbol{A} \times \boldsymbol{v})_{ij} = \mathcal{E}_{jkl} A_{ik} v_l. \tag{A.2}$$

The cross product of two second order tensors $\boldsymbol{A}$ and $\boldsymbol{B}$ to give a new second order tensor denoted $\boldsymbol{A} \times \boldsymbol{B}$ is defined so that for any arbitrary vectors $\boldsymbol{v}$ and $\boldsymbol{w}$ gives:

$$\boldsymbol{v} \cdot (\boldsymbol{A} \times \boldsymbol{B})\, \boldsymbol{w} = (\boldsymbol{v} \times \boldsymbol{A}) : (\boldsymbol{B} \times \boldsymbol{w})\, ; \quad (\boldsymbol{A} \times \boldsymbol{B})_{ij} = \mathcal{E}_{ikl}\mathcal{E}_{jmn} A_{km} B_{ln}. \tag{A.3}$$

In the framework developed in this paper the tensor cross product will be mostly applied between two-point tensors. For this purpose the above definition can be readily particularised to second order two-point tensors as,

$$(\boldsymbol{A} \times \boldsymbol{B})_{iI} = \mathcal{E}_{ijk}\mathcal{E}_{IJK} A_{jJ} B_{kK}. \tag{A.4}$$

When applied to a second order tensor $\boldsymbol{A}$ and a fourth order tensors $\mathbb{H}$, two possible operations are defined as:

$$(\mathbb{H} \times \boldsymbol{A})_{pPiI} = \mathcal{E}_{ijk}\mathcal{E}_{IJK} \mathbb{H}_{pPjJ} A_{kK}; \quad (\boldsymbol{A} \times \mathbb{H})_{iIpP} = \mathcal{E}_{ijk}\mathcal{E}_{IJK} A_{jJ} \mathbb{H}_{kKpP}. \tag{A.5}$$

Moreover, the double application of the tensor cross product between a fourth order tensor and two second order tensors is associative, namely:

$$\boldsymbol{A} \times \mathbb{H} \times \boldsymbol{B} = (\boldsymbol{A} \times \mathbb{H}) \times \boldsymbol{B} = \boldsymbol{A} \times (\mathbb{H} \times \boldsymbol{B})\,. \tag{A.6}$$

Finally, when applied to a second order tensor $\boldsymbol{A}$ and a third order tensors $\mathbb{Q}$, two possible operations are defined as:

$$(\mathbb{Q} \times \boldsymbol{A})_{PiI} = \mathcal{E}_{ijk}\mathcal{E}_{IJK} \mathbb{Q}_{PjJ} A_{kK}; \quad (\boldsymbol{A} \times \mathbb{Q})_{iIP} = \mathcal{E}_{ijk}\mathcal{E}_{IJK} A_{jJ} \mathbb{H}_{kKP}. \tag{A.7}$$

Some useful properties of new cross product are enumerated below. Let a be a scalar, $\boldsymbol{V}$ and $\boldsymbol{W}$ material vectors, $\boldsymbol{v}$ and $\boldsymbol{w}$ spatial vectors, $\boldsymbol{I}$ the identity tensor with Kronecker delta components $(\boldsymbol{I})_{ij} = \delta_{ij}$ and $\boldsymbol{A}$, $\boldsymbol{B}$ and $\boldsymbol{C}$ second order tensors

$$\boldsymbol{A} \times \boldsymbol{B} = \boldsymbol{B} \times \boldsymbol{A}; \tag{A.8}$$

$$\boldsymbol{A} \times \boldsymbol{B} = \boldsymbol{A}^T \times \boldsymbol{B}^T; \tag{A.9}$$

$$\boldsymbol{A} \times (\boldsymbol{B} + \boldsymbol{C}) = \boldsymbol{A} \times \boldsymbol{B} + \boldsymbol{A} \times \boldsymbol{C}; \tag{A.10}$$

$$a\,(\boldsymbol{A} \times \boldsymbol{B}) = (a\boldsymbol{A}) \times \boldsymbol{B} = \boldsymbol{A} \times (a\boldsymbol{B})\,; \tag{A.11}$$

$$(\boldsymbol{v} \otimes \boldsymbol{V}) \times (\boldsymbol{w} \otimes \boldsymbol{W}) = (\boldsymbol{v} \times \boldsymbol{w}) \otimes (\boldsymbol{V} \times \boldsymbol{W})\,; \tag{A.12}$$

$$\boldsymbol{v} \times (\boldsymbol{A} \times \boldsymbol{V}) = (\boldsymbol{v} \times \boldsymbol{A}) \times \boldsymbol{V} = \boldsymbol{v} \times \boldsymbol{A} \times \boldsymbol{V}; \tag{A.13}$$

$$\boldsymbol{A} \times (\boldsymbol{v} \otimes \boldsymbol{V}) = -\boldsymbol{v} \times \boldsymbol{A} \times \boldsymbol{V}; \tag{A.14}$$

$$(\boldsymbol{A} \times \boldsymbol{B}) : \boldsymbol{C} = (\boldsymbol{B} \times \boldsymbol{C}) : \boldsymbol{A} = (\boldsymbol{A} \times \boldsymbol{C}) : \boldsymbol{B}; \tag{A.15}$$

$$(\boldsymbol{A} \times \boldsymbol{B})\,(\boldsymbol{V} \times \boldsymbol{W}) = (\boldsymbol{A}\boldsymbol{V}) \times (\boldsymbol{B}\boldsymbol{W}) + (\boldsymbol{B}\boldsymbol{V}) \times (\boldsymbol{A}\boldsymbol{W})\,; \tag{A.16}$$

$$\boldsymbol{A} \times \boldsymbol{I} = (\mathrm{tr}\boldsymbol{A})\,\boldsymbol{I} - \boldsymbol{A}^T; \tag{A.17}$$

$$\boldsymbol{I} \times \boldsymbol{I} = 2\boldsymbol{I}; \tag{A.18}$$

$$(\boldsymbol{A} \times \boldsymbol{A}) : \boldsymbol{A} = 6\ \det\boldsymbol{A}; \tag{A.19}$$

$$\mathrm{Cof}\boldsymbol{A} = \frac{1}{2}\boldsymbol{A} \times \boldsymbol{A}; \tag{A.20}$$

$$(\boldsymbol{A}\boldsymbol{C}) \times (\boldsymbol{B}\boldsymbol{C}) = (\boldsymbol{A} \times \boldsymbol{B})\,(\mathrm{Cof}\boldsymbol{C})\,. \tag{A.21}$$

Appendix B. Proof of convexity of stabilised invariants

Appendix B.1. Stabilisation strategy 1 in Section 6.1

Convexity of invariant $W_{\boldsymbol{F}\boldsymbol{D}_0}(\boldsymbol{F},\boldsymbol{D}_0)$ in equation (92) is subject to positiveness of the variable $\mathcal{F}$ defined as

$$\mathcal{F} = \begin{bmatrix} \delta\boldsymbol{F} : & \delta\boldsymbol{D}_0 \cdot \end{bmatrix} \begin{bmatrix} \frac{\partial^2 W_{\boldsymbol{F}\boldsymbol{D}_0}}{\partial\boldsymbol{F}\partial\boldsymbol{F}} & \frac{\partial^2 W_{\boldsymbol{F}\boldsymbol{D}_0}}{\partial\boldsymbol{F}\partial\boldsymbol{D}_0} \\ \frac{\partial^2 W_{\boldsymbol{F}\boldsymbol{D}_0}}{\partial\boldsymbol{D}_0\partial\boldsymbol{F}} & \frac{\partial^2 W_{\boldsymbol{F}\boldsymbol{D}_0}}{\partial\boldsymbol{D}_0\partial\boldsymbol{D}_0} \end{bmatrix} \begin{bmatrix} :\delta\boldsymbol{F} \\ \delta\boldsymbol{D}_0 \end{bmatrix} \geq 0, \tag{B.1}$$

where each of the terms featuring in the Hessian of $W_{\boldsymbol{F}\boldsymbol{D}_0}$ in (B.1) are obtained as

$$\begin{aligned} \frac{\partial^2 W_{\boldsymbol{F}\boldsymbol{D}_0}}{\partial\boldsymbol{F}\partial\boldsymbol{F}} &= 8\boldsymbol{F}\otimes\boldsymbol{F} + 4(II_{\boldsymbol{F}} + \gamma^2 II_{\boldsymbol{D}_0})\boldsymbol{\mathcal{I}}; \\ \frac{\partial^2 W_{\boldsymbol{F}\boldsymbol{D}_0}}{\partial\boldsymbol{F}\partial\boldsymbol{D}_0} &= 8\gamma^2\boldsymbol{F}\otimes\boldsymbol{D}_0; \\ \frac{\partial^2 W_{\boldsymbol{F}\boldsymbol{D}_0}}{\partial\boldsymbol{D}_0\partial\boldsymbol{D}_0} &= 8\gamma^4\boldsymbol{D}_0\otimes\boldsymbol{D}_0 + 4\gamma^2(II_{\boldsymbol{F}} + \gamma^2 II_{\boldsymbol{D}_0})\boldsymbol{I}. \end{aligned} \tag{B.2}$$

Introduction of above equation (B.2) into (B.1) yields

$$\begin{aligned} \mathcal{F} = {} & \underbrace{8(\delta\boldsymbol{F}:\boldsymbol{F})^2 + 4II_{\boldsymbol{F}}II_{\delta\boldsymbol{F}}}_{\mathcal{F}_1} + \underbrace{4\gamma^2 II_{\boldsymbol{D}_0}II_{\delta\boldsymbol{F}}}_{\mathcal{F}_3} \\ & + \underbrace{8\gamma^4(\delta\boldsymbol{D}_0\cdot\boldsymbol{D}_0)^2 + 4\gamma^4 II_{\boldsymbol{D}_0}II_{\delta\boldsymbol{D}_0}}_{\mathcal{F}_2} + \underbrace{4\gamma^2 II_{\boldsymbol{F}}II_{\delta\boldsymbol{D}_0}}_{\mathcal{F}_4} \\ & + \underbrace{16\gamma^2(\delta\boldsymbol{F}:\boldsymbol{F})(\delta\boldsymbol{D}_0\cdot\boldsymbol{D}_0)}_{\mathcal{F}_5}. \end{aligned} \tag{B.3}$$

Application of the Cauchy-Schwarz inequality to the tensors $\boldsymbol{F}$ and $\delta\boldsymbol{F}$ and to the vectors $\boldsymbol{D}_0$ and $\delta\boldsymbol{D}_0$ reads as,

$$II_{\boldsymbol{F}}II_{\delta\boldsymbol{F}} \geq (\delta\boldsymbol{F}:\boldsymbol{F})^2; \quad II_{\boldsymbol{D}_0}II_{\delta\boldsymbol{D}_0} \geq (\delta\boldsymbol{D}_0\cdot\boldsymbol{D}_0)^2. \tag{B.4}$$

Equation (B.4) enables a set of inequalities for $\mathcal{F}_1$ and $\mathcal{F}_2$ in (B.3) to be written as,

$$\begin{aligned} \mathcal{F}_1 &= 8(\delta\boldsymbol{F}:\boldsymbol{F})^2 + 4II_{\boldsymbol{F}}II_{\delta\boldsymbol{F}} \geq 12(\delta\boldsymbol{F}:\boldsymbol{F})^2; \\ \mathcal{F}_2 &= 8\gamma^4(\delta\boldsymbol{D}_0\cdot\boldsymbol{D}_0)^2 + 4\gamma^4 II_{\boldsymbol{D}_0}II_{\delta\boldsymbol{D}_0} \geq 12\gamma^4(\delta\boldsymbol{D}_0\cdot\boldsymbol{D}_0)^2. \end{aligned} \tag{B.5}$$

Introduction of the inequalities for $\mathcal{F}_1$ and $\mathcal{F}_2$ in (B.5) into equation (B.3) yields the following inequality

$$\begin{aligned}\mathcal{F} \geq \underbrace{12(\delta \boldsymbol{F} : \boldsymbol{F})^2}_{\mathcal{F}_1^*} + \underbrace{4\gamma^2 II_{\boldsymbol{D}_0} II_{\delta \boldsymbol{F}}}_{\mathcal{F}_3} + \underbrace{12\gamma^4 (\delta \boldsymbol{D}_0 \cdot \boldsymbol{D}_0)^2}_{\mathcal{F}_2^*} \\ + \underbrace{4\gamma^4 II_{\boldsymbol{F}} II_{\delta \boldsymbol{D}_0}}_{\mathcal{F}_4} + \underbrace{16\gamma^2 (\delta \boldsymbol{F} : \boldsymbol{F})(\delta \boldsymbol{D}_0 \cdot \boldsymbol{D}_0)}_{\mathcal{F}_5}.\end{aligned} \tag{B.6}$$

Notice in above (B.6) that $\mathcal{F}_3 \geq 0$ and $\mathcal{F}_4 \geq 0$. Therefore, inequality (B.6) can be further modifed as

$$\mathcal{F} \geq \mathcal{F}^*; \qquad \mathcal{F}^* = \mathcal{F}_1^* + \mathcal{F}_2^* + \mathcal{F}_5. \tag{B.7}$$

Introduction of equation (B.6) into equation $(\text{B.7})_b$ enables the intermediate variable $\mathcal{F}^*$ in (B.7) to be written as

$$\mathcal{F}^* = \mathcal{F}_1^* + \mathcal{F}_2^* + \mathcal{F}_5 = 12\underbrace{(\delta \boldsymbol{F} : \boldsymbol{F})^2}_{a^2} + 12\underbrace{\gamma^4 (\delta \boldsymbol{D}_0 \cdot \boldsymbol{D}_0)^2}_{b^2} + 16\underbrace{\gamma^2 (\delta \boldsymbol{F} : \boldsymbol{F})(\delta \boldsymbol{D}_0 \cdot \boldsymbol{D}_0)}_{ab}. \tag{B.8}$$

Notice from equation (B.8) that $\mathcal{F}^*$ can be re-written in a more compact and clearer form in terms of a and b (B.8) as

$$\mathcal{F}^* = 12a^2 + 12b^2 + 16ab = 4(a^2 + b^2 + 2(a+b)^2) \geq 0. \tag{B.9}$$

Positiveness of $\mathcal{F}^*$ in above (B.9) yields positiveness of $\mathcal{F}$ in (B.6) (inferred from $(\text{B.7})_a$). Hence, the invariant $W_{\boldsymbol{F}\boldsymbol{D}_0}(\boldsymbol{F}, \boldsymbol{D}_0)$ in equation (92) is convex with respect to its arguments, namely $\{\boldsymbol{F}, \boldsymbol{D}_0\}$.

Appendix B.2. Stabilisation strategy 1 in Section 6.2

Convexity of invariant $\hat{W}_{\boldsymbol{H}\boldsymbol{D}_0}$ in equation (93) is subject to positiveness of the variable $\mathcal{G}$ defined as

$$\mathcal{G} = \begin{bmatrix} \delta \boldsymbol{H} : & \delta \boldsymbol{D}_0 \cdot \end{bmatrix} \begin{bmatrix} \frac{\partial^2 \hat{W}_{\boldsymbol{H}\boldsymbol{D}_0}}{\partial \boldsymbol{H} \partial \boldsymbol{H}} & \frac{\partial^2 \hat{W}_{\boldsymbol{H}\boldsymbol{D}_0}}{\partial \boldsymbol{H} \partial \boldsymbol{D}_0} \\ \frac{\partial^2 \hat{W}_{\boldsymbol{H}\boldsymbol{D}_0}}{\partial \boldsymbol{D}_0 \partial \boldsymbol{H}} & \frac{\partial^2 \hat{W}_{\boldsymbol{H}\boldsymbol{D}_0}}{\partial \boldsymbol{D}_0 \partial \boldsymbol{D}_0} \end{bmatrix} \begin{bmatrix} : \delta \boldsymbol{H} \\ \delta \boldsymbol{D}_0 \end{bmatrix} \geq 0, \tag{B.10}$$

where each of the terms featuring in the Hessian of $\hat{W}_{\boldsymbol{H}\boldsymbol{D}_0}$ in (B.10) are obtained as

$$\begin{aligned}\frac{\partial^2 \hat{W}_{\boldsymbol{H}\boldsymbol{D}_0}}{\partial \boldsymbol{H}\partial \boldsymbol{H}} &= 8\boldsymbol{H}\otimes\boldsymbol{H} + 4II_{\boldsymbol{H}} + 2\gamma^2\boldsymbol{\mathcal{T}};\\ \frac{\partial^2 \hat{W}_{\boldsymbol{H}\boldsymbol{D}_0}}{\partial \boldsymbol{H}\partial \boldsymbol{D}_0} &= 2\gamma^2\boldsymbol{\mathcal{S}};\\ \frac{\partial^2 \hat{W}_{\boldsymbol{H}\boldsymbol{D}_0}}{\partial \boldsymbol{D}_0\partial \boldsymbol{D}_0} &= 8\gamma^4\boldsymbol{D}_0\otimes\boldsymbol{D}_0 + 2\gamma^2(\boldsymbol{H}^T\boldsymbol{H} + 2\gamma^2 II_{\boldsymbol{D}_0}\boldsymbol{I})\boldsymbol{I}.\end{aligned} \tag{B.11}$$

with $\mathcal{T}_{iIjJ} = \delta_{ij}D_{0_I}D_{0_J}$ and $\mathcal{S}_{iIJ} = H_{iJ}D_{0I} + (\boldsymbol{H}\boldsymbol{D}_0)_i\,\delta_{IJ}$. Introduction of above equation (B.11) into (B.10) enables $\mathcal{G}$ in (B.10) to be re-written as

$$\begin{aligned}\mathcal{G} = &\underbrace{4II_{\boldsymbol{H}}II_{\delta\boldsymbol{H}}}_{\mathcal{G}_1} + \underbrace{4\gamma^4 II_{\boldsymbol{D}_0}II_{\delta\boldsymbol{D}_0}}_{\mathcal{G}_2} + \underbrace{4\gamma^2\left(\delta\boldsymbol{H}\boldsymbol{D}_0\cdot\boldsymbol{H}\delta\boldsymbol{D}_0 + \boldsymbol{H}\boldsymbol{D}_0\cdot\delta\boldsymbol{H}\delta\boldsymbol{D}_0\right)}_{\mathcal{F}_3}\\ &+ \underbrace{8\left(\delta\boldsymbol{H}:\boldsymbol{H}\right)^2 + 8\gamma^4\left(\boldsymbol{D}_0\cdot\delta\boldsymbol{D}_0\right)^2 + 2\gamma^2 II_{\delta\boldsymbol{H}\boldsymbol{D}_0} + 2\gamma^2 II_{\boldsymbol{H}\delta\boldsymbol{D}_0}}_{\mathcal{G}_4}.\end{aligned} \tag{B.12}$$

Application of the Cauchy-Schwarz inequality to the term $\mathcal{G}_1$ in above (B.12) yields the following inequality

$$\mathcal{G}_1 = 4II_{\boldsymbol{H}}II_{\delta\boldsymbol{H}} \geq 4\text{tr}\left(\boldsymbol{H}^T\boldsymbol{H}\delta\boldsymbol{H}^T\delta\boldsymbol{H}\right) = 4\text{tr}\left(\boldsymbol{H}^T\delta\boldsymbol{H}\delta\boldsymbol{H}^T\boldsymbol{H}\right). \tag{B.13}$$

Introduction of inequality (B.13) for $\mathcal{G}_1$ into equation (B.12) renders the following inequality for $\mathcal{G}$ (B.12)

$$\begin{aligned}\mathcal{G} \geq &\underbrace{4\text{tr}\left(\boldsymbol{H}^T\delta\boldsymbol{H}\delta\boldsymbol{H}^T\delta\boldsymbol{H}\right)}_{\mathcal{G}_1^*} + \underbrace{4\gamma^4 II_{\boldsymbol{D}_0}II_{\delta\boldsymbol{D}_0}}_{\mathcal{G}_2} + \underbrace{4\gamma^2\left(\delta\boldsymbol{H}\boldsymbol{D}_0\cdot\boldsymbol{H}\delta\boldsymbol{D}_0 + \boldsymbol{H}\boldsymbol{D}_0\cdot\delta\boldsymbol{H}\delta\boldsymbol{D}_0\right)}_{\mathcal{G}_3}\\ &+ \underbrace{8\left(\delta\boldsymbol{H}:\boldsymbol{H}\right)^2 + 8\gamma^4\left(\boldsymbol{D}_0\cdot\delta\boldsymbol{D}_0\right)^2 + 2\gamma^2 II_{\delta\boldsymbol{H}\boldsymbol{D}_0} + 2\gamma^2 II_{\boldsymbol{H}\delta\boldsymbol{D}_0}}_{\mathcal{G}_4}.\end{aligned} \tag{B.14}$$

Notice in above equation (B.14) that $\mathcal{G}_4 \geq 0$. Therefore, inequality (B.14) can be further modified as

$$\mathcal{G} \geq \mathcal{G}^*; \qquad \mathcal{G}^* = \mathcal{G}_1^* + \mathcal{G}_2 + \mathcal{G}_3. \tag{B.15}$$

Introduction of equation (B.14) into $(\text{B.15})_b$ enables the intermediate variable $\mathcal{G}^\star$ to be written as

$$\mathcal{G}^\star = \mathcal{G}_1^* + \mathcal{G}_2 + \mathcal{G}_3 = 4\text{tr}\left(\boldsymbol{B}^T\boldsymbol{B}\right); \quad \boldsymbol{B} = \delta\boldsymbol{H}^T\boldsymbol{H} + \gamma^2\delta\boldsymbol{D}_0\otimes\boldsymbol{D}_0. \tag{B.16}$$

Finally, positive definiteness of the tensor $\boldsymbol{B}^T\boldsymbol{B}$ in above equation (B.16) implies positiveness of $\mathcal{G}^\star$ and hence, positiveness of $\mathcal{G}$ (inferred from equation (B.15)$_a$). Therefore, convexity of invariant $\hat{W}_{\boldsymbol{H}\boldsymbol{D}_0}$ in (93) with respect to its arguments, namely $\{\boldsymbol{H}, \boldsymbol{D}_0\}$ is proved.

Appendix C. Material characterisation in the reference configuration

Proper material characterisation in nonlinear electro-elasticity is at its early stage. Experimental studies reporting the behaviour of specific materials at various high deformation scenarios and for large values of the applied electric fields are not available. Therefore, material characterisation in nonlinear electro-elasticity relies upon characterisation in the reference configuration [38]. The following section shows how the different constitutive tensors emerging in electro-elasticity (45) can be expressed in terms of the elements of the extended set $\mathcal{V}$. Then, material characterisation in the reference configuration is achieved by replacing $\{\boldsymbol{F}, \boldsymbol{H}, J, \boldsymbol{D}_0, \boldsymbol{d}\}$ with $\{\boldsymbol{I}, \boldsymbol{I}, 1, \boldsymbol{0}, \boldsymbol{0}\}$ in the expressions obtained for the different constitutive tensors.

Appendix C.1. Elasticity tensor

From equation (44), the second directional derivative of the internal energy e with respect to changes of the geometry can be obtained as

$$D^2 e\,[\delta \boldsymbol{u}; \boldsymbol{u}] = \boldsymbol{\nabla}_0 \delta \boldsymbol{u} : \boldsymbol{\mathcal{C}} : \boldsymbol{\nabla}_0 \boldsymbol{u}. \tag{C.1}$$

Comparison of equations (C.1) and (46) enables the elasticity tensor $\boldsymbol{\mathcal{C}}$ to be alternatively re-written in terms of the derivatives of the electro-kinematic variable set $\mathcal{V}$ as

$$\begin{aligned}\boldsymbol{\mathcal{C}} &= W_{\boldsymbol{FF}} + \boldsymbol{F} \times (W_{\boldsymbol{HH}} \times \boldsymbol{F}) + W_{JJ} \boldsymbol{H} \otimes \boldsymbol{H} + \boldsymbol{\mathcal{C}}_1 \\ &\quad + 2(W_{\boldsymbol{FH}} \times \boldsymbol{F})^{\text{sym}} + 2(W_{\boldsymbol{F}J} \otimes \boldsymbol{H})^{\text{sym}} + 2(W_{\boldsymbol{Fd}} \otimes \boldsymbol{D}_0)^{\text{sym}} \\ &\quad + 2((\boldsymbol{F} \times W_{\boldsymbol{H}J}) \otimes \boldsymbol{H})^{\text{sym}} + 2((\boldsymbol{F} \times W_{\boldsymbol{Hd}}) \otimes \boldsymbol{D}_0)^{\text{sym}} \\ &\quad + 2(\boldsymbol{H} \otimes (W_{J\boldsymbol{d}} \otimes \boldsymbol{D}_0))^{\text{sym}} + \boldsymbol{\mathcal{A}},\end{aligned} \tag{C.2}$$

where

$$\mathcal{A}_{iIjJ} = \mathcal{E}_{ijp} \mathcal{E}_{IJP} \left(\boldsymbol{\Sigma_H} + \Sigma_J \boldsymbol{\Sigma_H} \right)_{pP}; \quad \mathcal{C}_{1,iIjJ} = (W_{\boldsymbol{dd}})_{ij}\, D_{0I} D_{0J}. \tag{C.3}$$

Moreover, for any fourth order tensor $\boldsymbol{\mathcal{T}}$ included in equation (C.2), the symmetrised tensor $\boldsymbol{\mathcal{T}}^{\text{sym}}$ is defined as $\mathcal{T}^{\text{sym}}_{iIjJ} = \frac{1}{2} (\mathcal{T}_{iIjJ} + \mathcal{T}_{iJjI})$.

Appendix C.2. Piezoelectric tensor

From equation (44), the second directional derivative of the internal energy e with respect to changes in geometry and electric displacement field leads to the following expression

$$D^2 e\left[\delta \boldsymbol{u}; \Delta \boldsymbol{D}_0\right] = \left(\boldsymbol{\nabla}_0 \delta \boldsymbol{u} : \boldsymbol{\mathcal{Q}}^T\right) \cdot \Delta \boldsymbol{D}_0. \tag{C.4}$$

Comparison of equations (C.4) and (46) allows to re-express the piezoelectric tensor $\boldsymbol{\mathcal{Q}}^T$ in terms of the elements of the set $\mathcal{V}$ as

$$\begin{aligned} \boldsymbol{\mathcal{Q}}^T &= W_{\boldsymbol{F}\boldsymbol{D}_0} + \boldsymbol{F} \boldsymbol{\times} W_{\boldsymbol{H}\boldsymbol{D}_0} + \boldsymbol{H} \otimes W_{J\boldsymbol{D}_0} + \boldsymbol{\mathcal{Q}}_1^T \\ &+ \boldsymbol{\mathcal{Q}}_2^T + \boldsymbol{\mathcal{Q}}_3^T + \boldsymbol{\mathcal{Q}}_4^T + \boldsymbol{\mathcal{Q}}_5^T + \boldsymbol{\Sigma}_{\boldsymbol{d}} \otimes \boldsymbol{I}. \end{aligned} \tag{C.5}$$

where the expressions for the tensors $\boldsymbol{\mathcal{Q}}_i^T$ in above equation (C.5) are given as

$$\left(\boldsymbol{\mathcal{Q}}_1^T\right)_{iIJ} = \left(W_{\boldsymbol{d}\boldsymbol{D}_0}\right)_{iJ} D_{0I}; \tag{C.6a}$$

$$\left(\boldsymbol{\mathcal{Q}}_2^T\right)_{iIJ} = \left(W_{\boldsymbol{F}\boldsymbol{d}iIj}\right) F_{jJ}; \tag{C.6b}$$

$$\left(\boldsymbol{\mathcal{Q}}_3^T\right)_{iIJ} = (\boldsymbol{F} \boldsymbol{\times} W_{\boldsymbol{H}\boldsymbol{d}})_{iIj} F_{jJ}; \tag{C.6c}$$

$$\left(\boldsymbol{\mathcal{Q}}_4^T\right)_{iIJ} = (\boldsymbol{H} \otimes W_{J\boldsymbol{d}})_{iIj} F_{jJ}; \tag{C.6d}$$

$$\left(\boldsymbol{\mathcal{Q}}_5^T\right)_{iIJ} = \left(W_{\boldsymbol{d}\boldsymbol{d}}\right)_{ij} F_{jJ} D_{0I}. \tag{C.6e}$$

Appendix C.3. Dielectric tensor

The second directional derivative of the internal energy e with respect to changes in the electric displacement field can be identified from equation (44) as

$$D^2 e\left[\delta \boldsymbol{D}_0; \Delta \boldsymbol{D}_0\right] = \delta \boldsymbol{D}_0 \cdot \boldsymbol{\theta} \Delta \boldsymbol{D}_0. \tag{C.7}$$

Comparison of equations (C.7) and (46) enables the inverse of the dielectric tensor $\boldsymbol{\theta}$ to be re-expressed in terms of the elements of the set $\mathcal{V}$ as

$$\boldsymbol{\theta} = W_{\boldsymbol{D}_0\boldsymbol{D}_0} + \left(W_{\boldsymbol{D}_0\boldsymbol{d}}\boldsymbol{F} + \boldsymbol{F}^T W_{\boldsymbol{d}\boldsymbol{D}_0}\right) + \boldsymbol{F}^T W_{\boldsymbol{d}\boldsymbol{d}} \boldsymbol{F}. \tag{C.8}$$

Appendix C.4. Electrostrictive tensor

A very important constitutive tensor described as a second order effect (it does not appear in the tangent operator of the internal energy $e(\boldsymbol{\nabla}_0\boldsymbol{x}, \boldsymbol{D}_0)$ in (44)) is the electrostrictive tensor, defined as

$$\boldsymbol{\mathcal{B}}|_{\boldsymbol{F}=\boldsymbol{\nabla}_0\boldsymbol{x}} = \frac{\partial \boldsymbol{\mathcal{Q}}^T}{\partial \boldsymbol{D}_0}. \tag{C.9}$$

Introduction of equation (C.5) into (C.9) enables $\boldsymbol{\mathcal{B}}$ to be expressed in terms of the elements of the set $\mathcal{V}$ as

$$\begin{aligned}\left(\boldsymbol{\mathcal{B}}|_{\boldsymbol{F}=\boldsymbol{\nabla}_0\boldsymbol{x}}\right)_{iIJK} &= (W_{\boldsymbol{F}\boldsymbol{D}_0\boldsymbol{D}_0})_{iIJK} + (W_{\boldsymbol{F}\boldsymbol{D}_0\boldsymbol{d}})_{iIJm}\, F_{mK} \\ &+ (\boldsymbol{F}\times W_{\boldsymbol{H}\boldsymbol{D}_0\boldsymbol{D}_0})_{iIJK} + (\boldsymbol{F}\times W_{\boldsymbol{H}\boldsymbol{D}_0\boldsymbol{d}})_{iIJm}\, F_{mK} \\ &+ (\boldsymbol{H}\otimes W_{J\boldsymbol{D}_0\boldsymbol{D}_0})_{iIJK} + (\boldsymbol{H}\otimes W_{J\boldsymbol{D}_0\boldsymbol{d}})_{iIJm}\, F_{mK} \\ &+ (\boldsymbol{\mathcal{B}}_1+\boldsymbol{\mathcal{B}}_2+\boldsymbol{\mathcal{B}}_3+\boldsymbol{\mathcal{B}}_4+\boldsymbol{\mathcal{B}}_5)_{iIJK} + (W_{\boldsymbol{d}\boldsymbol{D}_0})_{iK}\,\delta_{IJ} + (W_{\boldsymbol{d}\boldsymbol{d}})_{im}\, F_{mK}\delta_{IJ},\end{aligned} \tag{C.10}$$

where $W_{\boldsymbol{ABC}} = \frac{\partial^3 W}{\partial\boldsymbol{A}\partial\boldsymbol{B}\partial\boldsymbol{C}}$ and with

$$(\boldsymbol{\mathcal{B}}_1)_{iIJK} = (W_{\boldsymbol{d}\boldsymbol{D}_0\boldsymbol{D}_0})_{iJk}\, D_{0I} + (W_{\boldsymbol{d}\boldsymbol{D}_0\boldsymbol{d}})_{iJm}\, F_{mK}D_{0I} + (W_{\boldsymbol{d}\boldsymbol{D}_0})_{iJ}\,\delta_{IK}; \tag{C.11a}$$

$$(\boldsymbol{\mathcal{B}}_2)_{iIJK} = (W_{\boldsymbol{F}\boldsymbol{d}\boldsymbol{D}_0})_{iIjK}\, F_{jJ} + (W_{\boldsymbol{F}\boldsymbol{d}\boldsymbol{d}})_{iIjk}\, F_{jJ}F_{kK}; \tag{C.11b}$$

$$(\boldsymbol{\mathcal{B}}_3)_{iIJK} = (\boldsymbol{F}\times W_{\boldsymbol{H}\boldsymbol{d}\boldsymbol{D}_0})_{iIjK}\, F_{jJ} + (\boldsymbol{F}\times W_{\boldsymbol{H}\boldsymbol{d}\boldsymbol{d}})_{iIjk}\, F_{jJ}F_{kK}; \tag{C.11c}$$

$$(\boldsymbol{\mathcal{B}}_4)_{iIJK} = (\boldsymbol{H}\otimes W_{J\boldsymbol{d}\boldsymbol{D}_0})_{iIjK}\, F_{jJ} + (\boldsymbol{H}\otimes W_{J\boldsymbol{d}\boldsymbol{d}})_{iIjk}\, F_{jJ}F_{kK}; \tag{C.11d}$$

$$(\boldsymbol{\mathcal{B}}_5)_{iIJK} = (W_{\boldsymbol{d}\boldsymbol{d}\boldsymbol{D}_0})_{ijK}\, F_{jJ}D_{0I} + (W_{\boldsymbol{d}\boldsymbol{d}\boldsymbol{d}})_{ijk}\, F_{jJ}F_{kK}D_{0I} + (W_{\boldsymbol{d}\boldsymbol{d}})_{ij}\, F_{jJ}\delta_{IK}. \tag{C.11e}$$

References

[1] J. Bonet, A. J. Gil, R. Ortigosa, A computational framework for polyconvex large strain elasticity, Computer Methods in Applied Mechanics and Engineering 283 (2015) 1061–1094.

[2] J. M. Ball, Convexity conditions and existence theorems in nonlinear elasticity, Archive for Rational Mechanics and Analysis 63 (1976) 337–403.

[3] R. de Boer, Vektor- und Tensorrechnung für Ingenieure, Springer-Verlag, 1982.

[4] A. O'Halloran, F. O'Malley, P. McHugh, A review on dielectric elastomer actuators, technology, applications, and challenges, Journal of Applied Physics 104 (2008).

[5] R. E. Pelrine, R. D. Kornbluh, J. P. Joseph, Electrostriction of polymer dielectrics with compliant electrodes as a means of actuation, Sensors and Actuators A: Physical 64 (1998) 77–85.

[6] R. Pelrine, R. Kornbluh, Q. Pei, J. Joseph, High-speed electrically actuated elastomers with strain greater than 100 %, Science 287 (2000) 836–839.

[7] G. Kofod, P. Sommer-Larsen, R. Kornbluh, R. Pelrine, Actuation response of polyacrylate dielectric elastomers, Journal of Intelligent Material Systems and Structures 14 (2003) 787–793.

[8] R. Pelrine, R. D. Kornbluh, Q. Pei, S. Stanford, S. Oh, J. Eckerle, R. J. Full, M. A. Rosenthal, K. Meijer, Dielectric elastomer artificial muscle actuators: toward biomimetic motion, 2002.

[9] T. Li, C. Keplinger, R. Baumgartner, S. Bauer, W. Yang, Z. Suo, Giant voltage-induced deformation in dielectric elastomers near the verge of snap-through instability, Journal of the Mechanics and Physics of Solids 61 (2013) 611–628.

[10] S. Chiba, M. Waki, T. Wada, Y. Hirakawa, K. Masuda, T. Ikoma, Consistent ocean wave energy harvesting using electroactive polymer (dielectric elastomer) artificial muscle generators, Applied Energy 104 (2013) 497–502.

[11] S. Skatulla, C. Sansour, A. Arockiarajan, A multiplicative approach for nonlinear electro-elasticity, Computer Methods in Applied Mechanics and Engineering 245-246 (2012) 243–255.

[12] A. Dorfmann, R. W. Ogden, Nonlinear electroelasticity, Acta Mechanica 174 (2005) 167–183.

[13] A. Dorfmann, R. Ogden, Nonlinear electroelastic deformations, Journal of Elasticity 82 (2006) 99–127.

[14] R. Bustamante, A. Dorfmann, R. Ogden, Nonlinear electroelastostatics: a variational framework, Zeitschrift für angewandte Mathematik und Physik 60 (2009) 154–177.

[15] R. Bustamante, A. Dorfmann, R. Ogden, On electric body forces and Maxwell stresses in nonlinearly electroelastic solids, International Journal of Engineering Science 47 (2009) 1131–1141.

[16] R. Bustamante, Transversely isotropic non-linear electro-active elastomers, Acta Mechanica 206 (2009) 237–259.

[17] R. Bustamante, J. Merodio, Constitutive structure in coupled non-linear electro-elasticity: Invariant descriptions and constitutive restrictions, International Journal of Non-Linear Mechanics 46 (2011) 1315 – 1323.

[18] A. W. Richards, G. M. Odegard, Constitutive modeling of electrostrictive polymers using a hyperelasticity-based approach, Journal of Applied Mechanics 77 (2009).

[19] R. M. McMeeking, C. M. Landis, Electrostatic forces and stored energy for deformable dielectric materials, Journal of Applied Mechanics 72 (2008) 581–590.

[20] Z. Suo, X. Zhao, W. H. Greene, A nonlinear field theory of deformable dielectrics, Journal of the Mechanics and Physics of Solids 56 (2008) 467–486.

[21] M. Itskov, V. N. Khiêm, A polyconvex anisotropic free energy function for electro- and magneto-rheological elastomers, Mathematics and Mechanics of Solids (2014) 1–12.

[22] R. Bustamante, J. Merodio, On simple constitutive restrictions for transversely isotropic nonlinearly elastic materials and isotropic magneto-sensitive elastomers, Journal of Engineering Mathematics 68 (2010) 15–26.

[23] J. E. Marsden, T. J. R. Hughes, Mathematical foundations of elasticity, 1994.

[24] A. Dorfmann, R. W. Ogden, Electroelastic waves in a finitely deformed electroactive material, IMA Journal of Applied Mathematics 75 (2010) 603–636.

[25] M. H. Siboni, P. P. Castañeda, Fiber-constrained, dielectric-elastomer composites: Finite-strain response and stability analysis, Journal of the Mechanics and Physics of Solids 68 (2014) 211–238.

[26] M. H. Siboni, R. Avazmohammadi, P. P. Castañeda, Electromechanical instabilities in fiber-constrained, dielectric-elastomer composites subjected to all-around dead-loading, Mathematics and Mechanics of Solids (2014).

[27] C. Miehe, D. Vallicotti, D. Zäh, Computational structural and material stability analysis in finite electro-elasto-statics of electro-active materials, International Journal for Numerical Methods in Engineering 102 (2015) 1605–1637. Nme.4855.

[28] J. M. Ball, Energy-minimising configurations in nonlinear elasticity, Archive for Rational Mechanics and Analysis 63 (1976) 337–403.

[29] J. M. Ball, Geometry, Mechanics and Dynamics, Springer, pp. 3–59.

[30] J. M. Ball, F. Murat, $W^{1,p}$-quasiconvexity and variational problems for multiple integrals, Journal of Functional Analysis 58 (1984) 225–253.

[31] B. Dacorogna, Direct Methods in the Calculus of Variations, Springer, 2008.

[32] P. Ciarlet, Existence theorems in intrinsic nonlinear elasticity, Journal des mathématiques pures et appliqués 94 (2010) 229–243.

[33] P. L. Tallec, Handbook of Numerical Analysis. Numerical Methods for Solids, North Holland.

[34] J. Schröder, P. Neff, D. Balzani, A variational approach for materially stable anisotropic hyperelasticity, International Journal of Solids and Structures 42 (2005) 4352–4371.

[35] J. Schröder, P. Neff, Invariant formulation of hyperelastic transverse isotropy based on polyconvex free energy functions, International Journal of Solids and Structures 40 (2003) 401–445.

[36] M. Aguirre, A. J. Gil, J. Bonet, A. A. Carreño, A vertex centred finite volume Jameson-Schmidt-Turkel (JST) algorithm for a mixed conservation formulation in solid dynamics, Journal of Computational Physics 259 (2014) 672–699.

[37] J. Schröder, P. Neff, V. Ebbing, Anisotropic polyconvex energies on the basis of crystallographic motived structural tensors, Journal of Mechanics and Physics of Solids 56 (2008) 3486–3506.

[38] J. Schröder, P. Neff, V. Ebbing, Polyconvex energies for trigonal, tetragonal and cubic symmetry groups, in: IUTAM-Symposium on variational concepts with applications to the mechanics of materials: Proceedings of the IUTAM-Syposium.

[39] J. Schröder, P. Wriggers, D. Balzani, A new mixed finite element based on different approximations of the minors of deformation tensors, Computer Methods in Applied Mechanics and Engineering 200 (2011) 3583–3600.

[40] J. Schröder, Anisotropic polyconvex energies, in: J. Schröder, P. Neff (Eds.), Poly-, quasi- and rank-one convexity in Applied Mechanics, volume 516 of CISM Courses and Lectures, volume 516 of CISM Courses and Lectures, Springer-Verlag, 2010, pp. 53–105.

[41] A. J. Gil, C. H. Lee, J. Bonet, R. Ortigosa, A first order hyperbolic framework for large strain computational solid dynamics - Part II: Total Lagrangian compressible, nearly incompressible and truly incompressible elasticity, Computer Methods in Applied Mechanics and Engineering (Under review).

[42] M. Itskov, N. Aksel, A class of orthotropic and transversely isotropic hyperelastic constitutive models based on a polyconvex strain energy

function, International Journal of Solids and Structures 41 (2004) 3833 – 3848.

[43] M. Itskov, A. Ehret, D. Mavrilas, A polyconvex anisotropic strain-energy function for soft collagenous tissues, Biomechanics and Modeling in Mechanobiology 5 (2006) 17–26.

[44] A. E. Ehret, M. Itskov, A polyconvex hyperelastic model for fiber-reinforced materials in application to soft tissues, Journal of Materials Science 42 (2007) 8853–8863.

[45] R. Ortigosa, A. J. Gil, J. Bonet, C. Hesch, A computational framework for polyconvex large strain elasticity for geometrically exact beam theory, Computational Mechanics (2015) In print.

[46] R. Rogers, Nonlocal variational problems in nonlinear electromagneto-elastostatics, SIAM Journal on Mathematical Analysis 19 (1988) 1329–1347.

[47] R. Ortigosa, A. J. Gil, A new framework for large strain electromechanics based on convex multi-variable strain energies: conservation laws and hyperbolicity, Computer Methods in Applied Mechanics and Engineering (Under review).

[48] A. N. Brooks, T. J. R. Hughes, Streamline upwind/Petrov-Galerkin formulations for convection dominated flows with particular emphasis on the incompressible Navier-Stokes equations, Computer Methods in Applied Mechanics and Engineering 32 (1982) 199–259.

[49] D. K. Vu, P. Steinmann, G. Possart, Numerical modelling of non-linear electroelasticity, International Journal for Numerical Methods in Engineering 70 (2007) 685–704.

[50] J. Zhou, W. Hong, X. Zhao, Z. Zhang, Z. Suo, Propagation of instability in dielectric elastomers, International Journal of Solids and Structures 45 (2008) 3739–3750.

[51] D. Vu, P. Steinmann, On 3-D coupled BEM-FEM simulation of nonlinear electro-elastostatics, Computer Methods in Applied Mechanics and Engineering 201-204 (2012) 82–90.

[52] D. Vu, P. Steinmann, A 2-D coupled BEM-FEM simulation of electro-elastostatics at large strain, Computer Methods in Applied Mechanics and Engineering 199 (2010) 1124–1133.

[53] F. Vogel, R. Bustamante, P. Steinmann, On some mixed variational principles in electro-elastostatics, International Journal of Non-Linear Mechanics 47 (2012) 341–354. Nonlinear Continuum Theories.

[54] D. P. Flanagan, T. Belytschko, A uniform strain hexahedron and quadrilateral with orthogonal hourglass control, International Journal for Numerical Methods in Engineering 17 (1981) 679–706.

[55] J. Bonet, P. Bhargava, A uniform deformation gradient hexahedron element with artificial hourglass control, International Journal for Numerical Methods in Engineering 38 (1995) 2809–2828.

[56] J. C. Simo, F. Armero, K. S. Pister, Variational and projection methods for the volume constraint in finite deformation elasto-plasticity, Computational Methods for Applied Mechanical Engineering 51 (1985) 177–208.

[57] R. Stenberg, A family of mixed finite elements for elasticity problems, Numerische Mathematik 48 (1988) 513–538.

[58] J. C. Simo, F. Armero, Geometrically non-linear enhanced strain mixed methods and the method of incompatible modes, International Journal for Numerical Methods in Engineering 33 (1992) 1413–1449.

[59] J. C. Simo, F. Armero, R. Taylor, Improved versions of assumed enhanced strain tri-linear elements for 3D finite deformation problems, Computational Methods for Applied Mechanical Engineering 110 (1993) 359–386.

[60] M. A. Puso, A highly efficient enhanced assumed strain physically stabilized hexahedral element, International Journal for Numerical Methods in Engineering 49 (2000) 1029–1064.

[61] F. Auricchio, L. B. de Veiga, C. Lovadina, A. Reali, A stability study of some mixed finite elements for large deformation elasticity problems, Computational Methods for Applied Mechanical Engineering 194 (2005) 1075–1092.

[62] F. Auricchio, L. B. de Veiga, C. Lovadina, A. Reali, The importance of the exact satisfaction of the incompressibility constraint in nonlinear elasticity: mixed fems versus nurbs-based approximations, Computational Methods for Applied Mechanical Engineering 199 (2008) 314–323.

[63] R. L. Taylor, A mixed-enhanced formulation for tetrahedral finite elements, International Journal for Numerical Methods in Engineering 47 (2000) 205–227.

[64] C. R. Dohrmann, M. W. Heinstein, J. Jung, S. W. Key, W. R. Witkowski, Node-based uniform strain elements for three-node triangular and four-node tetrahedral meshes, International Journal for Numerical Methods in Engineering 47 (2000) 1549–1568.

[65] Q. Tiehu, Symmetrizing nonlinear elastodynamic system, Journal of Elasticity 50 (1998) 245–252.

[66] D. H. Wagner, Symmetric-hyperbolic equations of motion for a hyperelastic material, Journal of Hyperbolic Differential Equations 06 (2009) 615–630.

[67] J. Bonet, R. D. Wood, Nonlinear Continuum Mechanics for Finite Element Analysis, Cambridge University Press, second edition, 2008.

[68] A. J. Gil, C. H. Lee, J. Bonet, M. Aguirre, A stabilised Petrov-Galerkin formulation for linear tetrahedral elements in compressible, nearly incompressible and truly incompressible fast dynamics, Computer Methods in Applied Mechanics and Engineering 276 (2014) 659–690.

[69] C. H. Lee, A. J. Gil, J. Bonet, Development of a stabilised Petrov-Galerkin formulation for conservation laws in lagrangian fast solid dynamics, Computer Methods in Applied Mechanics and Engineering 268 (2014) 40–64.

[70] I. A. Karim, C. H. Lee, A. J. Gil, J. Bonet, A two-step Taylor-Galerkin formulation for fast dynamics, Engineering Computations 31 (2014) 366–387.

[71] G. Scovazzi, B. Carnes, X. Zeng, A simple, stable and accurate tetrahedral finite element for transient, nearly incompressible, linear and nonlinear elasticity: A dynamic variational multiscale approach, International Journal for Numerical Methods in Engineering (2015). Under review.

[72] C. H. Lee, A. J. Gil, J. Bonet, Development of a cell centred upwind finite volume algorithm for a new conservation law formulation in structural dynamics, Computers & Structures 118 (2013) 13–38.

[73] M. Aguirre, A. J. Gil, J. Bonet, C. H. Lee, A vertex centred upwind finite volume method for solid dynamics, Journal of Computational Physics (2015). In Press.

[74] R. Ortigosa, A. J. Gil, A new framework for large strain electromechanics based on convex multi-variable strain energies: Finite Element discretisation and computational implementation, Computer Methods in Applied Mechanics and Engineering (Under review).

[75] J. Bonet, A. J. Gil, R. Ortigosa, On a tensor cross product based formulation of large strain solid mechanics, International Journal of Solids and Structures (Under review).

[76] X. Zhao, Z. Suo, Electrostriction in elastic dielectrics undergoing large deformation, Journal of Applied Physics 104 (2008) 123530.

[77] R. Hill, On uniqueness and stability in the theory of finite elastic strain, Journal of the Mechanics and Physics of Solids 5 (1957) 229–241.

[78] B. D. Coleman, W. Noll, On the thermostatics of continuous media, Archive for Rational Mechanics and Analysis 4 (1959) 97–128.

[79] P. G. Ciarlet, Mathematical Elasticity. Volume 1: Three Dimensional Elasticity, 1988.

[80] O. Gonzalez, A. M. Stuart, A first course in Continuum Mechanics, Cambridge University Press, 2008.

[81] J. Bonet, A. J. Gil, C. H. Lee, M. Aguirre, R. Ortigosa, A first order hyperbolic framework for large strain computational solid dynamics - Part I: Total Lagrangian isothermal elasticity, Computer Methods in Applied Mechanics and Engineering 283 (2015) 689–732.

[82] B. Li, L. Liu, Z. Suo, Extension limit, polarization saturation, and snap-through instability of dielectric elastomers, International Journal of Smart and Nano Materials 2 (2011) 59–67.

[83] C. B. T. Böhlke, Graphical representation of the generalised Hooke's law, Technische Mechanik 21 (2001) 145–158.